Met Office

Scientific and Technical Review 2002/3

An Executive Agency of the Ministry of Defence

Scientific and Technical Review 2002/3

Met Office

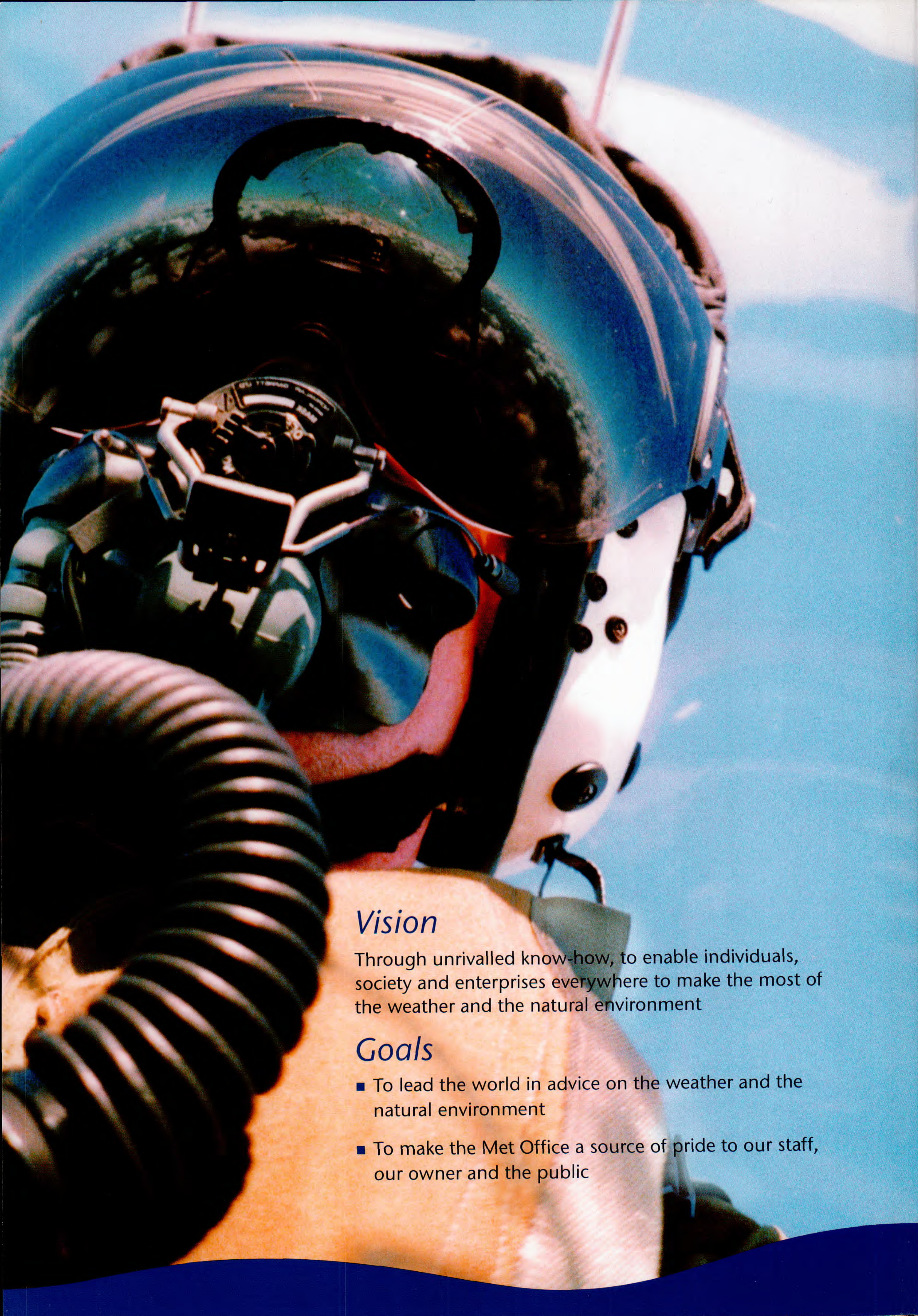

Vision

Through unrivalled know-how, to enable individuals, society and enterprises everywhere to make the most of the weather and the natural environment

Goals

- To lead the world in advice on the weather and the natural environment
- To make the Met Office a source of pride to our staff, our owner and the public

Contents

From the cockpit of an RAF Hawk jet, the distant horizon is reflected in the pilot's visor. Whatever you do, wherever you are, keep your goals in sight and we will help you achieve them, by using the weather to your advantage.

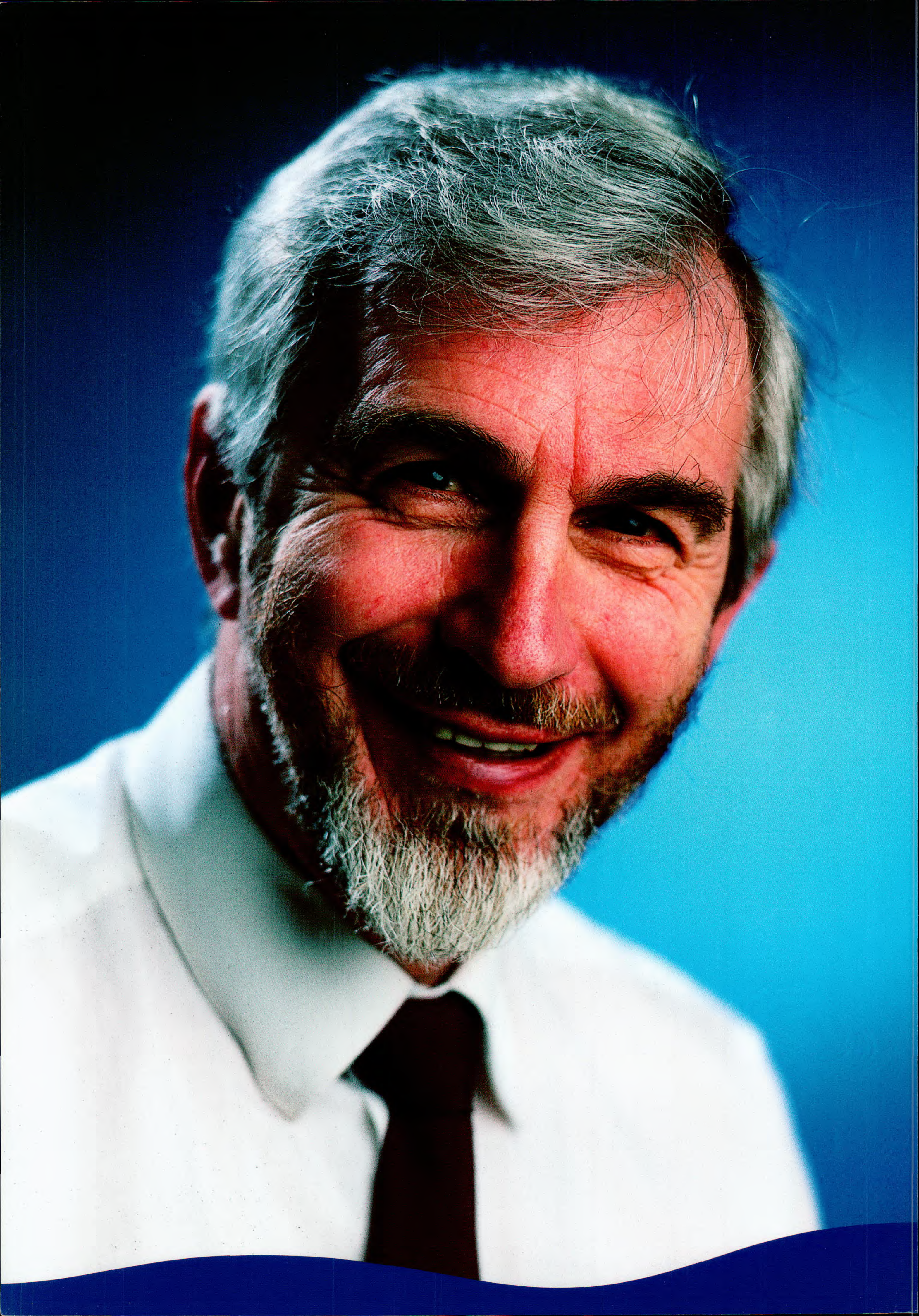

Chief Scientist's introduction

The past year has again seen many successes in the scientific and technical development of the Met Office. In particular, significant progress has been made in numerical weather prediction and climate research. Our New Dynamics scheme, which has been developed over the past few years, has been integrated into our numerical weather prediction models and is now operational. This scheme has greatly contributed to the continued improvement in the numerical weather prediction index, and also provides the scientific foundation for the future development of a high resolution forecasting capability. Our Hadley Centre for Climate Prediction and Research remains at the forefront of climate change modelling, with many pioneering projects under way, including work on the quantification of uncertainty in climate predictions.

High-performance computing is critical to our forecasting ability and, therefore, our business as a whole, so it is with some anticipation that we look forward to switching over to the new NEC SX6 supercomputer towards the end of this year. Its introduction will help us further develop the use of ensemble techniques for both climate and weather prediction, and its additional computing power will also be essential for developing very high resolution forecast models to improve the prediction of severe weather events.

By the end of 2003, the majority of Met Office staff will have relocated to our new building in Exeter. Such a large-scale move inevitably provides many challenges for our organisation, both from a technical point of view and for our staff on a personal level. Preparations are, in both cases, well under way and our drive towards relocation is progressing well. Our move also provides many new opportunities, such as an improved computing infrastructure and new working environment. In particular, we hope that this will lead to improved communication within the Office and a greater synergy between the different parts of our business.

John Mitchell, Chief Scientist

"On a day-to-day basis, I'm working with other Board Members and those in the Research Process to develop our science strategy and see that it is implemented. I enjoy the combination of being involved in state-of-the-art science and demonstrating to people the importance of having a world-class scientific foundation for our products."

Chief Executive's overview

Success in the front line

As I write this brief overview for 2002/3, the Met Office is fully engaged in supporting UK and coalition forces in Iraq. Staff from our Mobile Met. Unit (MMU) are in uniform, based in Kuwait or at the front line, serving in very difficult conditions. Preparing forecasts while being constantly interrupted by air-raid warnings is difficult enough, but, with the added threat of gas or chemical attacks, the task becomes truly daunting. I thank them for all that they are doing and acknowledge the disruption and concern it causes their families.

Of course, success in the front line requires the support of many other teams across the Met Office, including developers, forecasters, support staff and communication staff. Together they have delivered the goods and have considerably enhanced the Met Office's reputation within the Ministry of Defence, the armed forces and the wider coalition community. This is the Met Office at its best, and I offer my congratulations to everyone involved.

Making the most of the weather

Turning to the weather in 2002/3, the winter months again saw floods, road chaos and storm damage to businesses and domestic properties. Even though we successfully forecast these events well in advance, there were still fatalities and substantial losses to business. We are now working with a range of customers to see what measures can be taken to mitigate the worst effects of the weather and to manage the residual risk. Our overall aim remains to enable our many customers to make the most of the weather and achieve their desired outcomes.

A challenging year

The past year has been a difficult trading year for the Met Office, and the signs are that 2003/4 will be just as difficult. While we have made further substantial improvements in our forecasting accuracy and in the quality of the services we provide to our customers, we have not had the same success in reducing our operating costs and increasing our revenue. For the first time since we became a trading fund, we will miss our annual efficiency target,

Peter Ewins, Chief Executive

"As Chief Executive, I am personally accountable to the Secretary of State for Defence for the efficient and effective management of the Met Office. Together with my Board, I formulate the strategy for developing the business and maintaining its scientific reputation and international status. I promote Met Office services and look for opportunities to collaborate both nationally and internationally to improve upon them."

although we remain well ahead of our long-term target. We will, therefore, revisit our plans to ensure we still achieve our medium-term cost reduction targets. We have also failed to achieve the expected growth in revenue, and revised plans are already in place to reinvigorate our sales and marketing strategy.

Our commercial contribution, which is a measure of the extent to which our non-government business has helped to offset the cost to the taxpayer, has risen by 12% in 2002/3 compared to 2001/2. In the current economic climate, this is an excellent performance and it is a pity that we have missed the formal target by just £150,000.

Investing in the future

2002/3 has been a year of major investment in our future. We have signed the contract for a new supercomputer — one of Europe's fastest — that will allow us to achieve more-detailed and more-accurate numerical weather prediction, greatly enhancing our weather forecasting and climate prediction capability. Our new Headquarters and Operations Centre at Exeter has already grown from a muddy field a year ago to an increasingly attractive set of buildings. The first computer links have been established and the first of our staff are at work in Exeter, getting everything ready for the rest of us to move, on schedule, later in 2003.

Investment in research and development has continued, with a new formulation for the numerical modelling of the dynamics of the atmosphere coming to successful conclusion and implementation.

All these investments will help to ensure that we continue to be the world leader in weather forecasting and the benchmark for national met. services in Europe.

Moving forward

The theme for this year's *Scientific and Technical Review* and *Annual Report and Accounts* is 'Met Office on the move'. This is not only about our move to Exeter later in the year, important as that is, but it is also about all the other ways in which we are moving forward: into new fields of research, advancing our knowledge of meteorology and the environment, developing new markets, forging new relationships and leading the development of met. services, not only in the UK but also worldwide.

I hope you will be able to take the time to at least browse through our *Scientific and Technical Review*, and that you will pass it on to others who might be interested.

“2002/3 has been a year of major investment to help ensure that we continue to be the world leader in weather forecasting and the benchmark for national met. services in Europe.”

Peter Ewins, Chief Executive, Met Office

Developments in observing of the environment

Surface observing development

A major objective of our observing strategy is full automation of the surface observing networks in the next five to ten years, thus obtaining maximum benefit from the networks both now and in the future.

Camborne trials facility

The move of the Met Office HQ to Exeter means that the trials facility at Beaufort Park will be lost. However, significant investment in the observing site at Camborne has enabled the continuation of detailed instrument and observing techniques studies (Fig. 1).

Figure 1. The observing trials facility at Camborne.

The collocation of surface observations, radiosonde measurements, remote sensing profiles of wind, temperature and humidity, and a Baseline Surface Radiation Station, creates a very powerful operational observing tool that can be used for instrument studies that were not possible at Beaufort Park. The Camborne facility now forms an important part of the developers' tool kit, as any new observational technique requires a benchmark to be judged against.

Observations automation

The rollout of surface observing automation is progressing. The focus this year has been on the provision of consistent performance from the new measurement systems across the observing networks. Consistency tests for present weather and laser cloud-base recorders (LCBRs) have been established. This important element of verifying sensor performance is key to ensuring that all sites equipped with the new instrumentation are performing at their optimum level. It also ensures that we can monitor the quality of their output. Any deterioration in quality is very quickly identified and can be swiftly addressed, often in conjunction with the manufacturers.

SAMOS enhancements

The Semi-automatic Meteorological Observing System (SAMOS) forms the backbone of the UK observing network, with over 100 of the 150 routine synoptic observing stations in the UK using this system. The latest version was installed at all sites, including civil aviation stations — such as Heathrow and Manchester Airport — that were still using the legacy version of SAMOS. Even St Helena, the most remote of the Met Office-managed sites, was upgraded during the autumn. A common observing platform helps minimise the costs of network management, as well as providing a consistent performance level across the network. To further automate the observing process at aviation stations, we have developed a meteorological condition alarm to draw attention to significant changes in key meteorological elements, such as a change in cloud base or the surface temperature falling below freezing. The introduction of this tool will be an important step towards the automation of all observing at airfields.

Tim Oakley, Remote Sensing Team Leader

"I'm responsible for developing automated instruments, and testing new measurement and software processing techniques, with the aim of providing high-resolution upper-air data to forecasters and for use in our numerical models. Leading the wind profiler team, we've been making tropospheric systems operational and have just installed a new wind profiling radar on South Uist in the Hebrides, Scotland."

Humidity measurement

Humidity is a basic parameter that is measured at every synoptic station in the UK. The current basis for this measurement is the psychrometer, which is a combination of dry- and wet-bulb thermometers. Although this technique has served the Met Office well, the high maintenance requirement and the potential for gross error (if not correctly maintained) make it no longer suitable as we move towards full automation. Although sensors that measure relative humidity directly are available, they have always been seen as a back up to the psychrometer. We are carrying out a review of the latest technology to determine the most appropriate method for humidity measurement in future. Most modern sensors measure the capacitance change as water molecules are absorbed onto a thin polymer film. Such a method is sufficiently accurate for our requirements but is susceptible to contamination. The effect of this contamination on the measurement is apparent at observing sites that experience salty coastal air or the presence of aviation fuel exhaust. These contamination effects form part of the review.

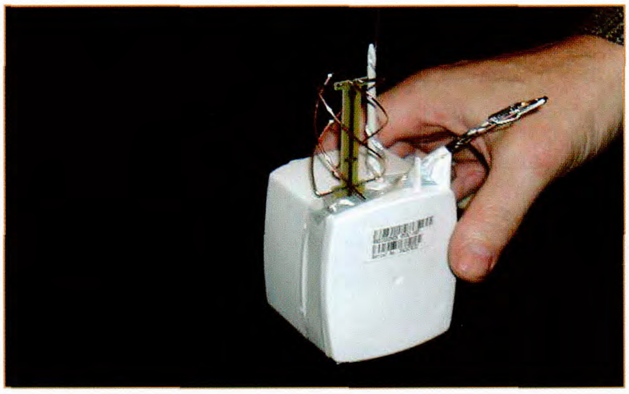

Figure 2. Prototype of the next-generation Vaisala RS92 radiosonde.

Cloud cover measurement

Although a significant improvement in our automated cloud cover measurement capability has been achieved with the introduction of a new type of LCBR, there are still weaknesses in cloud-cover measurement in certain circumstances. The cloud has to be directly overhead for the LCBR to make the measurement and no integrating algorithm, no matter how sophisticated, will produce the correct cloud cover measurement if the cloud is not overhead. However, a new technique using a combination of LCBR integration and whole sky infrared measurement by a pyrgeometer has been developed for possible use at sites where the traditional LCBR method is known to underperform. The development of this technique is the first step towards production of the Cloud Cover Arbiter.

Ground-based upper-air observing systems

We are continuing work on ground-based observing systems in order to meet the ongoing requirement for accurate measurements of wind, temperature and relative humidity at a better vertical resolution than can be achieved by current satellite systems.

New generation of radiosondes

During the past year, we have performed prototype testing on a new generation of radiosondes (weather balloon systems) in collaboration with the manufacturer (Fig. 2). The radiosonde will transmit over a narrower bandwidth than the current systems and will reduce the radio frequency spectrum required by our operations. The improved signal transmission link will allow smaller batteries to be used in the radiosonde, thus making balloon operations safer. Wind measurements are derived by tracking the movement of the system with signals from Global Positioning System (GPS) navigation satellites. The signals are decoded using a code-correlating receiver in the radiosonde — a change of method by our manufacturer. We expect it to lead to an improvement in the reliability of the GPS radiosonde system. The new radiosonde is controlled by application-specific integrated circuits. These allow more-sophisticated control of the radiosonde sensors. For instance, the heaters used to drive off contamination from the sensing system for relative humidity can be adjusted to cope with the cloud conditions found over the UK. This should result in a significant improvement in the accuracy of our relative humidity measurements.

Wind profilers

The number of sites hosting vertically pointing radars capable of measuring winds (wind profilers) in clear air has been expanded to include South Uist in the Outer Hebrides (Fig. 3). The development system, temporarily installed in August 2002, will be replaced by a new operational system operating at longer wavelengths. This will allow winds to be measured continuously up to a height of 12 km in all weathers and will complement the upper-wind monitoring of the Mesosphere-Stratosphere-Troposphere wind profiler, Aberystwyth, and a similar profiler operated near Paris by Météo-France.

Figure 3. Antenna installation for 64 MHz tropospheric wind profiler on South Uist.

Water vapour measurements from GPS signals

We have made a start in building up a network of sites where integrated water vapour can be measured from the reception of GPS navigation satellite signals. This work depends on strong collaboration with a number of universities and Government agencies. The UK real-time ground-based GPS water vapour network consists of 17 receivers operating remotely, with automated contribution of hourly data to the national archive at the Institute of Engineering and Space Geodesy at the University of Nottingham. Eight of these receivers have been deployed. The GPS data are also forwarded to the real-time demonstration network of the European programme COST-716 so that development work on assimilating the measurements into numerical forecast models can continue. This network is expected to reveal information about the smaller-scale structures in water vapour distribution that cannot be resolved by the limited number of weather balloon ascents in a day.

Microwave radiometer and cloud radar

We are carrying out investigations into the use of a 12-channel microwave radiometer for measuring temperature, water vapour and cloud properties from the surface up to about 4 km at high temporal resolution. The radiometer was set up at Camborne in February 2002, and has operated very reliably. However, we found problems with the calibration and scanning cycle of the system, but the manufacturer has responded quickly to revise the software. The radiometer now retrieves profiles of temperature, humidity and cloud every two minutes using a neural network algorithm (Fig. 4).

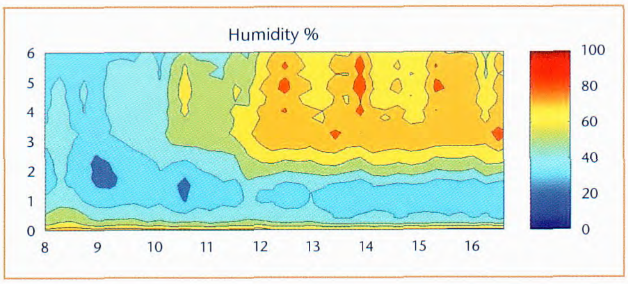

Figure 4. Time series of humidity measurements at 15-minute temporal resolution, from the Microwave Radiometer (16 May 2002, Camborne).

We are developing a variational assimilation technique to use radiance data from this instrument directly in mesoscale numerical weather prediction (NWP) models and to combine these with data from active sensors (wind profilers, ceilometers, cloud radars) to enhance the vertical resolution of the resultant profiles.

We have made progress in testing a prototype, vertically-pointing 78.2 GHz cloud radar, developed by the Space Science and Technology Department of the Rutherford Appleton Laboratory (Fig. 5). This cloud radar is designed to be relatively cheap to manufacture and operate, and has good potential for measuring fog depth and multiple layers of cloud.

Figure 5. Deployment of the cloud radar at Camborne, with the microwave radiometer visible in the background.

Satellite observing systems and weather radar

Making effective use of the information from the new series of satellites is a key component of our observations strategy. We are also making fundamental changes to the way rainfall products are generated from weather radar data.

Meteosat Second Generation

The first of the new series of Meteosat Second Generation satellites (MSG-1) was launched on 28 August 2002. Compared with first generation Meteosat, which went into operation in 1978, MSG's principal imaging instrument, SEVIRI, is a major advance in terms of spatial sampling, frequency of coverage, number of spectral channels and radiometric accuracy. From 2003 until at least 2014, the series will provide greatly improved products to support nowcasting and very-short-range forecasting, including the monitoring of severe storms and fog. It will contribute to short- and medium-range NWP through improved cloud-tracked winds and will also provide environmental monitoring, including detection and tracking of volcanic ash.

Re-engineering the radar data processing chain

The changes to the processing of radar data are aimed at delivering improvements in the accuracy of surface rainfall estimates, product timeliness, and providing the capacity to process data from a much larger number of radars in continental Europe.

The main structural change achieves a greater centralisation of the processing, which is currently distributed between three systems: the 'Cyclops' computer at the radar sites, 'Radarnet III' and 'Nimrod' workstation-based systems at Bracknell (Fig. 6 (a)). We are now developing a new 'Radarnet IV' system, which is designed to receive raw radar data from Cyclops and

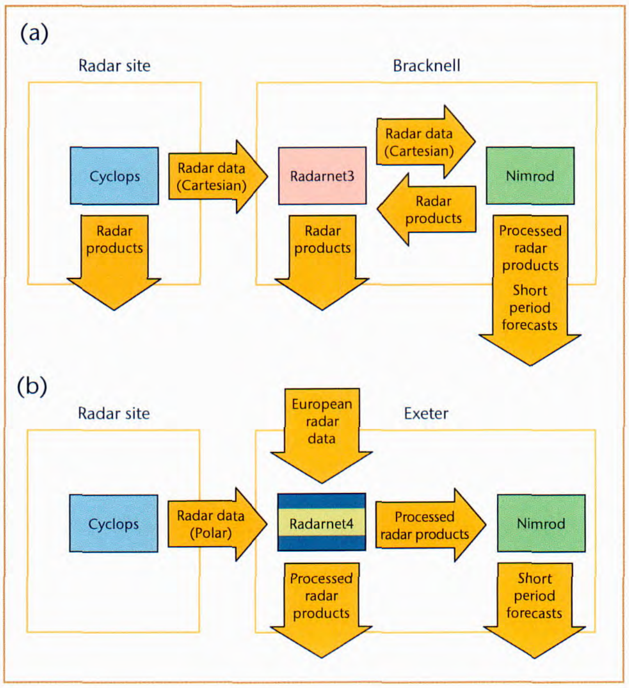

Figure 6. Radar data processing chain (a) as at 2003, (b) re-engineered chain to come into operation in 2004.

generate all the required radar-based rainfall products (Fig. 6 (b)). The Nimrod system will then focus on the generation of forecast products.

The raw data transmitted from the radar sites will be in polar co-ordinates, rather than the Cartesian format used at present. Access to these raw polar data presents opportunities for improving the quality control and correction algorithms that convert the radar measurements into estimates of surface rainfall. As the polar format data are much larger in volume, this change has only been made possible by development of the new Met Office wide-area network, MORSN. The scientific development of new algorithms is proceeding in parallel with the Radarnet IV system development. We have produced new clutter-discrimination methods in-house (ref. *Scientific and Technical Review 2001/2*) and work on relating radar measurements aloft and rainfall at the ground has been contracted to the University of Reading.

Climatological data

Gridded climate statistics, derived from conventional observations, are now available for the UK for each month from January 1961 to December 2000 for each of 26 weather parameters, such as temperature and rainfall (Fig. 7). These data sets, produced in association with the UK Climate Impacts Programme, can be downloaded for research purposes, free of charge, from the Met Office web site at www.metoffice.com/research/hadleycentre/obsdata/ukcip/index.html. The data sets have been used to generate a consistent set of monthly statistics for the UK, its constituent countries and various regions.

As part of our work to calculate long-term averages, we have developed new software to estimate values for periods of missing data. An estimate is generated for an observing site using available data from several neighbouring sites. The relationship between the target site and each neighbour is obtained by using regression analysis of the period when both sites have data. Neighbours are selected according to the level of correlation during the period of overlap.

To meet the increasing demand for real-time assessments of exceptional weather, we have enhanced our historical archive of noteworthy weather events. The information is now contained in an Oracle database and a new intranet-based search facility provides users with interactive access.

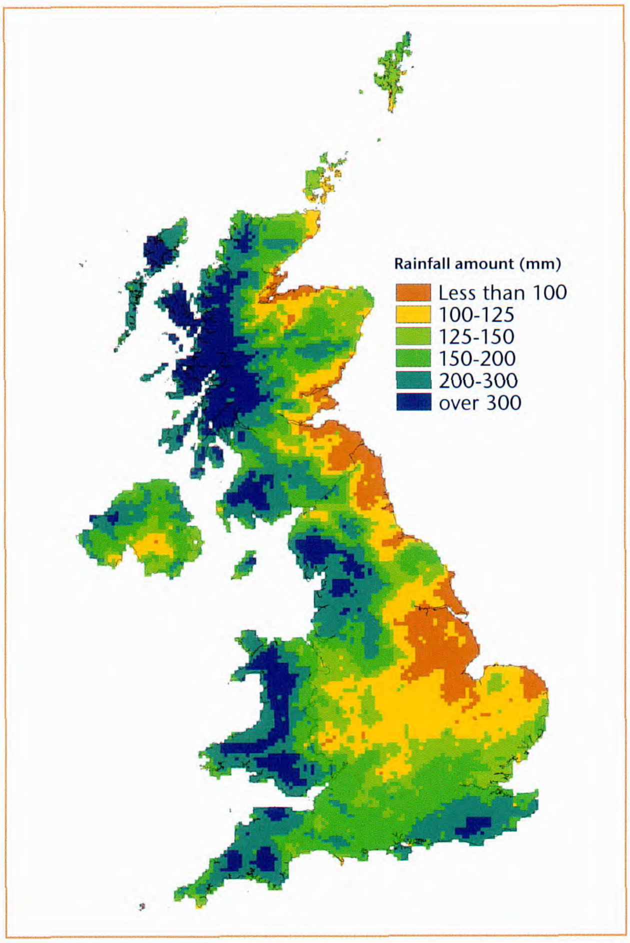

Figure 7. 5-km UK-gridded rainfall for October 2000.

High-performance computing in numerical modelling

Why do we need more power?

The Met Office's supercomputer facility lies at the heart of our Numerical Weather Prediction (NWP) and Climate Research and Production processes. Our position amongst the world's best demands a powerful computing facility. However, our twin Cray T3Es are underpowered for the research and development we now wish to do. As a result, we are replacing them with an SX-6 system built by NEC — one of the most powerful supercomputers in the world.

This will enable us to deliver the improved NWP forecasts and climate predictions required by our customers. Key components of these plans are as follows.

- Tackling the main forecast problems associated with fog, low cloud and heavy precipitation. To properly resolve some of these features requires a substantial increase in resolution, particularly for local area regional models where the primary benefit to customers will be obtained. This can be expensive — for example, doubling the resolution requires sixteen times more computational power.
- Increasing the resolution and complexity of our Production Climate model and providing the opportunity to explore more climate scenarios and quantify the climate uncertainties in greater detail.
- Increasing the sophistication of numerical schemes and physical parametrizations. Our success in improving predictions of fog, low cloud and precipitation depends on increasing the complexity of our modelling of the moisture processes. In a climate context, the models are becoming even more complicated — for example, we are introducing a chemistry sub-model to simulate important climate feedback mechanisms.
- Coping with the ever-increasing data volumes flowing from next-generation satellite observing systems. At present, cost constraints mean we use only a small subset of available data. Higher-resolution models require more observations.
- Implementing four-dimensional variational data assimilation, which has had proven benefits at other met. centres, but is substantially more costly than our current 3D analysis. We hope to reduce the frequency of poor forecasts attributed to misanalysis.

About the NEC SX-6

The basic building block of the SX-6 system is the NEC-designed vector processor, which has a theoretical peak performance of 8 Gflops.

Eight processors form a node, all sharing a single 32-Gbyte shared memory. The Met Office's SX-6 will be split into two 15-node clusters, with each cluster residing in a separate computer hall to enable maximum resilience for our operational services. The combined 2-cluster SX-6 will have a total peak performance of 1.9 Tflops with a total memory of near 1 Tbyte (Fig. 8).

Connected to the clusters is the TX-7, a 24-processor front-end system, which acts as the host controller, allowing all the processors to have a consistent view of a single shared file system. Each input/output request from a processor is routed to the TX-7, which will then forward it on to the appropriate disk controller via a fibre-channel switch. The disk system will be distributed between the two computer halls, allowing access to all file systems from both halls, with key file systems mirrored between the two halls for operational resilience. The TX-7 will also be used for compiling codes, executing the Unix control scripts and communicating with other systems.

Robin Pallister, Supercomputer Support Manager

"Our supercomputers are vital for delivering accurate and timely weather forecast and climate predictions. After procurement, installation and acceptance of the new supercomputer, my job is to run the system from acceptance until it's decommissioned. I have to deliver a reliable service, liaising with both the suppliers and internal users to ensure that their requirements are understood and met."

Figure 8. 2-cluster SX-6

Transition to the SX-6

Installing the hardware

The installation is being staged, enabling us to both phase the development and implementation during the transition to Exeter and benefit from new, cheaper hardware that will be available later next year (Table 1). The final system, available in early 2005, will provide an increase of 12.5 times over the current combined T3E machines. The first SX-6 machine at Exeter will go through a period of acceptance testing during Autumn 2003 in readiness for operational use early in 2004.

Moving the application codes

Ten years ago, the Met Office had a shared-memory, modestly parallel vector Cray C90 supercomputer. Five years ago, we moved to the opposite end of the spectrum after the acquisition of a scalar, distributed-memory, massively parallel Cray T3E. The NEC SX-6 can be considered as a fusion of the architectures of the previous two supercomputers. A single SX-6 node is similar to an entire Cray C90. The transition from Cray C90 to Cray T3E was radical and entailed a major development effort to use a distributed-memory architecture. This time, the transition from a Cray T3E to the NEC SX-6, will be an easier process.

The major application codes, and particularly the Unified Model (UM), have been deliberately designed and developed with portability in mind, so the basic transfer of the codes to the SX-6 should be straightforward.

Date	Location	Description	Total power (cf T3Es)
January 2003	Bracknell Headquarters	4-node SX-6 system for software migration	x 0.8
July 2003	Exeter Headquarters Computer Hall 'B'	15-node SX-6 system available for use	x 3
August 2003	Exeter Headquarters Computer Hall 'A'	15-node SX-6 system available for use	x 6
January 2005	Exeter Headquarters Computer Hall 'A'	15-node 'SX-6 successor' available for use	x 12.5
January 2005	Exeter Headquarters Computer Hall 'B'	Combine the two 15-node SX-6 systems into a single 30-node SX-6 system	x 12.5

Table 1. Timetable of SX-6 installation during transition to Exeter.

Optimising the application codes

Once the basic transfer is achieved, the next stage is to make the codes run faster. The benchmark version of the UM reached an acceptable level of performance after less than 0.5% of the code was revised. With half a million lines of code, this remains a substantial task.

As the UM code was originally developed for the Cray C90, the data structures and general loop constructs are still appropriate for the SX-6. Some later codes were not written for vector machines, so more work is required to adapt them, for example making 'do' loops suitable for vectorisation.

Challenges

In the longer term, there are a number of areas where we will be looking to make further optimisations, such as input/output, communications and parallelisation. At present, the Cray T3E deals with all aspects of running a model suite. In future, the SX-6 will do the numbercrunching task it is best suited to, while its TX-7 front end will deal with running control scripts and compilations. We may need to make some substantial changes to enable proper integration of the front-end system with the supercomputer. As a result, we are also likely to need a more complicated job scheduling system.

Some early performance results

Figure 9 shows the performance measurements taken during the benchmarking process for the global forecast model run at a higher resolution, shown relative to the same code running on a similar fraction of our T3E.

Two lines are shown that demonstrate the effect of using different decompositions (how the work is partitioned across the processors). The upper (higher performance) line shows results from running the code with a one-dimensional decomposition, only decomposing in the north/south dimension. Here, we obtain a six-fold increase in computational speed, relative to the T3E for the same percentage of machine usage. The lower line (lower performance) shows results when running with a two-dimensional decomposition (using two processors in the east/west dimension and a variable number in the north/south dimension). This early result demonstrates that a simple transfer of codes may not achieve optimal performance.

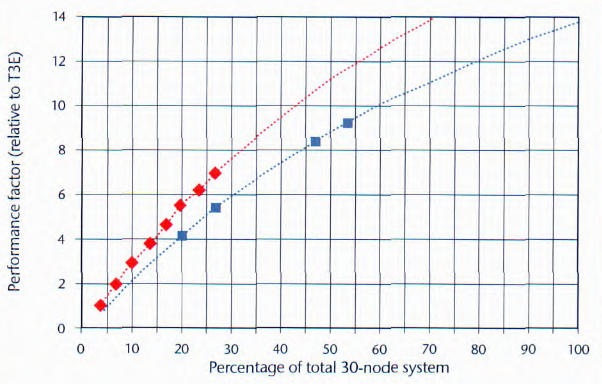

Figure 9. Performance measurements taken during the benchmarking process for the global forecast model run at a higher resolution, shown relative to the same code running on a similar fraction of our T3E.

Forecasting

Nowcasting

During 2002, the Met Office's nowcasting capability, which is based on the well-established Nimrod system, was expanded to include three separate domains. The principal domain continues to cover the UK and surrounding waters with a 5-km grid and an hourly update cycle for most products. In September, the 2-km GANDOLF precipitation system was implemented operationally across England, Wales and southern Scotland, primarily to support flood forecasting. Then, in December, we implemented an expanded 5-km grid domain across Europe (EuroNimrod). The latter domain benefits from recent progress in the exchange of radar data amongst European countries. Figure 10 shows an example of a 15-minute precipitation accumulation forecast for the EuroNimrod area.

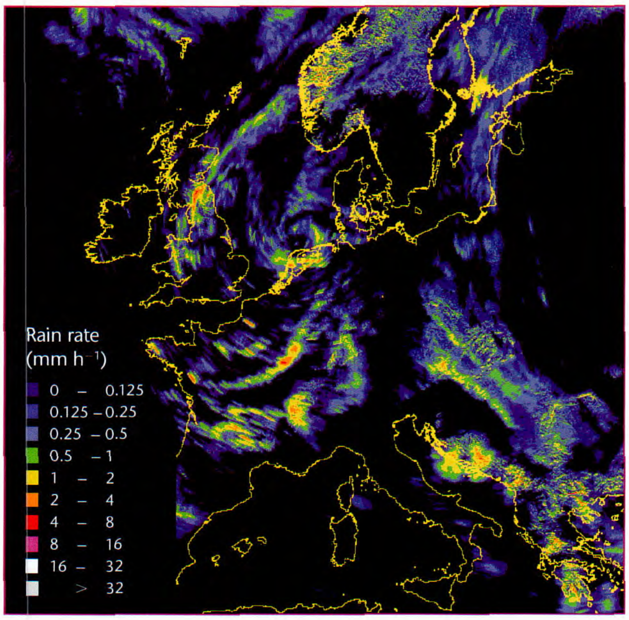

Figure 10. One-hour European Nimrod forecast of rain accumulation (15-minute accumulation period) for 1600 UTC on 22 January 2003.

GANDOLF upgrade

In September 2002, as part of a major upgrade, we introduced a new advection algorithm into the GANDOLF precipitation nowcast scheme. This algorithm is based on a solution of the Optical Flow Constraint (OFC) equation, widely used in the computer animation industry, and has a number of advantages over other widely used schemes. These include avoiding having to identify contiguous rain areas, and application of a field constraint that generates realistic advection velocities while minimising errors in regions with sparse data and at domain boundaries. Figure 11 shows a comparison between the old scheme and the OFC

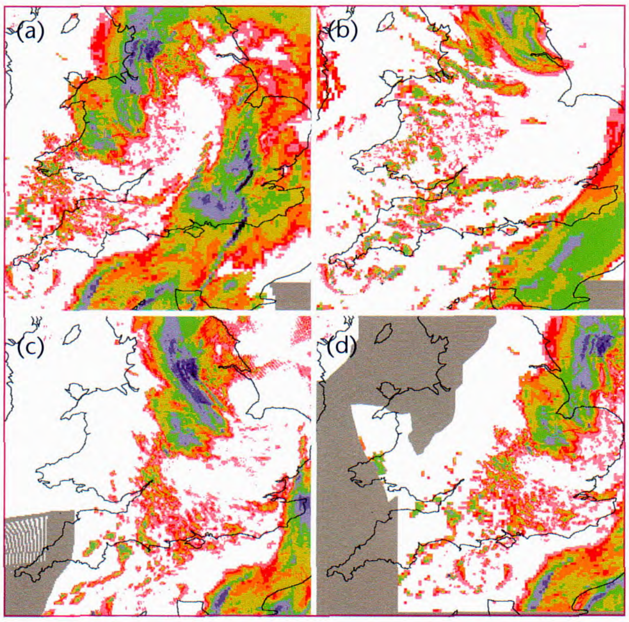

Figure 11. GANDOLF nowcasts for 30 October 2000. (a) Observed precipitation distribution at 0645 UTC, (b) observed precipitation distribution at 0945 UTC, (c) GANDOLF OFC three-hour forecast for 0945, (d) old GANDOLF three-hour forecast for 0945. Grey areas are missing data.

Clive Pierce, Precipitation Forecasting Scientist

"I am based at the Joint Centre for Hydro-Meteorological Research in Oxfordshire. My work is an exciting mix of applied research in short-range rainfall prediction and the design of computer-based systems for automatic forecasts of rainfall at short range. I'm currently working on a Nimrod rainfall forecasting system in Poland for their Institute of Meteorology and Water Management."

scheme for a case when passage of a deep depression over northern England resulted in localised flooding on 30 October 2000. The precipitation area over northern England, near the centre of the depression, remained almost stationary during the three-hour period between Figs 11 (a) and (b), while the cold front over southern England moved rapidly south-east. The forecast from the OFC scheme (Fig. 11 (c)) captured this difference more successfully than the old scheme (Fig. 11 (d)).

Polish Nimrod

Following the devastating floods of the rivers Odra and Vistula in July 1997, a major infrastructure development project was initiated in Poland, with World Bank funding, to mitigate the impact of future severe flooding events. The Met Office is providing a version of Nimrod, configured for Poland, to the Polish Institute of Meteorology and Water Management (IMGW) in Warsaw as a component of the Hydrological and Meteorological Monitoring and Forecasting System (SMOK). Figure 12 shows a test rainfall forecast from the Polish Nimrod system, carried out prior to delivery using historical data.

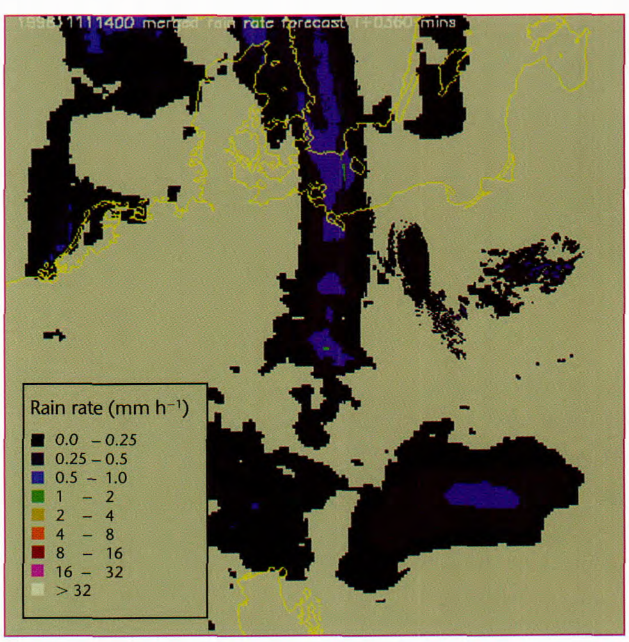

Figure 12. Six-hour forecast of rain rate for 1400 UTC, 11 November 1998, produced by Polish Nimrod.

Cloud-top height

A critical component of much Nimrod processing is the cloud-top height field, which is diagnosed principally from Meteosat infrared imagery. It has been known for several years that the diagnosis scheme occasionally assigns low cloud to the mid-troposphere due to a combination of biases in the brightness temperature seen by the satellite and deficiencies in the model representation of low-level inversions. To overcome this, we have carried out a major revision of the code, from the perspective that the model is much more likely to correctly estimate the height of a stable layer than its temperature. As a result, we have achieved substantial improvements in the height assignment of low cloud and fog. Figure 13 shows an example where low cloud

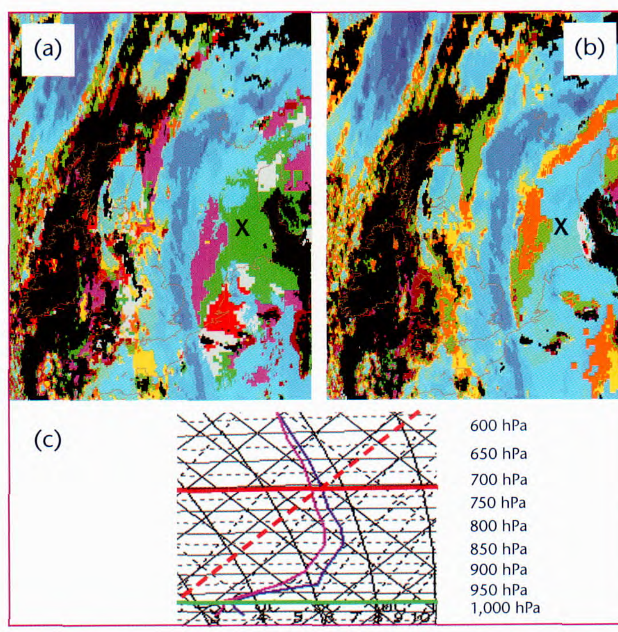

Figure 13. Nimrod cloud-top height maps derived from Meteosat IR imagery for 1030 UTC on 12 February 2003, for an area covering the British Isles, the North Sea and the low countries. Cloud-free areas are black, high cloud tops are in blue shades, and low cloud tops are in red, grey, green and purple as height increases. (a) New scheme, (b) old scheme, (c) tephigram showing cloud-top height derivation — blue line: model temperature; purple line: model brightness temperature; red dashed line: satellite brightness temperature; red solid line: old cloud top; green line: new cloud top. The location of (c) is shown by a cross in (a) and (b).

and fog over the southern North Sea, near Denmark, have been diagnosed at a much lower height by the new scheme. Figure 13 (c) shows the relationship between the old and new cloud-top heights in this area to the model temperature profile. The height indicated by the old scheme is not only too high, but is also inconsistent with the presence of stratiform cloud.

Wind nowcasts

The wind nowcasting scheme in Nimrod is an important source of information for inshore waters forecasts and hazard warnings for severe winds over land. It is formulated to extrapolate deviations from the mesoscale model surface-wind forecast, assuming that they propagate with the model wind. Unfortunately, part of the deviation arises from the influence of local topographic effects, unresolved by the model, which are stationary. A new representation of the influence of local topography, based on the linear theory of flow over hills, has been developed to allow the separation of these stationary and propagating signals. Figure 14 shows how the adjustment scheme (Fig. 14 (a)) improves the representation of winds over the high ground, relative to the raw model output (Fig. 14 (b)). The improvement is summarised by a comparison with the observations in Figs 14 (c) and (d).

More sophisticated models of the impact of topography on wind flow have been under development for several years. Experiments with the Unified Model (UM), run at very high resolution, have shown that it can successfully reproduce the observed wind maximum associated with north-easterly winds through the Strait of Dover. Over the past year, our collaborative work with Leeds University has shown that a simpler model, called 3dVOM, developed for simulating orographic lee waves and rotors, can also reproduce this feature. A comparison of the simulations by the two models is shown in Fig. 15.

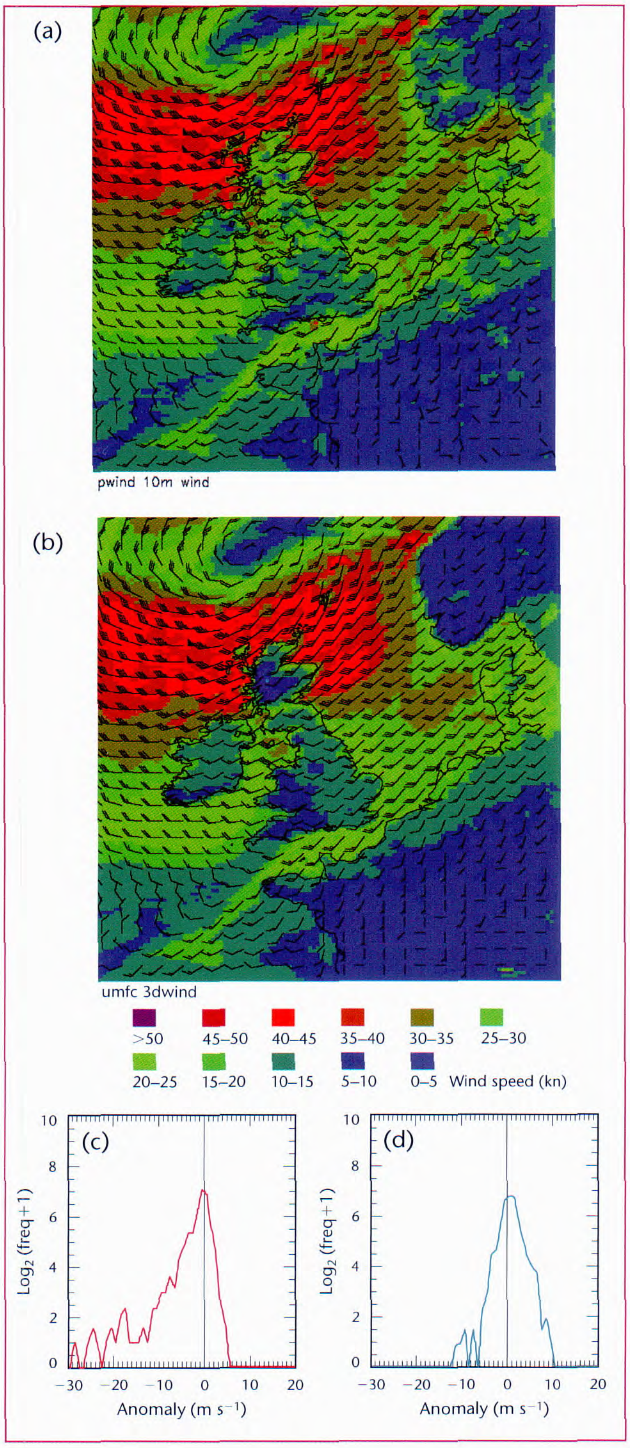

Figure 14. Nimrod wind speed and direction for 1200 UTC on 15 January 2003. (a) From the mesoscale model after topographic adjustment, (b) raw mesoscale model output, (c) graph of observation–model differences from the raw model output, (d) graph of observation–model differences from the adjusted model output.

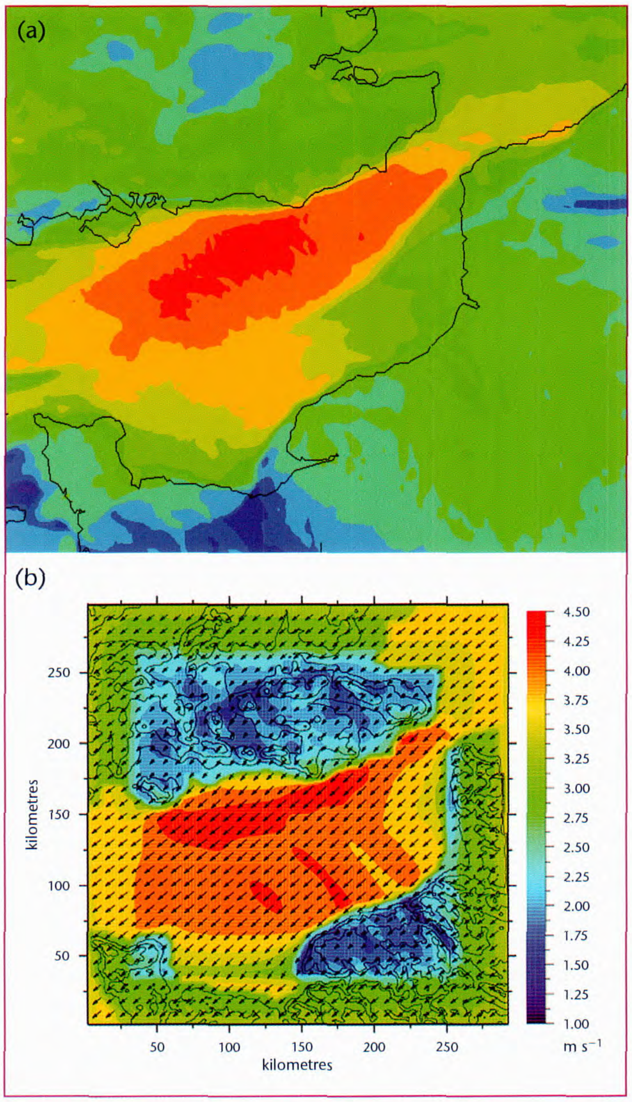

Figure 15. Simulation of wind flow through the Strait of Dover on 23 July 2000 using (a) a 2 km-resolution version of the UM, (b) the 3dVOM model.

Man–machine mix

Over several years, we have progressively moved from manual forecasting methods to more automated techniques. While much production is now done automatically, forecasters still add important value to forecasts. A key strand of our forecasting strategy is to 'change once, use often' by adopting a central quality control of numerical weather prediction (NWP) output using Fields Modification (FM). FM makes it possible to 'correct' data streams before they are transformed into a variety of products. This ensures that the process of issuing guidance and adding value to products is made as beneficial and efficient as possible. Field modification will:

- deliver consistency throughout a range of outputs;
- allow our guidance forecasters to make significant changes on those rare occasions when the model products are seriously in error;
- have the potential to substantially increase the efficiency of the production process.

A good example of the power of this technique is demonstrated by the events of 15 October 2002. Figure 16 shows the T+36 forecast from the global run of the UK model with a shallow low close to the Netherlands at 1200 UTC on the 15th. However, there was a good signal from the European Centre for Medium-range Weather Forecasts (ECMWF) ensembles of a more vigorous development and this was supported by a variety of deterministic solutions from other centres. Also, the satellite picture at 0200 UTC on the 15th indicated a developing cloud head with dry intrusion to the west of Spain, symptomatic of vigorous cyclonic development. Using this information resulted in the guidance forecaster issuing a forecast that was very different from that produced by the model (Fig. 16 (a)). The analysis at 1200 UTC on the 15th (Fig. 16 (c)) shows a vigorous low close to south-west England. The forecaster had correctly predicted the general development and depth of the low, and issued timely warnings to emergency authorities of heavy rainfall and gales in coastal areas.

This has revolutionised the guidance issued from our operations centre. During October 2002, the production and delivery of Met Office guidance changed from being a text product delivered to customers at fixed times, to an intranet-based graphical product that is available at all times. This new guidance:

- introduces the modification of key model fields, such as cloud and precipitation, to produce graphical output better at reflecting the perceived short-range evolution;

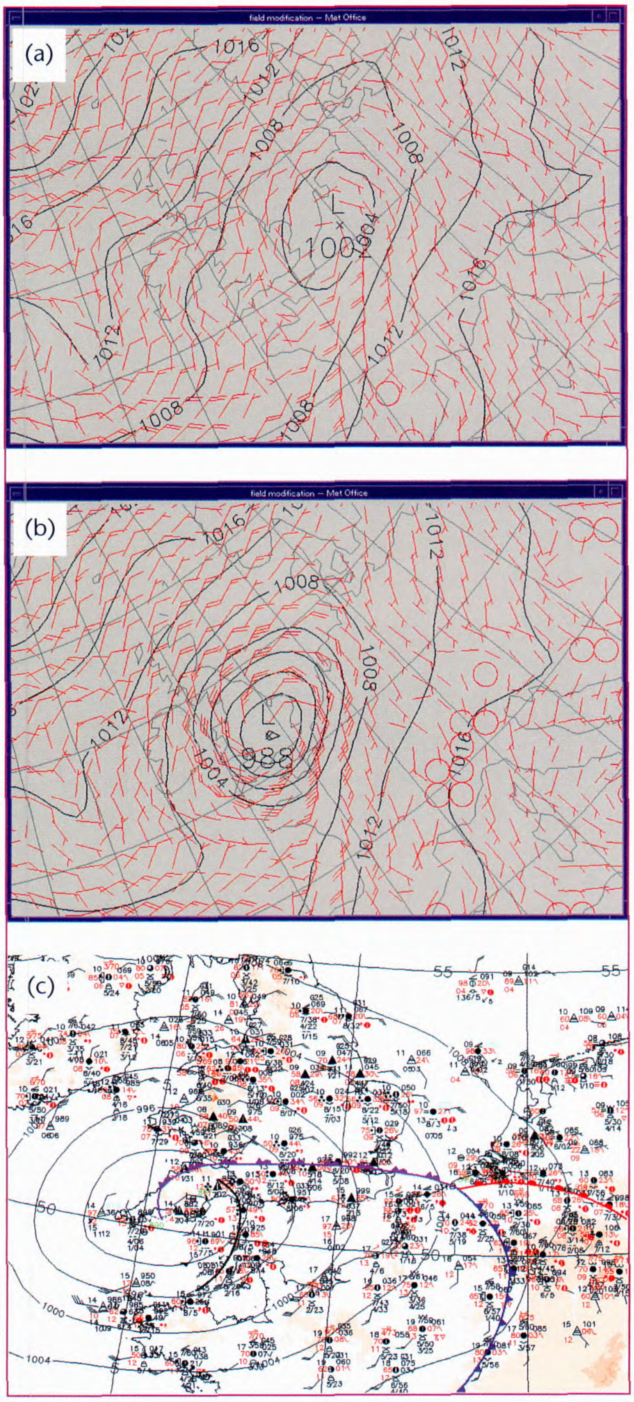

Figure 16. Forecasts for 1200 UTC 15 October 2002. (a) 36-hour model forecast, (b) modified forecast, (c) manual analysis.

- provides guidance that has a substantially higher information content, enhanced by the use of graphical output;
- provides graphical products that will become a common source of information for many users, including regional offices and TV companies, significantly enhancing the service we offer.

Medium-range forecasting

Forecasting the weather with numerical models involves significant uncertainty due to the strong sensitivity of the forecast to small errors in the initialising analysis. This uncertainty is particularly important when forecasting several days ahead and in potential severe weather situations. To help assess this uncertainty, we use output from the Ensemble Prediction System (EPS) run by the ECMWF. The EPS uses 51 separate numerical forecasts, each started from slightly different initial conditions — the differences are small and are within typical analysis errors.

First-guess early warnings of severe weather

Using the EPS output, we have developed an application to estimate the probability of severe weather to support early warnings, as issued under the National Severe Weather Warning Service. Probabilities of heavy rain, severe gales and snowfall are assessed automatically, and forecasters receive different levels of alert according to the risk, along with appropriate warning messages ready for issue (Fig. 17). Assessment of the system shows that it is often not possible to issue warnings with high confidence, due to the fundamental uncertainty in the forecasts; however, when the system does provide a strong signal, severe weather is correspondingly more likely, and forecasters have been able to issue more timely warnings to customers on a number of occasions, for three to four days ahead.

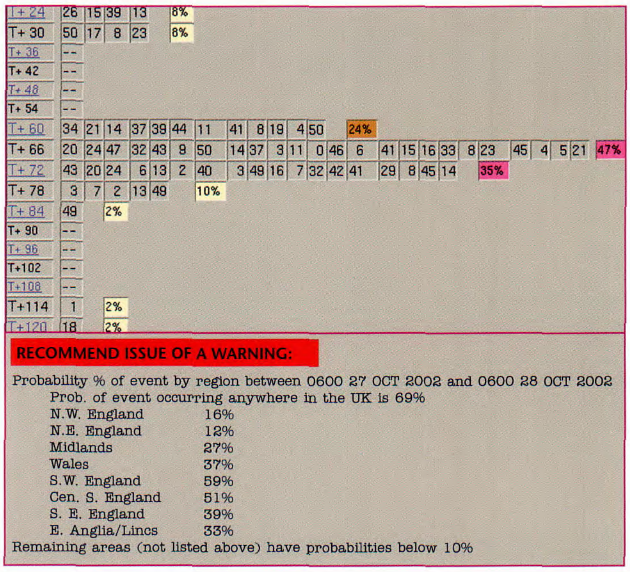

Figure 17. Sample alert from severe weather early warnings system showing a three-day warning of severe gales for the storm that struck southern Britain on 27 October 2002. The top panel gives probabilities each six hours, listing ensemble members so that the forecaster can investigate detail. The lower panel gives a draft warning with regional probabilities.

Probabilities of blocking

Blocking is a phenomenon in which the normal eastward progression of weather systems in the atmosphere ceases, typically due to a large stationary high-pressure system. Blocking can lead to prolonged periods of either fine or unsettled weather, depending on the precise location of the block. Prediction of the onset or decay of blocking is therefore vital for successful medium-range forecasting (three to ten days ahead), but it is often sensitive to small errors, so ensemble prediction is appropriate. Applying research by a Met Office-sponsored PhD student, we have introduced probability forecasts of blocking, including onset and decay, based on the EPS (Fig. 18). The research results showed that the EPS has skill in predicting the onset of blocking up to seven days ahead, and decay up to ten days ahead.

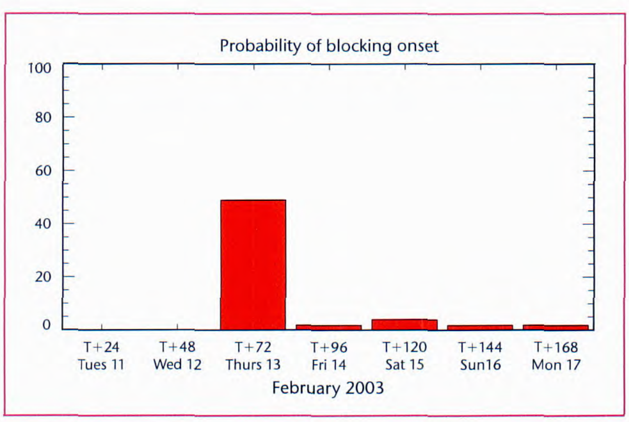

Figure 18. Probabilities of blocking for the Euro-Atlantic area from the EPS. This example shows a high probability of a transition to blocked flow on day three of the forecast.

Evaluation

We are employing a new view on the verification of categorical forecasts, e.g. rain/no-rain forecasts. Instead of looking at the forecast accuracy, which is strongly influenced by the weather itself, we can look at the *benefits* that the model brings to a forecast using climatology. This is done using the odds ratio, which can be interpreted as a product of the odds for getting the rain forecast right and the odds for getting the no-rain forecast right.

For instance, we find that the odds for a successful slight (heavy) rain forecast (Fig. 19 (a)) increase from roughly 1:2 (1:100) from using climatology to 1:1 (1:3) when the Met Office model forecasts such an event. The final odds do not look too impressive due to the rarity of the event, but using the model improves the odds for getting a rain forecast right by a factor of 2 (30). However, this is only half of the story and it is important *not* to neglect the other half — namely to forecast no-rain. The odds for correctly rejecting rain (Fig. 19 (b)) improve from 2:1 (100:1), when using climatology, to 8:1 (200:1) after using the model, i.e. they increase by a factor of 4 (2). Note that the odds for the correct rejection of rain are impressively high, largely due to the abundance of the no-rain event. Finally, in the odds ratio (Fig. 19 (c)), the climatological odds cancel out and it increases from about 10 for slight rain to about 60 for heavy rain. The advantage over a persistence forecast rises similarly.

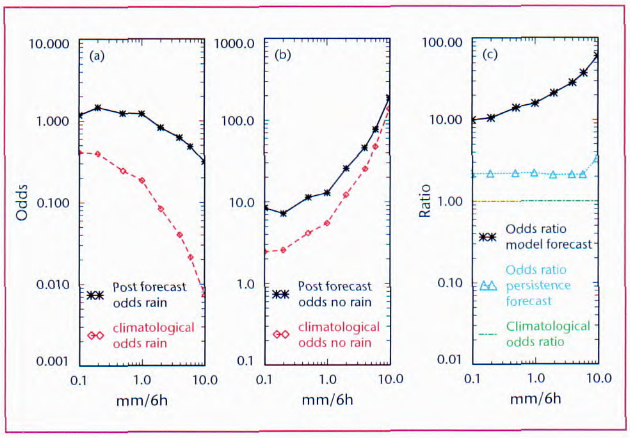

Figure 19. Odds-based verification of six-hour rainfall accumulations against threshold for August 1995 to September 2002. Model forecast results are shown in black, climatology in red ((a) and (b) only) and persistence in blue (odds ratio only). (a) Odds of rain, (b) odds of no-rain, (c) odds ratio.

Aviation services

The Met Office acts as the London Volcanic Ash Advisory Centre and, as such, has responsibility for monitoring and forecasting volcanic ash dispersion for the North Atlantic. We have developed two tools to provide information to forecasters fulfilling this role. One is a product derived from Advanced Very High Resolution Radiometer (AVHRR) satellite imagery to aid forecasters in locating volcanic ash and the other is NAME, an atmospheric dispersion model that predicts the dispersion of the ash. Forecasters monitored an eruption of Mount Etna, which began on 27 October 2002, using these two tools to track and forecast movement of the ash (Fig. 20).

Defence services

A critical defence requirement is to be able to predict what various electro-optical sensors will be able to 'see'. We have made considerable progress in developing a new support tool based on Met Office expertise in radiative and heat transfer modelling. Figure 21 shows an output from the component of this tool that diagnoses the thermal contrast of a target.

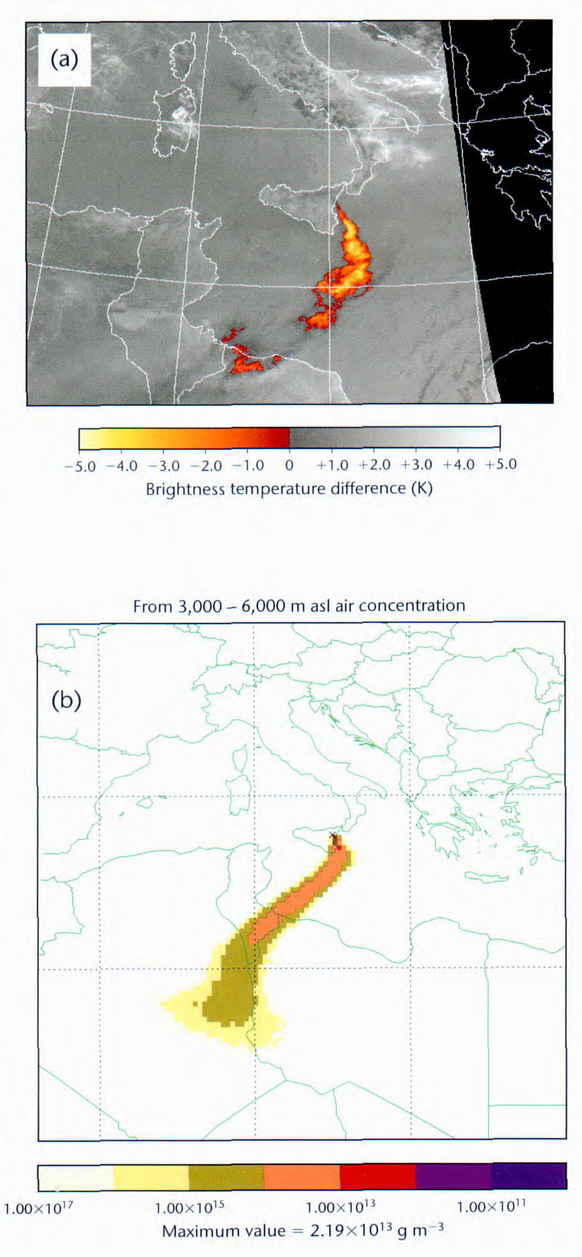

Figure 20. Observed and forecast location of the volcanic ash cloud from Mount Etna on 28 October 2002.
(a) AVHRR image (difference between 10.8 μm and 12.0 μm channels) showing the location of volcanic ash, indicated by the negative values, at 1315 UTC,
(b) NAME output showing the forecast concentration of volcanic ash at 1200 UTC.

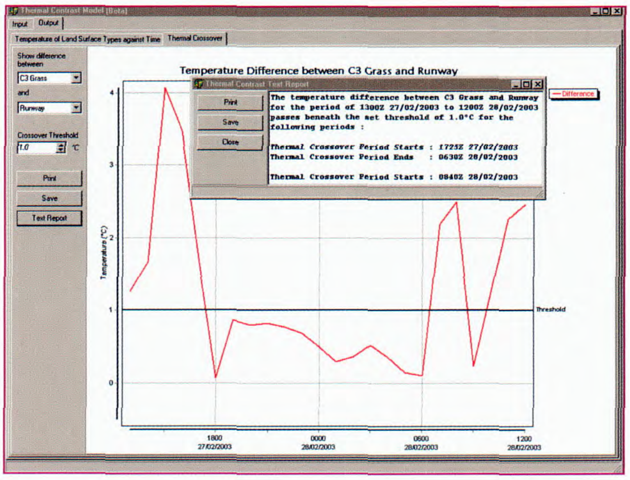

Figure 21. Time series of thermal contrast between grass and runway. Superimposed at the top is a test report that identifies when the temperature falls below a user-specified threshold.

We have also continued to make progress in developing a simple-to-use CD-based global climatology facility for use in defence operations (Fig. 22). Based on a mix of data received in real time, together with data sets obtained through international exchange, the climatologies have been subjected to extensive quality control and post-processing. They now include surface and upper-air data over both sea and land, and have been augmented in data-sparse areas with synthetic climatologies generated for representative locations with the Met Office site-specific model.

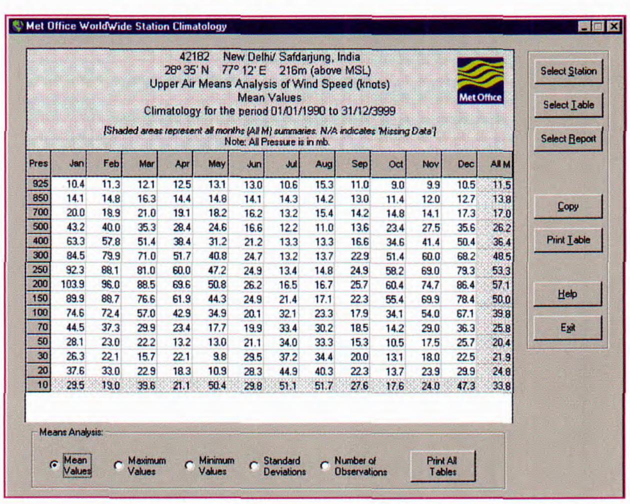

Figure 22. Screen shot from the global climatology CD, showing monthly mean upper-air wind speed for New Delhi.

Commercial services

We have been working in collaboration with GAB Robins to develop weather-related tools for the insurance industry, both to enable quick claims checking, and to provide advance warning of forthcoming peaks in enquiries. The results are being incorporated into GAB Robins' WeatherEYE service. Figure 23 shows a prototype display that depicts forthcoming severe weather by region, using a simple set of coloured indicators tied to user thresholds.

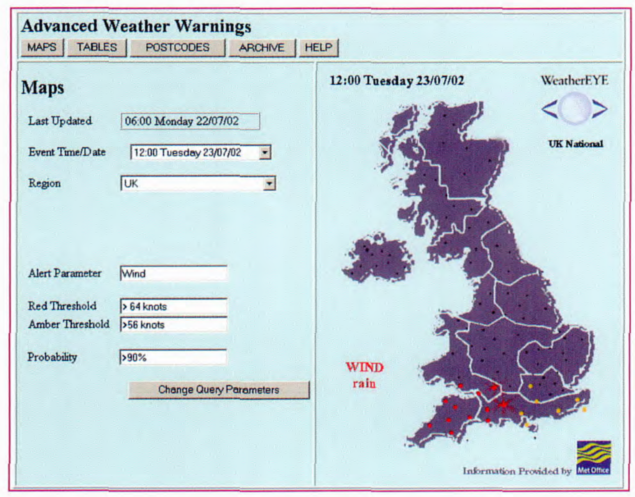

Figure 23. Screen shot of the prototype severe weather display developed with GAB Robins for their WeatherEYE service.

Numerical weather prediction

Over the past ten years, we have seen unprecedented advances in the accuracy of the numerical weather prediction (NWP) that underpins most of the Met Office's business. This comes as a direct result of harnessing increased computer power to improved data from new satellite missions, better numerical algorithms and a more complete representation of the key physical processes in the atmosphere. Our understanding of these processes is founded on more basic research supported by the observational data facilities at the Met. Research Flight based at Farnborough and the Met. Research Unit based at Cardington.

The numerical models used to produce these forecasts are developed within the Unified Model (UM) system, which provides the computational and scientific framework required for both NWP and climate prediction. These models are run at regular intervals throughout the day, to tight deadlines, in order to provide up-to-date forecast information. A global configuration of the UM provides forecasts out to five days ahead and we use a higher-resolution UK regional configuration to provide more-detailed forecasts for the UK for up to two days ahead.

Research is under way into all aspects of the NWP system, with the aim of improving the accuracy of the operational forecasts. A number of areas are singled out for more-detailed discussion in this chapter. Recent developments in the operational formulation of the UM are examined, along with developments in the operational processing and assimilation of satellite data. Looking further ahead, we review progress with ongoing research into the use of very high resolutions and the development of new boundary-layer and convection parametrizations. Finally, we take a closer look at how we use and analyse the information collected by our observational data facilities.

Unified Model

In previous editions of the *Scientific and Technical Review*, we have described our Unified Model (UM) and, more recently, the New Dynamics version. This new version of the model has a non-hydrostatic dynamical core and much-revised physical parametrizations and has been a major component of our research programme over the past five years. Extensive trials of the new formulation, some of which were described in last year's *Review*, demonstrated its benefits over its predecessor. Operational implementation required substantial changes to the suite of programs that provide products to customers in order to adapt to the new grid. After much work by a large team across the Met Office, the new model became operational in late summer.

However, even lengthy trials do not enable us to fully understand the characteristics of a new model. As with all developments, the overall positive signal encompassed some negatives as well as many positives and we have been working to understand and resolve some of the outstanding problems. In the following sections, we describe some new features that have been introduced since the summer, a number of problems that have been resolved and some interesting forecasts.

A new surface exchange scheme

The second version of the Met Office Surface Exchange Scheme, MOSES2, introduces a significant advance in our modelling of the land surface–atmosphere interactions. The changes include an improved specification of vegetation type and coverage, and improved treatment of evaporation and the surface energy balance.

Terry Davies, Numerical Modeller in Dynamics Research
"As an applied mathematician, I help develop and maintain the computer models that are essential to many of the Met Office's activities. We regularly monitor the models and use mathematics, physics and programming techniques to improve them, using some of the most powerful computers in the world. It's very rewarding when we see the forecasts improving!"

This revision gave a substantial benefit in the summer seasons, resulting from a change in the surface energy balance with less sensible heating of the lowest atmospheric layers and more latent heating in the mid-troposphere, due to a moister surface in the semi-arid regions. The impact on forecasts was:

- a reduced warm bias in lower troposphere temperatures;
- a beneficial moistening of the lower troposphere over land in summer;
- a reduced tendency for excessive low pressure over land during summer;
- reduced root-mean-square error (RMSE) in mean sea-level pressure (MSLP) and tropical winds.

The improvement obtained in sea-level pressure forecasts is illustrated in Fig. 24. In terms of geographical patterns, the reduction in the RMSE during the summer is mostly confined to the land regions, with improvements over the central US, North Africa, China and Eurasia. These changes are correlated with a reduction in the negative bias in sea-level pressure and a reduced warm bias in the lower troposphere.

Improvements to tropical convection and model stability

During trials, we noticed a disappointing aspect of the new version of the UM was its relative performance in the Tropics. Occasional numerical and physical instability associated in part with tropical convection and increased errors in the large-scale tropical circulation were noted, although these deficiencies did not damage the forecasts of tropical cyclones, where our skill levels have reached an all time high. After a very careful analysis of the problems, we implemented a package of changes early in 2003.

Shallow convection is now diagnosed only when we have subsidence at the top of the boundary layer (vertical velocity <0). This prevents the misdiagnosis of shallow convection in the deep convective regimes. Such misdiagnosis was thought to be inhibiting deep convection and thus was a potential cause of instabilities. The change removes excessive cloud in the trade-cumulus regions of the subtropics. The resulting improvement in forecast cloud climatology is illustrated in Fig. 25. In addition, there is an overall reduction in tropical precipitation and diabatic heating, with some alleviation of the excessive Hadley and Walker circulation errors.

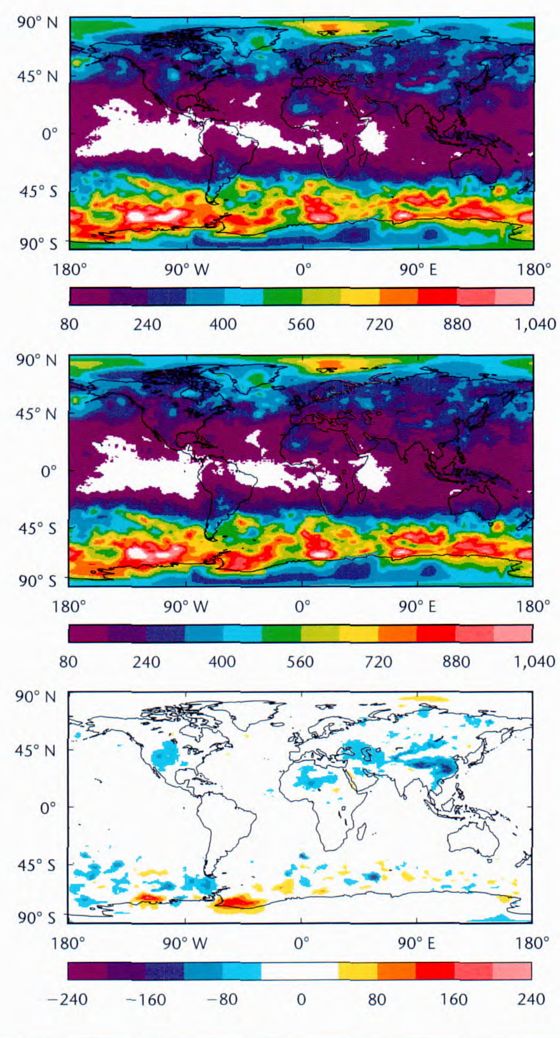

Figure 24. RMSE of T+72 MSLP forecasts from a July–August 2000 trial of MOSES II. MOSES I (top panel), MOSES II (middle panel), difference (MOSES II – MOSES I) (lower panel). Blue shading in the difference plot signifies reduced RMSE in MOSES II formulation.

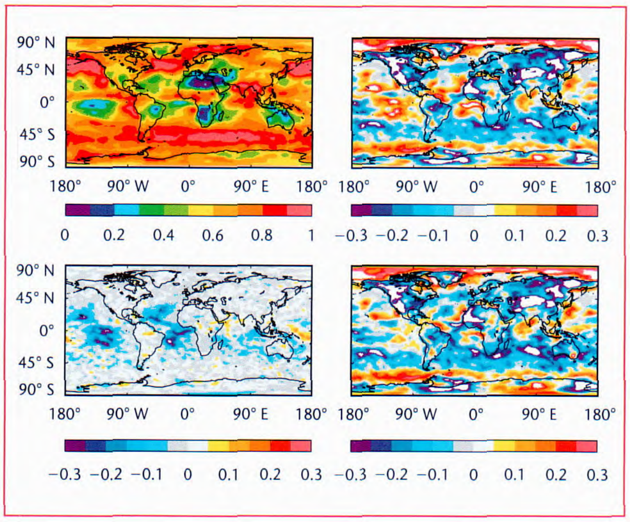

Figure 25. Mean cloud amount for T+120 forecasts for a June–July 2001 trial of changes to convection (experiment). The reference cloud amount is the International Satellite Cloud Climatology Project (ISCCP) estimate for July 2001 (top left). The differences from ISCCP of control (top right) and experiment (bottom right), and the experiment–control difference (bottom left) show beneficial reductions in cloud from the convection changes over the sub-tropical oceans.

European flood events — a new high-resolution model for Europe

Soon after the New Dynamics version of the UM became operational, two major flooding events occurred in Europe. The Dresden/Prague floods in the second week of August 2002 provided the first test, with rainfall totals in excess of 300 mm further swelling rivers already high from heavy rain earlier in the month. A similarly notable event occurred one month later when the area around Nimes in south-west France experienced barely credible rainfall totals of up to 600 mm in less than two days.

Our current forecast guidance for Europe is based on our Global Modelling System, which, with a resolution of only 60 km, is not capable of providing the necessary detail for these relatively small-scale features. Deficiencies in the global model predictions are particularly marked in regions of significant orography, where the precipitation is orographically enhanced.

To improve the forecast detail over Europe to near that provided over the UK from our mesoscale model, we are preparing a new European model. This currently has a horizontal resolution of 20 km, which is three times higher than the global model. This model (Fig. 26) also covers the Atlantic to enable the Atlantic weather systems to be defined with more detail as they approach Europe.

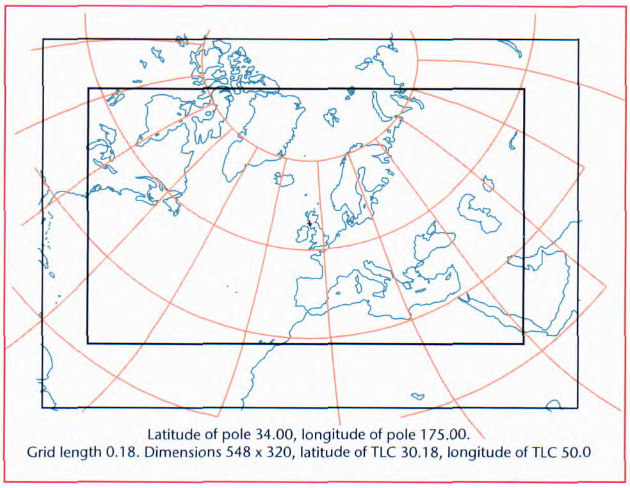

Figure 26. The domain of the European model (inner box).

The Prague/Dresden Flood event on 12 August 2002 provided an early test of the European model. The model forecast of 187 mm was a good match to what was observed (Fig. 27), although the peak rainfall area was displaced slightly too far east. In Fig. 28, we compare global and European model forecasts of the Nimes Flood event on 9 September 2002. Although both models forecast similar totals, the global model is clearly unable to resolve any detail on this scale. Note that the observation plot is indicative only, as the data cover the whole event and not just a 24-hour period. These early successes provided evidence that the European model should be run routinely and the model became semi-operational in December 2002.

Applications of satellite data

Successful developments in the processing and assimilation of satellite data have continued to lead to improvements in global NWP performance.

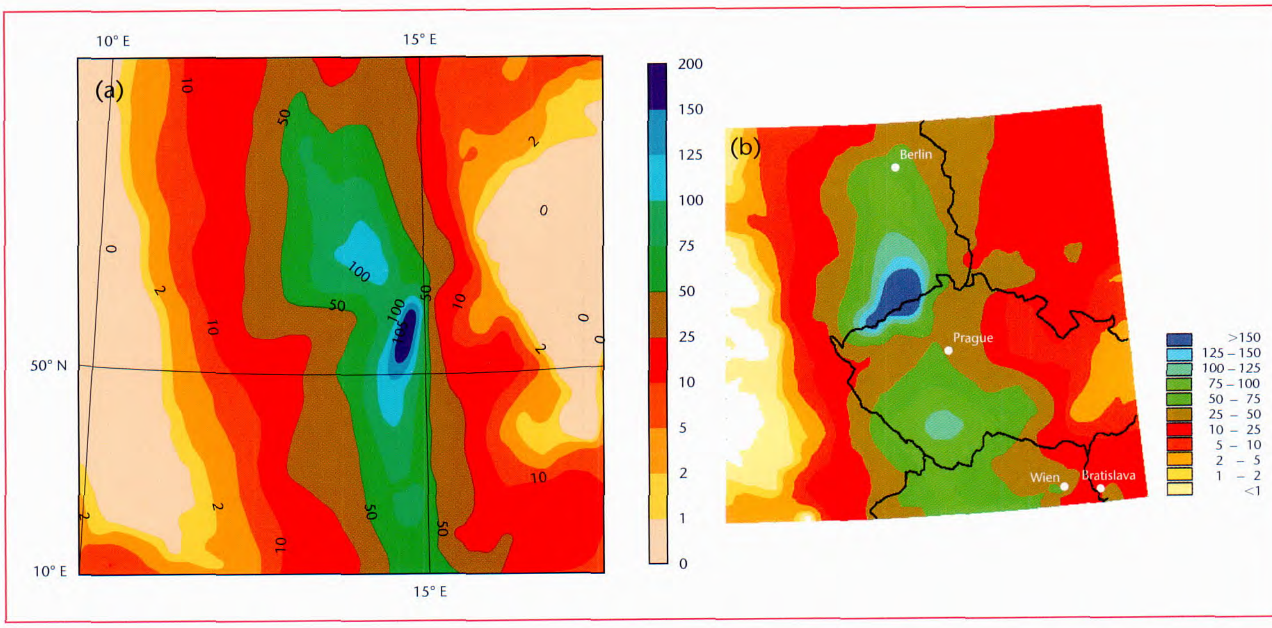

Figure 27. 24-hour rainfall totals (mm) from the European Model (T+6 to T+30) from (a) a forecast starting at 00 UTC on 12 August 2002, compared with (b) the observed rainfall distribution (kindly provided by Deutscher Wetterdienst).

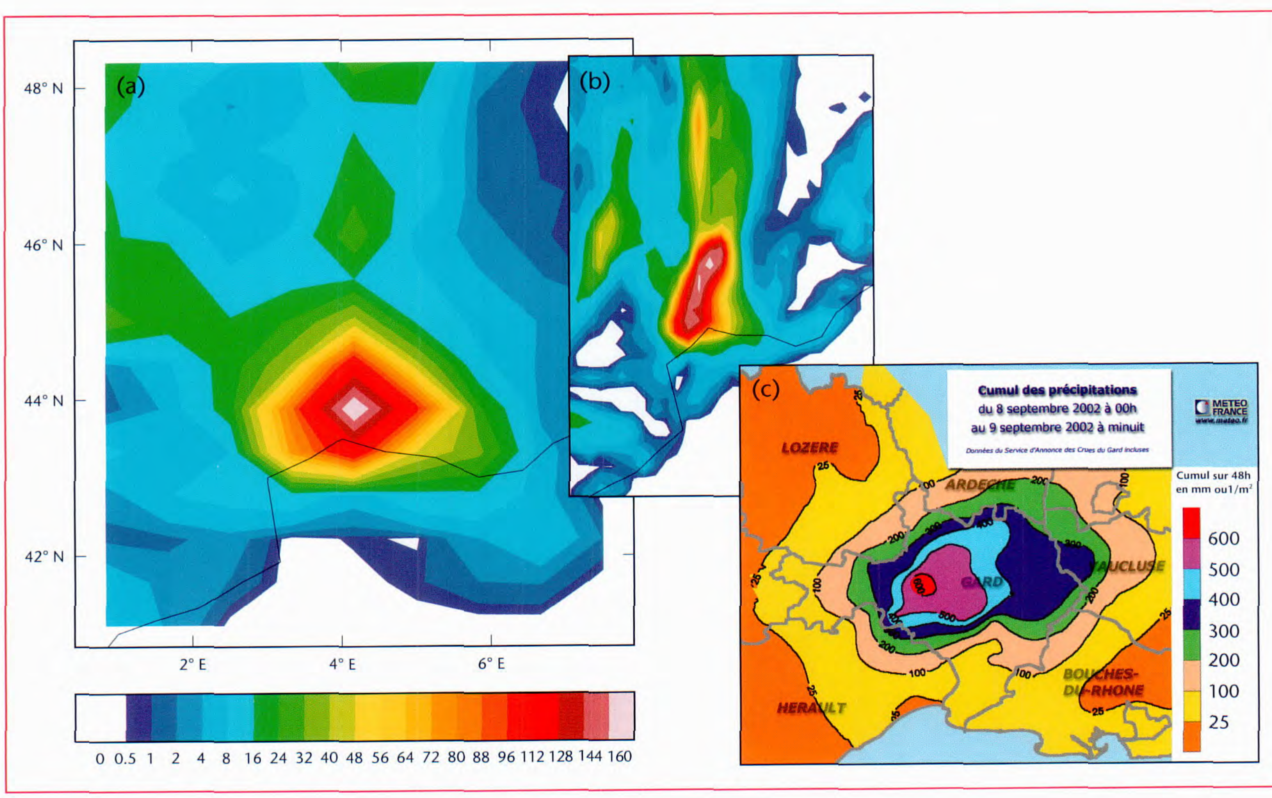

Figure 28. 24-hour rainfall totals (mm) from the (a) global and (b) European models for T+0 to T+24, from a forecast starting at 12 UTC on 18 September 2002. The observed plot (c) is a 48-hour total for the event (kindly provided by Météo-France).

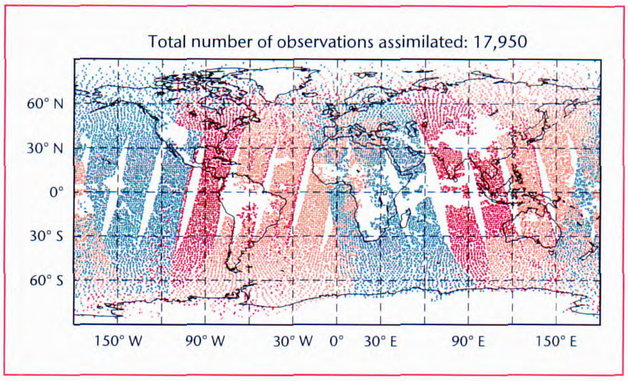

Figure 29. Coverage in a six-hour data assimilation window of data from ATOVS instruments on three NOAA satellites.

ATOVS data from NOAA-17

On 1 October 2002, ATOVS data from NOAA-17, launched in June 2002, were assimilated alongside NOAA-15 and NOAA-16 data. This was the first time we have simultaneously assimilated data from three polar-orbiting satellites and it was also our shortest period between launch and assimilation of data from a new satellite. There were three benefits: firstly, the negative impact on forecast scores if one satellite was lost (due to instrument failure, for example) is reduced by 85%, compared to a two-satellite system. Therefore the system is more robust. Secondly, two satellites do not give global coverage in a single six-hour data assimilation window, whereas three satellites achieve this, as the orbit of NOAA-17 lies between those of NOAA-15 and NOAA-16 (Fig. 29). Thirdly, the forecast skill for three satellites is better than for two satellites, especially in the southern hemisphere.

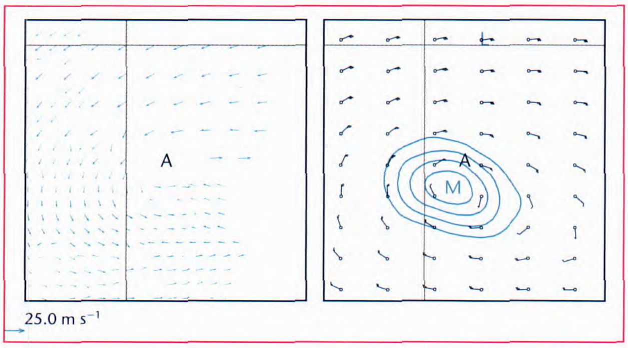

Figure 30. Seawinds observations of the surface wind field in the vicinity of a tropical cyclone in the Western Pacific. The letter A denotes the centre of the cyclone estimated from the observations. On the right panel, the observed centre is compared with the corresponding global NWP analysis of wind and relative vorticity in the region of the cyclone. M denotes the analysed centre of the cyclone.

Operational implementation of Seawinds data

The amount of marine wind observations used in the global NWP model was substantially increased from 11 December 2002 with the introduction of data from the Seawinds scatterometer on the satellite 'Quikscat'. This instrument provides almost complete coverage of the world's oceans in one day. Careful quality control is required, as the observations can be degraded in the presence of rain. Studies have revealed a positive impact for forecasts of surface variables out to three days, particularly in the extra-tropics. Another important benefit of these scatterometer winds is improved description of the wind field around tropical cyclones (Fig. 30).

AIRS

The Advanced Infrared Sounder (AIRS) was launched on NASA's Aqua satellite in May 2002. It is the first 'hyperspectral' sounder, making measurements in 2,378 spectral channels and giving information on profiles of

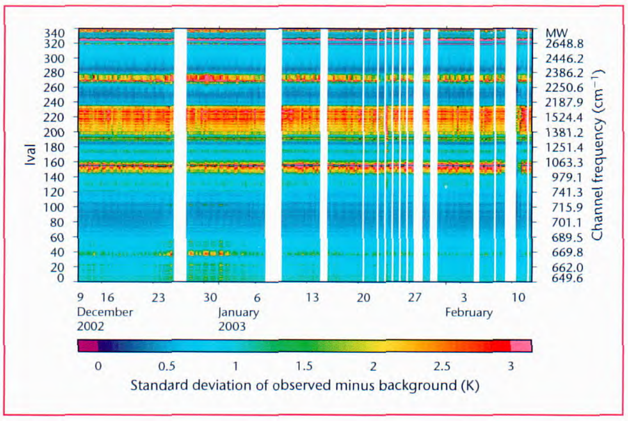

Figure 31. Plot of the global standard deviation of the difference between measured AIRS cloud-free brightness temperatures and the NWP model equivalents computed from six-hour forecast fields for 324 AIRS channels during the period December 2002 to February 2003. The 15 channels uppermost in the plot are from the AMSU-A sensor on the same platform.

temperature and humidity at considerably enhanced vertical resolution compared with the current generation of operational satellite sounders. AIRS is a research forerunner for instruments with similar performance on operational satellites later in the decade. Through collaboration with NASA and NOAA/NESDIS, we are obtaining AIRS observations in near real time. To reduce the data volumes for NWP applications, we receive only 324 channels, carrying most of the information on the vertical atmospheric profiles of temperature, water vapour and ozone. In preparation for data assimilation trials, AIRS radiances are being continuously monitored by comparing them with model simulated radiances (see Fig. 31).

High-resolution modelling

Current operational models are unable to resolve the convective clouds, including thunderstorms, that lead to the highest rainfall rates and can cause flash flooding.

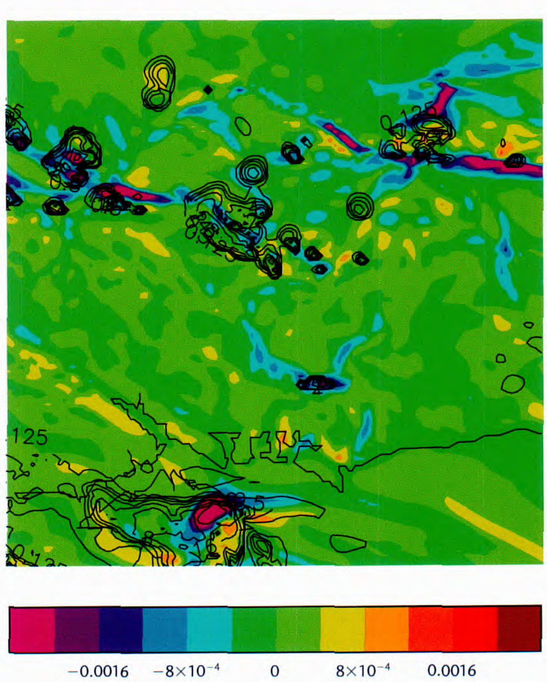

Figure 32. Results from a 1-km resolution version of the UM covering south England at 15 UTC on 31 July 2002, showing horizontal divergence (colour) of the low-level wind with contours of precipitation.

Instead, we parametrize their effects — an approximate process that can lead to errors. We are investigating the use of resolutions of about 1 km for very short range forecasting — this resolution can represent the larger storms reasonably well and we have shown that such resolutions can simulate strongly forced, organised storms remarkably accurately. We are beginning to study the mechanisms that lead to the formation of convective cloud in our high-resolution models. Figure 32 shows a snapshot of the horizontal divergence of the low-level wind (colour) overlaid with contours of precipitation, just after the first rain from convective showers reaches the ground. The convective cells are clearly forming along mesoscale convergence lines that existed before the clouds, the origin of which is not yet fully understood. These clouds went on to form severe thunderstorms (in reality and in the model), which caused localised flooding. Less-strongly forced storms often form more randomly within a region but may still be organised by larger-scale features of the meteorology or the surface (such as hills).

Even where little organisation occurs, the high resolution provides improved forecasts by, for example, realistically continuing to rain into the evening and

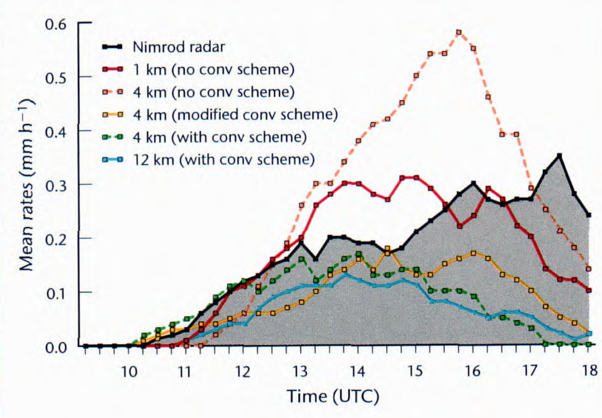

Figure 33. Area-averaged rainfall rate from a case with widespread, scattered convection (3 May 2002). Models using parametrized convection are, in this case, unable to show the continued growth of showers into the evening as well as the high-resolution model, though probably give a better indication of the initial formation of rain.

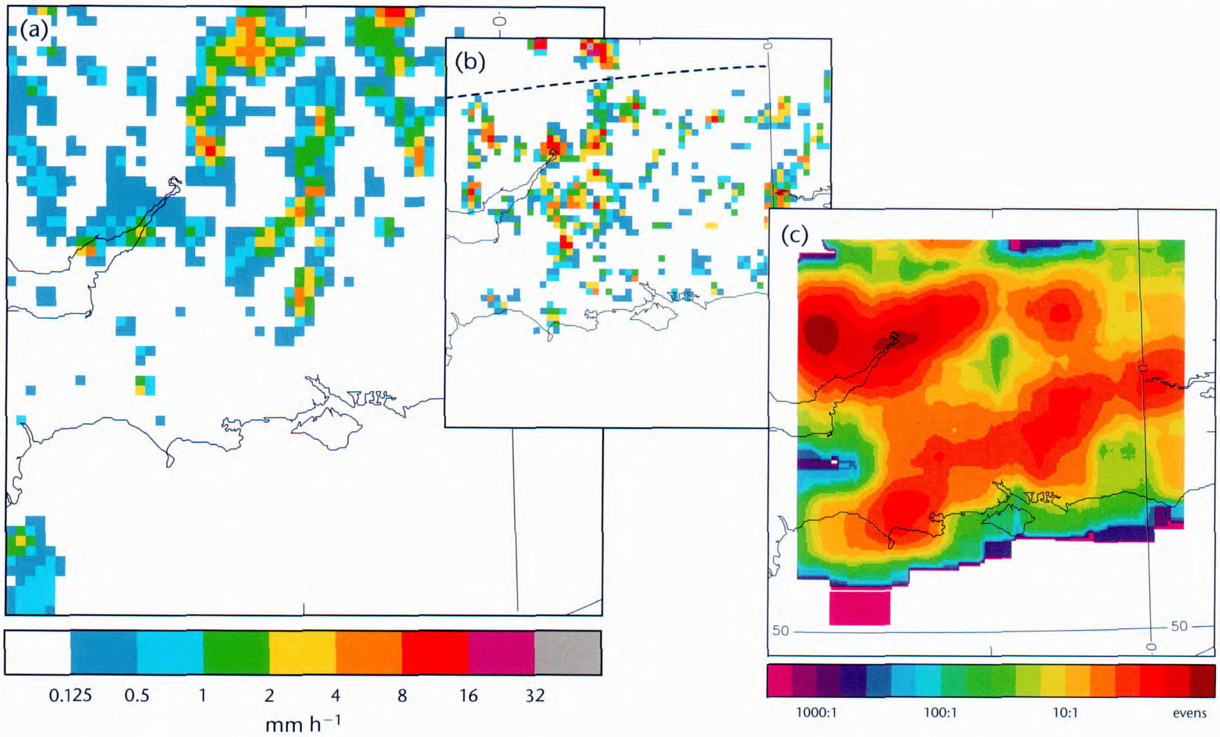

Figure 34. A radar image (a) showing the widespread convection on 3 May 2002, with an equivalent 14-hour forecast (b) from a 1-km resolution model, averaged to the same 5-km grid as the radar. There is clearly similarity but a lack of precision in forecasting the detailed location of rain. Information such as this has been used to estimate a risk of large accumulations of rain over the period 10 to 18 UTC on 3 May 2002 (c).

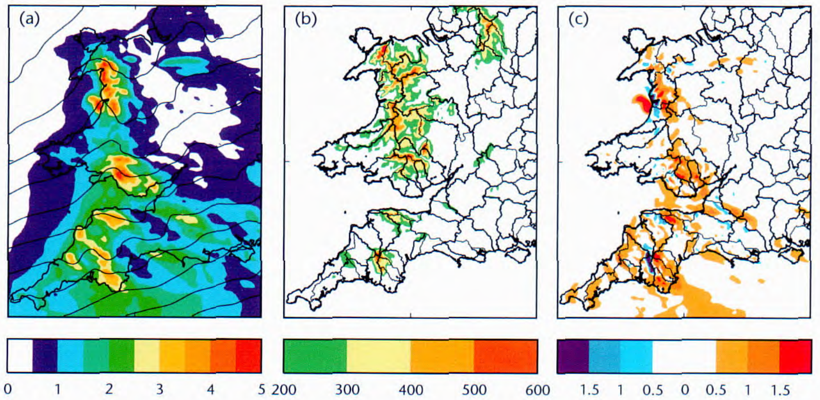

Figure 35. (a) Surface rainfall rate (mm h^{-1}) overlaid with MSLP contours (1 hPa interval) at 12 UTC on 29 November 2001 from a six-hour forecast using a 2-km resolution version of the UM including rain advection. (b) Height of orography (m) and boundaries of major river catchments. (c) The difference in surface rainfall rate (mm h^{-1}) between a forecast with rain advection and one without rain advection. Dipole anomalies in regions of orographically enhanced rainfall indicate the significant downwind displacement of the rain to the lee side of the orography (the wind is from the south-west); this is sufficient to move significant rain to different river catchments.

night where parametrized convection tends to die out (Fig. 33). Furthermore, even though, at this stage, the precise location of the highest rainfall is unlikely to be well forecast in our high-resolution model, we may still be able to use the results to obtain guidance on features such as the likelihood of extremely heavy rain. We are looking at ways of using the output to provide useful and reliable forecasts, even when we have little confidence in the precise location of individual clouds (Fig. 34).

To use high resolution, we need to enhance some of the model parametrizations, since assumptions such as the neglect of horizontal transport no longer apply. This is particularly true of cloud microphysics, and work is well under way to produce an enhanced microphysics scheme appropriate for high resolution (Fig. 35).

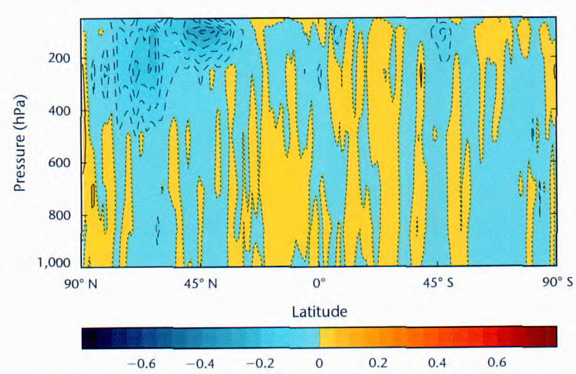

Figure 36. Changes in zonally-averaged root-mean-square errors in the zonal wind (m s^{-1}) at T+24, resulting from an increase in the parametrized drag associated with flow blocking and a decrease in that associated with propagating waves.

Representation of physical processes

With the operational introduction of the New Dynamics version of the UM, the representation of many important physical processes in the global NWP model was upgraded, including improvements to the treatment of radiation, cloud microphysics, turbulent transports in the convective boundary layer, and convective transports in the free atmosphere. In addition, a completely new orography package was introduced. This includes a new parametrization of the effects of unresolved orography, which includes a representation of the effects of flow blocking. Recent trials have shown

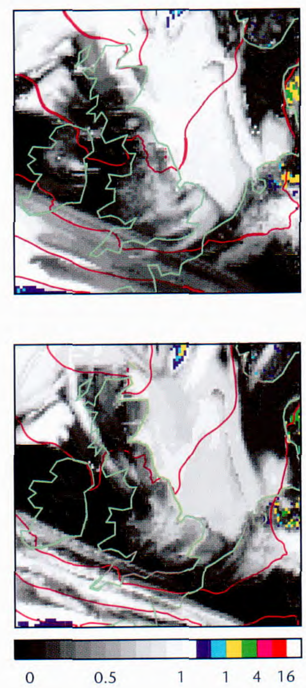

Figure 37. Cloud fraction (black and white scale), precipitation rate (mm h^{-1}, colour scale) and MSLP (isobars at 4 hPa intervals) at 12 UTC on 22 July 2000 for the prognostic scheme (top) and control scheme (bottom).

that further increasing the low-level drag associated with flow blocking, while decreasing the upper-level drag associated with propagating gravity waves, leads to significant improvements in many aspects of model performance. In particular, the errors in the stratospheric and upper-tropospheric winds are reduced north of around 30° N in winter (Fig. 36).

Some of our current research is aimed at further improving the representation of clouds, convection and the stable boundary layer, using observational research and high-resolution modelling to aid our understanding of atmospheric processes.

We have written a prognostic cloud and condensation scheme and tested it within the UM. Processes, such as convection and radiation, are modelled as updating liquid and ice condensates and cloud fractions. The prognostic scheme can predict liquid water clouds that contain less liquid water but are more extensive. Figure 37 shows stratocumulus cloud in an easterly flow penetrating further into Wales in the prognostic scheme.

The atmospheric boundary layer is the region adjacent to the Earth's surface, in which active heat, moisture and momentum exchange takes place with the surface. It becomes stably stratified, but often remains turbulent over land during the night and in regions of persistent surface cooling such as Antarctica. While the convective boundary layer is typically 1 km deep, the stable boundary layer is much shallower (of order 100 m or even less). The representation of this stable boundary layer regime in our numerical forecast is important for applications such as fog and surface-temperature forecasting.

The current stable boundary-layer parametrization employed in our forecast models has a known problem of producing a turbulent layer that, in some circumstances, is too deep. This tends to produce temperatures at the surface that are too warm, so we have developed a new scheme to counteract the problem. The new parametrization employs a sound theoretical framework from turbulence theory, based on the turbulent kinetic energy budget, which allows, among other things, the control of the depth of the turbulent layer. Use of the Met Office Large Eddy Simulation (LES) model at very high resolution has enabled us to explicitly simulate the turbulence of stable boundary layers. Using data from these simulations and also published observations, we have configured the new scheme with physically sound parameters.

We have incorporated the new scheme as an alternative to the current one in the forecast and climate models. Figure 38 compares the time evolution of vertical profiles of (potential) temperature from a single column of the forecast model using the old scheme and the new scheme. This is for a situation of prescribed surface temperature, decreasing with time. Also shown are the results from a LES (for the final time), which explicitly models the turbulence. The new scheme produces the desired effect of a shallower boundary layer, and more-closely matches the large eddy data. Figure 39 shows the difference between the new and the old schemes for a five-year climate simulation for the southern-hemisphere winter, in terms of surface temperature. The new scheme has the effect of producing significantly more cooling over the Antarctic, where stable conditions prevail.

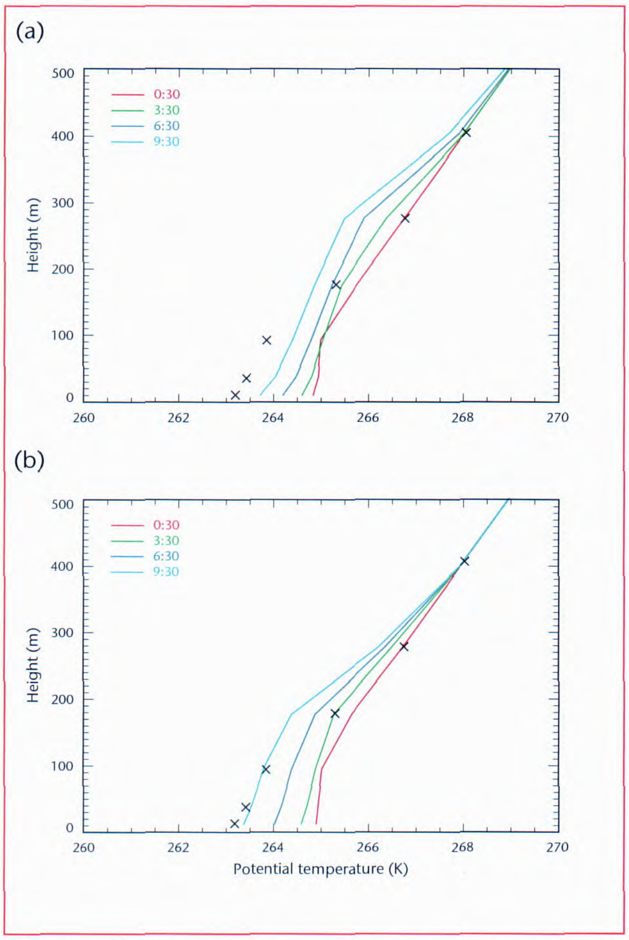

Figure 38. Vertical profiles of potential temperature every three hours (solid lines), and the Large Eddy Simulation at final time (crosses) for (a) the current scheme and (b) the new scheme. The key shows the time in hours and minutes since the start of the simulation.

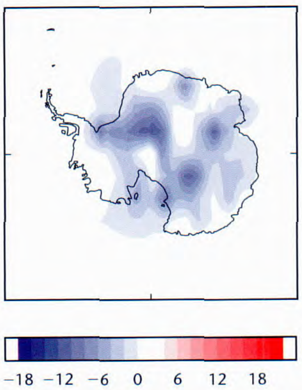

Figure 39. Difference between new and current stable boundary layer schemes in terms of surface temperature over Antarctica, averaged over five successive winter seasons, simulated using Met Office climate model.

Observations-based research

One of the methods we use to develop the representation of physical processes in NWP involves collecting and analysing special observational data sets. We have two facilities — a group using instrumented aircraft and a group using surface-based instrumentation. The aircraft group normally operates the scientific equipment on board the Met Office C-130 aircraft but they are currently transferring their equipment onto a BAe146-300 aircraft, which will be operated in partnership with the UK university community, called the Facility for Airborne Atmospheric Measurements (FAAM). Being involved in these facilities enables us to interact and benefit from a wider national and international observational resource.

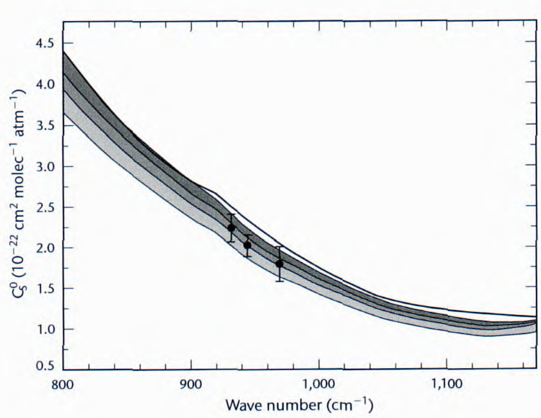

Figure 40. The self-broadening coefficient of the water vapour continuum.

Work in support of satellite applications

In 1995, the Met Office installed an interferometer system on its C-130 aircraft to conduct research in support of satellite-borne high-resolution sounding instruments (AIRS and Infrared Atmospheric Sounding Interferometers (IASIs)). Initial results comparing AIRS observations with NWP model fields show significant differences in regions of the thermal infrared spectra dominated by water vapour absorption. Such differences could arise from errors in the prescription of water vapour in the forecast model or errors in the spectroscopy of water vapour used in the forward radiative transfer models.

Our airborne data are being analysed to study whether this absorption is being correctly modelled. One aspect of the water vapour absorption is the so-called 'continuum' absorption, which represents a spectrally slowly varying component rather than strong 'line' absorption features. Our results show that the currently used parametrization of the continuum absorption, as represented by a self-broadening component, is too strong by between 6% and 15%. The disagreement is shown in Fig. 40, which also depicts some very recent laboratory measurements that are consistent with our airborne measurements. In the figure, the solid line is the standard formulation (known as CKD2.4) of the continuum. The darker shaded region indicates our best estimate of the strength of the continuum with the lighter shaded areas indicating our range of uncertainty. The three data points, with their associated one standard deviation error bars, are the new results of Cormier et al.

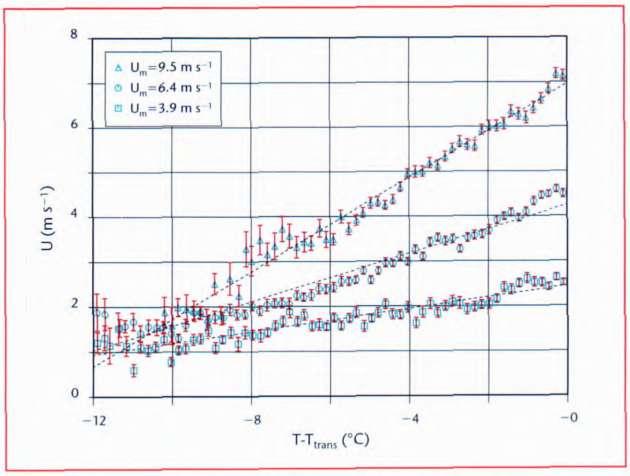

Figure 41. Mean curve of 10 m wind speed, U, against the screen temperature change $(T - T_{trans})$ after the transition for three maximum daytime wind speed $(U_m, m\ s^{-1})$ bands. The error bars shown are for the variance of the mean values.

Surface wind strength

It is commonly observed that, in stable conditions, the surface wind strength can decline markedly around sunset, allowing surface temperatures to fall dramatically and potentially giving rise to fog formation. Observations taken over five years from our instrumented surface site at Cardington have been used to examine factors determining this 'evening transition'. In particular, the data have been analysed to identify any predictable relationships that may interrelate the parameters in the stable boundary layer. The main results of this analysis show that there are statistically well-defined relationships between the decrease in screen temperature, measured at 1.2 m above the surface, and the near-surface wind, together with the drag and heat conducted by the flow. The reductions in wind speeds, measured at 10 m height, were linearly dependent on the reduction in screen temperature for a particular wind speed above the effects of the boundary layer (Fig. 41). The mechanisms involved have been studied by comparing these results with outputs from both a numerical and a semi-analytical model. These have shown that the reason for the observed increase in 10-m wind/screen temperature gradient with generally stronger upper-level flow is due to the greater thickness of the stable boundary layer at higher wind regimes. Observations from a tethered balloon facility have been used to confirm the deeper atmospheric structure.

The cloud physics of mixed-phase clouds

Understanding the disposition of ice and liquid in mixed-phase cloud is important for predicting the radiative impact of mixed-phase clouds and the evolution of precipitation systems, and has implications for predicting the occurrence and severity of aircraft icing.

Observations of mixed-phase cloud have been hampered by a lack of instrumentation capable of determining the phase of particles and have relied on manual or automatic techniques of identifying 2D images, which are only feasible for particles larger than 125 μm. Recently, in collaboration with the Met Office, the University of Hertfordshire designed and built a new aircraft probe, the Small Ice Detector (SID), which is capable of determining the sphericity of individual particles in the 2–50 μm range. By assuming that particles deemed spherical are liquid, we can observe the occurrence of supercooled liquid water along an aircraft transect.

Figure 42 shows results from coincident Chilbolton radar and the Met Office C-130 flight as part of the Natural Environment Research Council's (NERC's) Clouds, Water Vapour and Climate thematic programme. In Fig. 42 (a), the higher dBZ values indicate the presence of greater condensed water content. The black line shows the track of the Met Office C-130 at the time of the radar scan. The average air temperature along the run was 28 °C. Fig. 42 (b) and (c) show aircraft data obtained along the flight track; (b) shows the fraction of spherical particles in each one-second interval as determined by the SID. The blue colour indicates regions that are dominated (number weighted) by liquid in the 2-50 μm particle size range, while the red colour indicates ice domination. Fig. 42 (c) shows examples of ice crystal images captured with the 2D-C probe. The maximum width of the images is 0.8 mm.

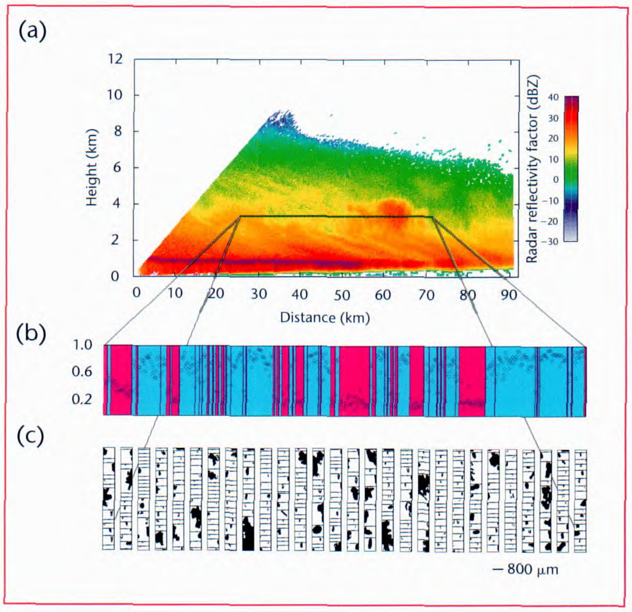

Figure 42. Results from coincident Chilbolton radar and Met Office C-130 flight. (a) Radar reflectivity values from Chilbolton radar as a function of height and range from the radar. (b) Fraction of spherical particles in each one-second interval (~100 m horizontal distance) as determined by the SID. (c) Examples of ice crystal images captured by 2D-C probe.

Figure 43. A large fire that was investigated during SAFARI2000. (Photograph, courtesy of Peter Hobbs, was taken from the University of Washington's Convair aircraft.)

The figure shows the complicated intermittent structure of mixed-phase regions within a frontal cloud. In this case, the orange ~20 dBZ radar reflectivity contour, at an altitude of 4 km, marks a shear-driven turbulent layer that gives rise to supercooled liquid water. At the same time, the 2D imaging probe that measures larger ice crystals indicates the presence of ice that will rapidly deplete the liquid water via the Bergeron–Findeisen process and enhance the precipitation rate. The analysis of the radar data was conducted by Dr R. Hogan of the University of Reading, using Chilbolton radar data provided by the Rutherford Appleton Laboratory.

Measurements and modelling of the radiative effects of biomass burning aerosol

Accurate treatment of the effects of atmospheric aerosols on both weather and climate models demands a better knowledge of the nature of these very variable particulates and an understanding of how they evolve and interact in the atmosphere. In Autumn 2000, we became involved in a multinational measurement campaign studying biomass burning in southern Africa when the seasonal burning of scrubland takes place. Instrumentation on the Met Office C-130 aircraft measured the optical properties of biomass burning aerosol directly over the fires (Fig. 43) and progressively downwind to determine the effects of ageing on the aerosol optical parameters. Scanning electron microscope images show that black carbon is emitted as a chain-like structure at source (Fig. 44 (a)), which collapses as time progresses to a more compact structure. This collapse has been modelled by applying Mie scattering theory to quasi-random chain structures (Fig. 44 (b)) with differing aspect ratios. The results suggest that the increase in absorption due to the collapse of the chain structure is not sufficient to explain the observed increase in the particle absorption; condensation of gaseous volatile organic species is the more likely cause.

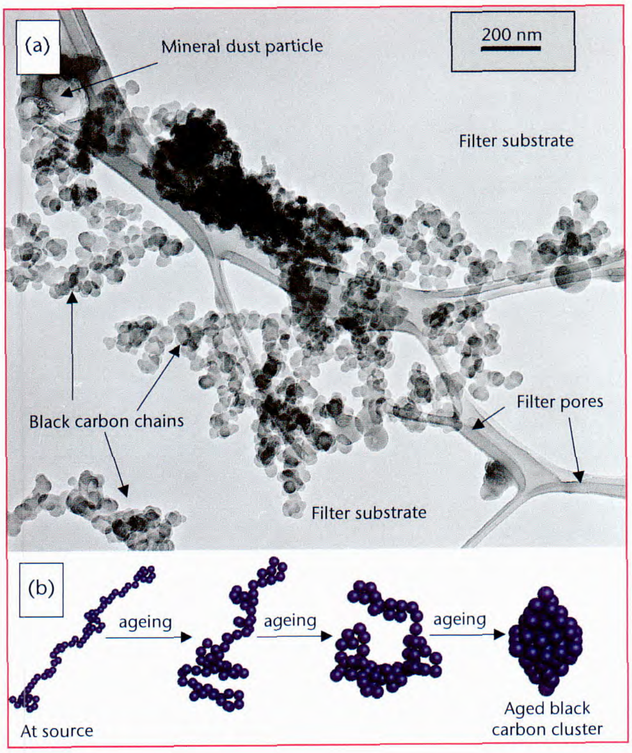

Figure 44. (a) Scanning electron microscope image of a typical black carbon chain collected in a smoke plume near the emission source (courtesy of Peter Buseck, Arizona State University). (b) Model representation of the ageing of the chain structure of black carbon that is used in Mie scattering calculations.

Climate research and ocean applications

International collaboration

Intergovernmental Panel on Climate Change

With the completion of the Intergovernmental Panel on Climate Change's (IPCC's) Third Assessment Report, there was international agreement that a Fourth Assessment Report would be prepared.

Co-Chair of Working Group I (WGI) Sir John Houghton has retired, and his Technical Support Unit (TSU), which had been at the Met Office's Hadley Centre for Climate Prediction and Research since the beginnings of the IPCC, has now moved to the United States. WGI deals with the underpinning climate science of the IPCC.

At the same time, the IPCC's WGII, dealing with impacts of climate change, has transferred to the UK with Professor Martin Parry as one of the WG Co-Chairs; the second Co-Chair is Dr Osvaldo Canziani of Argentina.

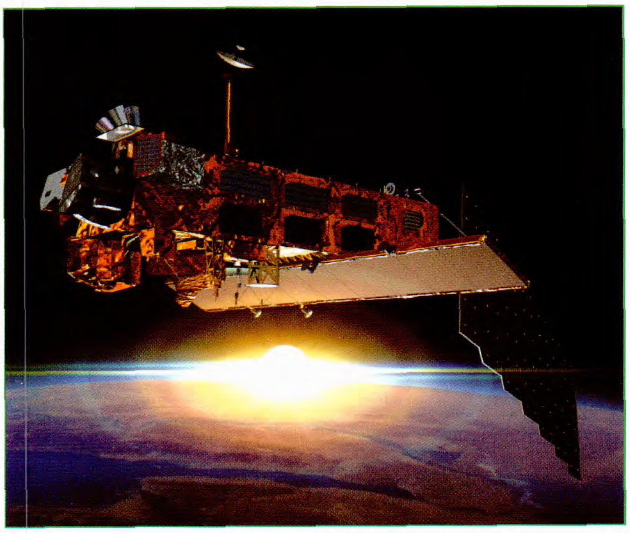

Figure 45. Artist's impression of ESA's ENVISAT satellite in orbit above the Earth. The AATSR is seen here at far left and nearest to the reader. Courtesy of ESA.

Our Hadley Centre was successful in its bid to host the WGII TSU, and our TSU team is now working on the Fourth Assessment Report.

We also contributed to the Second Report to the UN Framework Convention on Climate Change on the Adequacy of the Global Climate Observing System. We had a major input to the World Meteorological Organization's 7th Global Climate System Review.

Sea-surface temperatures from Envisat

The polar-orbiting Envisat (Fig. 45) was launched on 1 March 2002, and is the largest civilian satellite ever constructed in Europe. It carries ten instruments to monitor the Earth's environment; one of these is the Advanced Along-Track Scanning Radiometer (AATSR). This instrument measures sea-surface temperature (SST) to better than 0.3 °C accuracy, as required for monitoring climate trends and improving predictions of climate change.

Infrared data from AATSR are processed in near-real time at the Met Office to provide an SST product suitable for climate research (Fig. 46). We have played a key

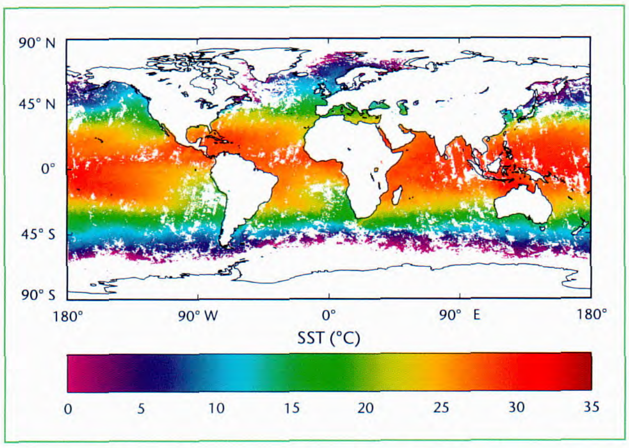

Figure 46. Monthly mean SST from AATSR at half-degree resolution.

Nick Rayner, Marine Data Research Scientist

"I'm part of a team developing data sets of variables such as sea-surface temperature and sea ice. These data come from ships, buoys and satellites and are updated regularly. Records stretch back 150 years and measurement methods have changed over time, so we adjust data to remove relative biases and make estimates of uncertainty. This allows us to analyse past climate variability and provide up-to-date information to Government."

role in AATSR validation activities since the launch, as we are the only partner to have obtained any substantial validation results. Our comparisons of SST from the AATSR to in-situ observations (from buoys) and analyses (such as HadISST1) have shown that, in the global mean, both the instrument and retrieval schemes are functioning within specification (Fig. 47). At the start of its mission, the AATSR is providing high-quality data that should admirably achieve its aim to continue the ATSR-series SST record for climate studies.

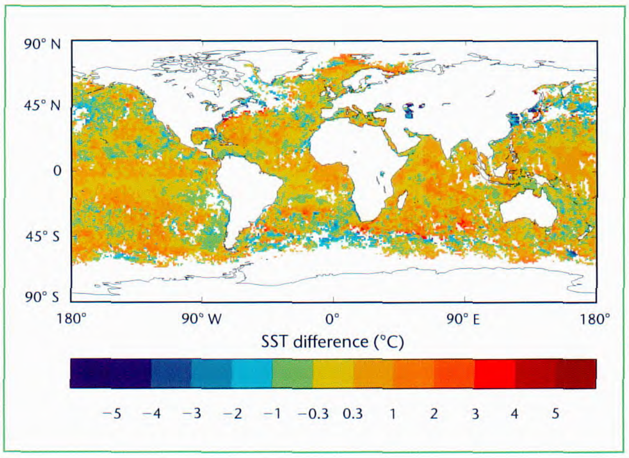

Figure 47. The difference, at one-degree resolution, between SST from AATSR and the Hadley Centre's global SST analysis (HadISST1, preliminary version); both for November 2002.

Climate variability

Global and UK climate trends

The year 2002 was the second warmest globally in the 142-year global temperature record, 0.48 °C above the 1961–90 normal. Only 1998 was warmer, at 0.55 °C above normal. This verified our global temperature forecast for 2002 made in 2001. For 2003 we predict the same global temperature as 1998. The year 2002 was the fourth warmest in the 344-year Central England Temperature (CET) record, being 1.1 °C above the 1961–90 average. February, October, November and December were notably wet over England and Wales, but not record-breaking.

We developed an improved system for automated processing of monthly worldwide climatic data. With the University of East Anglia, we use its output to brief the media and policy makers on global climate.

Marine temperatures

With Southampton Oceanography Centre, we developed improved adjustments to night-time marine air temperatures (NMAT) since the 1970s, to compensate for the increasing, geographically variable heights of ships' decks (Fig. 48). The adjustments add about 0.1 °C to the overall warming of NMAT since the 1860s and reduce the divergence between NMAT and SST trends in the southern hemisphere in the most recent decade.

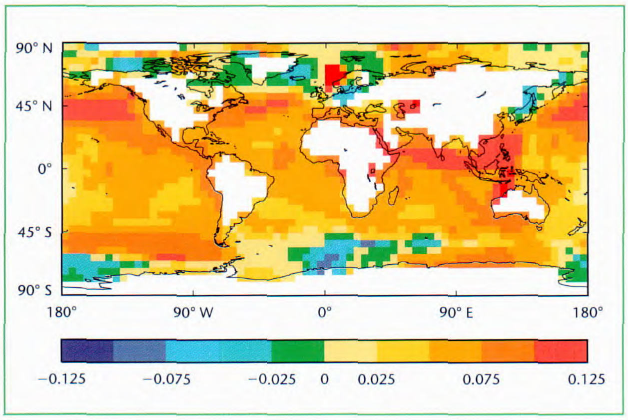

Figure 48. Adjustments (°C) to NMAT to allow for deck-heights, 2000.

European projects

We analysed Atlantic SSTs and observed atmospheric circulation to identify the patterns of SST most likely to induce a response in the North Atlantic/European atmosphere. We then used these SST patterns to force several European atmospheric climate models under the EU-funded 'Mechanisms and Predictability of Decadal Fluctuations in Atlantic–European Climate' (PREDICATE) project. The models yielded mainly consistent worldwide signals. North Atlantic SST variations influenced European seasonal-mean surface temperatures by about 1 °C and southern US precipitation by about

1 mm/day; in the Indian summer monsoon, there was a signal of around 3 mm/day. These signals are smaller than interannual variability but they could be important on decadal and longer timescales.

Another EU project, 'Simulations, Observations and Palaeoclimate data: Climate Variability over the past 500 years' (SOAP), has begun. It will compare partners' abilities to simulate the last 500 years and to quantify the relative contribution of natural and anthropogenic factors to climate variability. A simulation with only natural forcings replicated reasonably well northern hemispheric temperature for the period 1500–1950 (Fig. 49). The largest differences are in the mid-17th century when the simulations show more warming than the palaeo-reconstructions, and after the eruption of Tambora in the early 19th century. Both simulation and reconstruction show multi-decadal climate variability of order ±0.2 °C, much smaller than the expected warming in the 21st century.

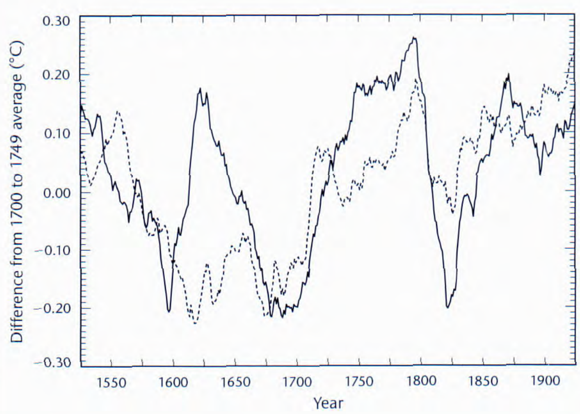

Figure 49. Comparison of simulated (solid line) and reconstructed (dashed line) 25-year running average summer half-year northern hemisphere land temperatures from 1500 to 1950. The reconstructed temperature time series is based on tree-ring densities from many northern hemisphere sites and was supplied by collaborators at the Climatic Research Unit, University of East Anglia.

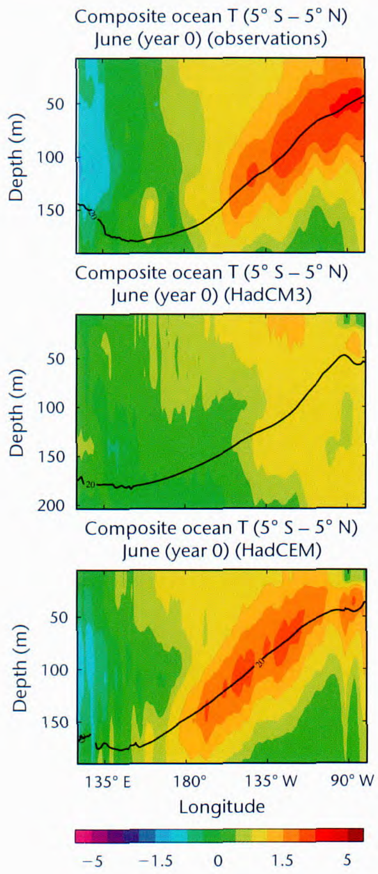

Figure 50. Composite upper Pacific ocean temperature anomalies and climatological 20 °C isotherm in the band 5° S–5° N in June (six months before the El Niño peaks) for the observations (top), HadCM3 (middle) and HadCEM (bottom) simulations.

Simulation of El Niño Southern Oscillation

El Niño Southern Oscillation (ENSO) is the largest mode of interannual variability in the coupled ocean-atmosphere system over the tropical Pacific. It affects the whole globe through atmospheric 'teleconnections'. We have analysed ENSO variability in observations, and in simulations using the HadCM3 model, and HadCEM, which has finer oceanic resolution. The observational and model results indicate

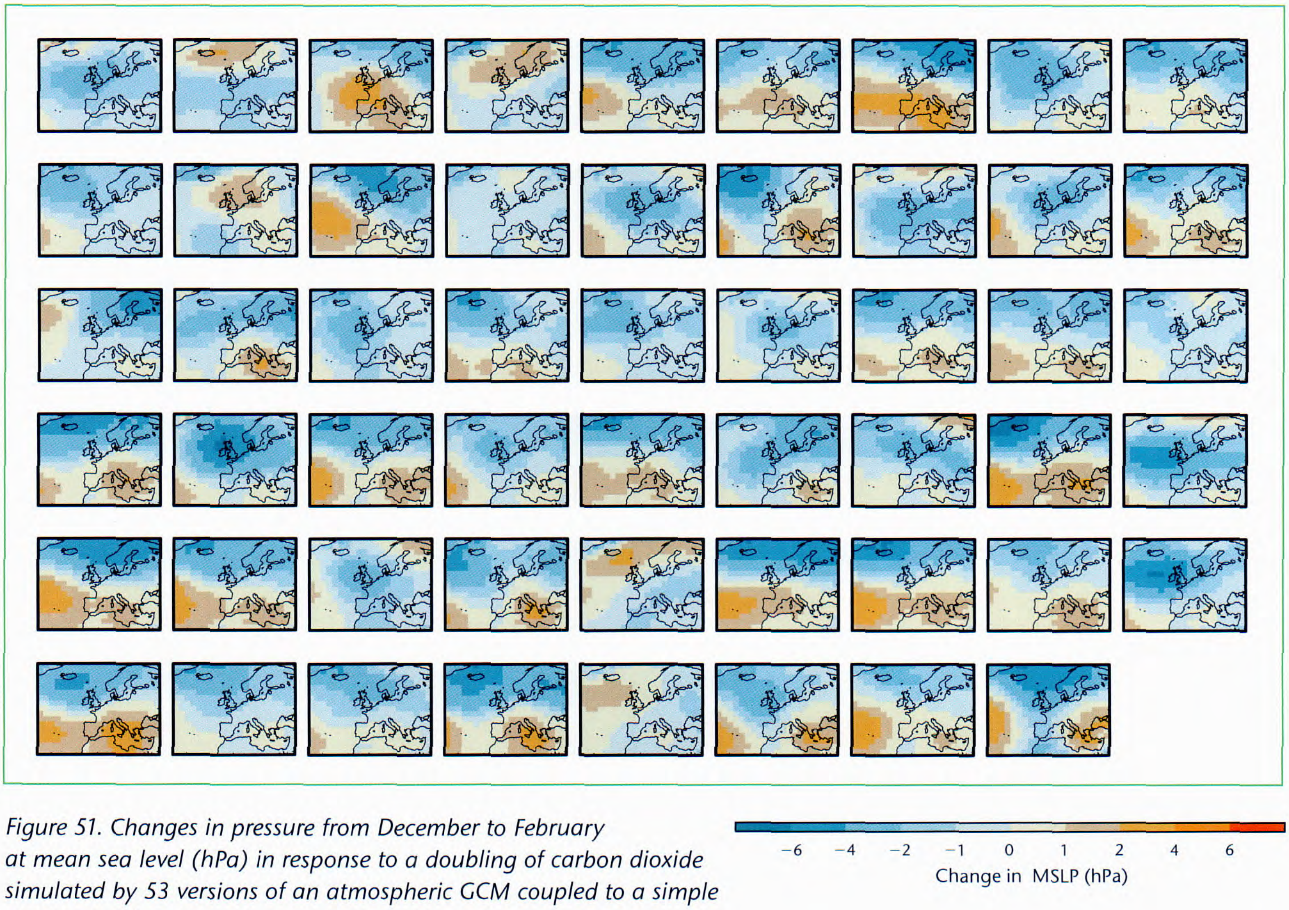

Figure 51. Changes in pressure from December to February at mean sea level (hPa) in response to a doubling of carbon dioxide simulated by 53 versions of an atmospheric GCM coupled to a simple ocean model.

that subsurface ocean temperature anomalies form over the western tropical Pacific about 12–14 months before ENSO peaks. These anomalies spread eastward and upwards along the thermocline (Fig. 50). When they reach the surface over the central and eastern Pacific, they amplify rapidly due to positive air–sea interactive feedbacks, marking the 'mature' or 'El Niño' stage of ENSO. The subsurface temperature anomalies are stronger and more realistic in HadCEM than in HadCM3.

Climate change predictions

Predictions of future climate change are subject to uncertainties arising from emissions of greenhouse gases and aerosols, the effects of natural variability and the representation of processes in the climate model. These uncertainties imply a range of outcomes, which needs to be quantified to allow policy makers and planners to develop optimal response strategies. In principle, this range can be estimated from a large ensemble of general circulation model (GCM) predictions. During the past year, we have produced the first such experiment to be carried out worldwide. The ensemble consists of 53 versions of the atmospheric model HadAM3 coupled to a simple ocean model. The standard model version is joined by 52 versions distinguished by a change to a parameter controlling a key physical atmospheric process. Figure 51 shows the change in winter circulation over Europe predicted by each ensemble member in response to a doubling of carbon dioxide. The results reveal substantial uncertainty in this aspect of future European climate. Work is now in progress to develop a 'Climate Prediction Index' that can be used to weight the individual ensemble members according to reliability — this will allow us to present results from future ensembles as probabilistic predictions.

The responsiveness of the climate system to an imposed radiative forcing is quantified by the 'climate sensitivity', defined as the steady-state response of global average surface temperature to a doubling of carbon dioxide. The climate sensitivity represents the greatest source of uncertainty in climate change projections for the 21st century. On the basis of GCM experiments, it is estimated to lie between 1.5 and 4.5 °C. The range has remained essentially unchanged during the last two decades, despite ongoing development and improvement of GCMs.

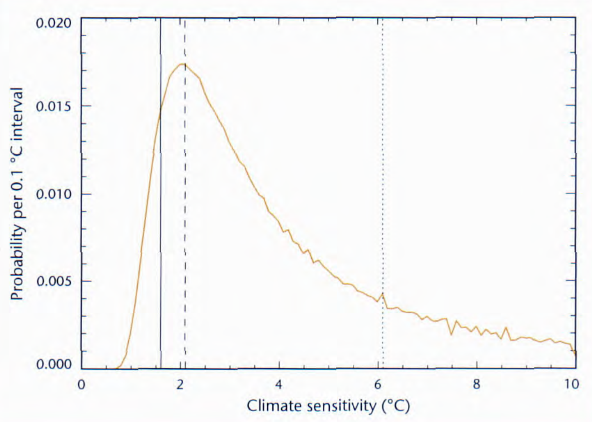

Figure 52. Probability distribution for the climate sensitivity. The bin width is 0.1 °C. The vertical solid line marks the lower bound of the 90% confidence interval (1.6 °C), the vertical dashed line the mode (2.1 °C) and the vertical dotted line the median (6.1 °C). Although the distribution is shown here only up to 10 °C, the probability of larger values was accounted for in deriving the statistics and confidence interval.

We have investigated an alternative approach of determining the climate sensitivity from measurements of the real climate system. The climate sensitivity was estimated from observed 20th century climate using estimates of the surface temperature change, the rate at which heat is being stored in the ocean (inferred from the warming of the ocean interior), and the radiative forcing due to greenhouse gases, sulphate aerosols, volcanic aerosols and solar variability. Since all these quantities are uncertain, we obtain a probability distribution for the result rather than a single number (Fig. 52). The uncertainty is dominated by our poor knowledge of the sulphate aerosol forcing and precludes us from setting an upper bound on climate sensitivity. We can, however, conclude that there is only a 5% chance that the climate sensitivity is less than 1.6 °C. This result is valuable because it is independent of GCMs and hence increases our confidence in predicting that substantial climate change will occur during the 21st century.

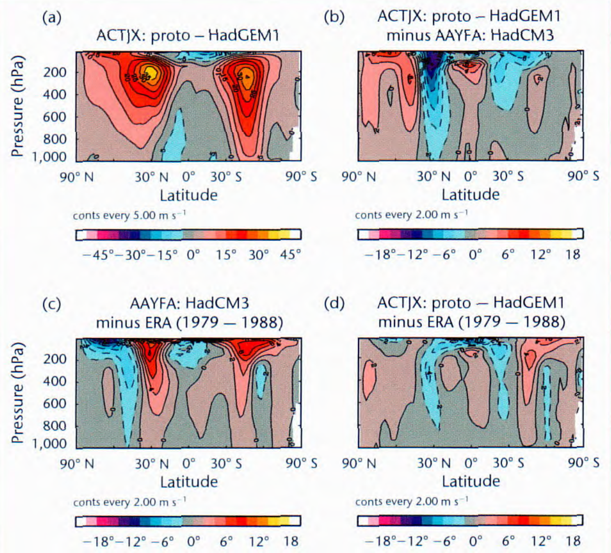

Figure 53. Latitude-height distributions of zonally averaged westerly wind (m s^{-1}) for December to February. (a) Values simulated by a prototype version of HadGEM run at similar resolution to HadCM3. The difference relative to HadCM3 is shown in (b), and biases relative to observed climatological values are shown in (c) and (d) for HadGEM1 and HadCM3, respectively.

Policy makers require increasingly sophisticated information about possible climate change, both in terms of regional effects and the impact and interaction of environmental processes. The Hadley Centre has nearly completed development of a new Global Environmental Model (HadGEM1) in order to meet this challenge. This model represents a significant advance on our existing Global Climate Model (HadCM3). The main improvements in the atmospheric component of the model are already included in the operational weather forecast model — these are New Dynamics, new physical parametrizations of boundary layer, convection, orographic and microphysical processes. In addition, the model will have enhanced resolution, an improved ocean simulation and enhanced coupling of climate processes, with online chemistry, aerosols, and biogeochemical processes. The teams working on HadGEM1 require a range of modelling and evaluation tools to diagnose and correct problems. One new tool used to great effect this year has been the 'aquaplanet' model. In this model, the interactions between the physical parametrizations and the dynamics are retained, while the surface boundary is global sea-surface everywhere with an idealised temperature distribution. Simplified warm or cold pools, or islands can be added for various tests.

HadGEM1 already shows improved skill relative to HadCM3 in simulating some aspects of the general circulation (e.g. Fig. 53), with further improvements anticipated as the resolution is increased and the model tuned.

Atmospheric dispersion

There is continued interest in understanding and predicting the processes by which airborne pollutants are transported in the atmosphere, both for emergency response and planning purposes, and for understanding a range of atmospheric pollution problems. Our atmospheric dispersion model, NAME, continues to be developed and applied to an ever-increasing range of problems.

Model developments

The introduction of the New Dynamics version of the Unified Model (UM) required a major upgrade, and a number of improvements were also made. These included a much simplified input and output, an extended chemistry scheme representing over 30 species, a better attribution facility for investigating source-receptor relationships and increased speed. A detailed review of boundary layer turbulence parametrizations, including extensive comparisons with surface and balloon measurements, resulted in many improvements.

New service

As a Volcanic Ash Advisory Centre, the Met Office is responsible for forecasting the spread of volcanic ash plumes from eruptions originating in the North Atlantic. This includes Iceland, an area of regular volcanic activity that is situated beneath some of the world's busiest airways. Following discussions with the Icelandic met. service, we have started running daily volcanic ash forecasts using NAME to improve emergency response preparedness.

Air quality

An interesting episode study was carried out to determine the origin of high PM_{10} levels (particulate matter) over much of the United Kingdom on 12 September 2002. A combination of NAME and satellite data analyses showed that the origin was smoke from forest fires in northern Russia (Fig. 54).

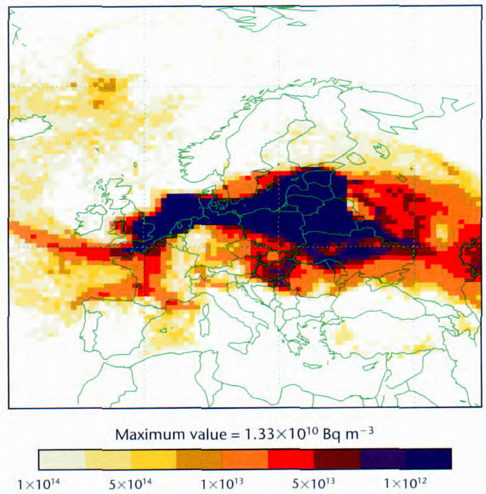

Figure 54. NAME derived map of possible source regions for 09 UTC on 12 September 2002.

Following the introduction of a new plume rise scheme to better represent the buoyancy of 'hot' plumes, a modelling study of fumigation events was completed. During fumigation events, pollutants released above the boundary layer are entrained into the boundary layer as it deepens during the day. This process can result in short periods of high surface concentrations some distance downwind of a source. A one-year simulation of emissions from a hypothetical power station revealed a number of such events, at ranges of up to 200 km (Fig. 55). A strong seasonal cycle was evident in the timing, strength, number and horizontal extent of events. Further work is planned to assess the impact on air quality.

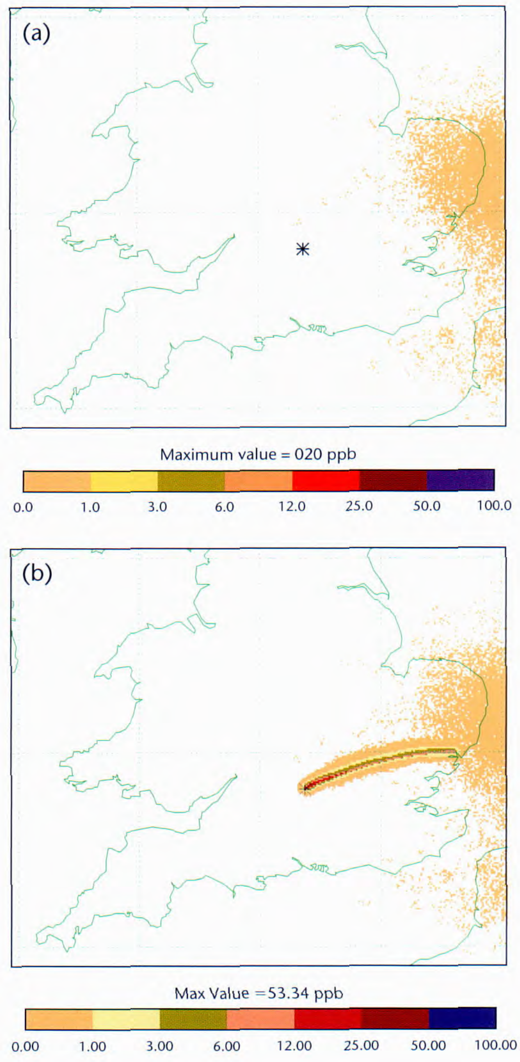

Figure 55. Example of a NAME predicted fumigation event from a 200 m chimney. (a) At 10 UTC, no material reaches the surface as pollutants are released above the inversion; (b) one hour later, the inversion level has risen, allowing material to reach the ground.

Determining source strengths

The Lagrangian nature of the NAME model allows it to be used to investigate source-receptor relationships. This capability continues to be used in support of the Global Atmosphere Division of Defra to interpret measurements of radiatively-active and ozone-depleting trace gases taken at the Mace Head monitoring station on the west coast of Ireland. The NAME model is used to predict the likely transport of material to Mace Head from all possible source regions, then a new inversion technique called 'simulated annealing' is applied to best 'fit' the model predictions to observations, thus providing emission estimates for the UK and a number of European countries. This technique offers an independent estimate of emission trends for a range of monitored species, allowing verification of internationally agreed emission quotas.

Environmental stresses

A new approach to examining the linkages between the environment and issues of socio-economic relevance, including conflict, has been developed further during the past year. A process leading to the implementation of this approach through a Geographical Information System has been fully scoped out. In part, the scoping process was handled through an international workshop held at the Government's Wilton Park facility in January/February 2003.

Climate, chemistry and ecosystems

Introduction

Climate change over the next 100 years will be driven by changes in atmospheric composition, through the radiative effects of greenhouse gases and aerosols. The primary cause will be human emissions, but most of the relevant chemical species also have significant chemical and biological sources and sinks. The role of the new Climate, Chemistry and Ecosystems team is to include interactions between the physical, chemical and biological components of the Earth's system within projections of 21st century environmental change.

Ecosystem-chemistry interactions

Ecosystems control the fluxes of important chemical species from surface to atmosphere, thereby influencing both atmospheric chemistry and climate (through the concentrations of greenhouse gases and aerosols).

For example, the most prevalent source of volatile organic compounds (VOCs) to the atmosphere is from vegetation. A particularly important emission from vegetation is isoprene (C_5H_8). VOCs interact with oxides of nitrogen (NO_x) in the troposphere to form ozone. Surface ozone is harmful to humans and causes significant reductions in crop production. It is also a greenhouse gas. We have coupled the diagnostics produced by the vegetation scheme (TRIFFID) to the tropospheric chemistry scheme (STOCHEM) in order to calculate interactive isoprene emissions. The important parameters are: vegetation type, leaf area index, temperature and photosynthetically active radiation. Figure 56 shows the effects of changing anthropogenic and natural emissions on the surface ozone. Comparing (a) and (b), (where the vegetation distribution is fixed) shows large increases in ozone over industrialised regions due to predicted increases in anthropogenic emissions of both NO_x and VOCs. The increases over Amazonia, and central and southern Africa are due to increased emissions of isoprene from vegetation due to the warmer climate. Comparing (b) and (c), (where the climate and anthropogenic emissions are fixed) shows the effect of the vegetation changes predicted by the TRIFFID model. Ozone levels have decreased, particularly over Amazonia as the Amazon forest dies back and emits fewer VOCs.

Chemistry in HadGEM

The STOCHEM atmospheric chemistry model has been included as an integral part of HadGEM, representing a considerable upgrade to the STOCHEM resolution (now 3.75° x 2.5° x 20 levels). HadGEM will allow various components of the model to be coupled together efficiently, allowing, for example, the role of climate change to impact on the chemistry. As an example, Fig. 57 shows the coupling between the annual methane growth increment and the Niño3 temperature index (the sea-surface temperature anomaly for part of the Equatorial Pacific). The correlation between the two is striking and is caused in this model by variations in the methane sink rate, promoted by humidity fluctuations that occur in response to surface temperature changes. As water vapour increases in response to a rise in temperature, the source rate for the hydroxyl radical (OH) increases, promoting the destruction of methane.

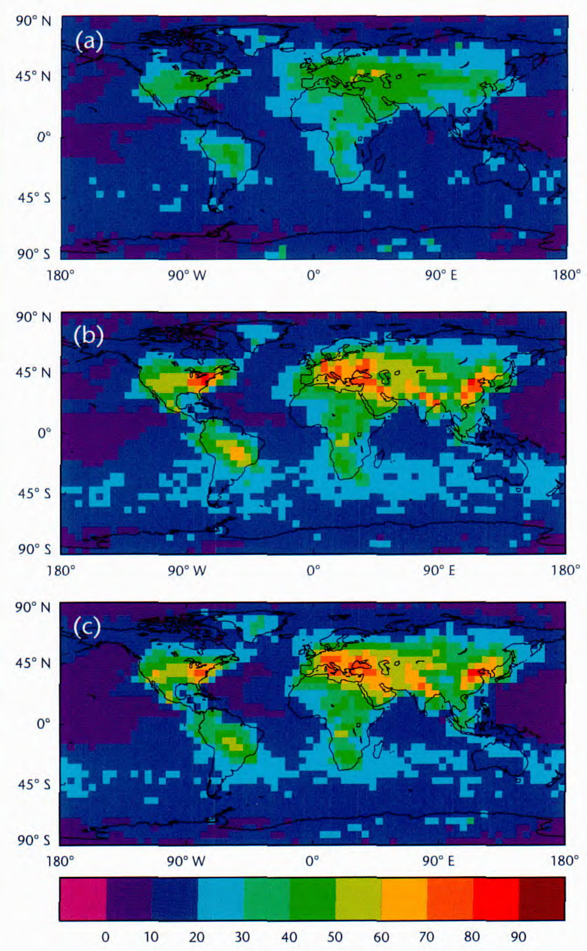

Figure 56. Impact of VOC emissions from vegetation on modelled surface ozone concentrations in parts per billion (under SRES A2 scenario). (a) 1990 emissions and climate, and vegetation, (b) 2090 emissions and climate, 1990 vegetation, and (c) 2090 emissions and climate, and vegetation.

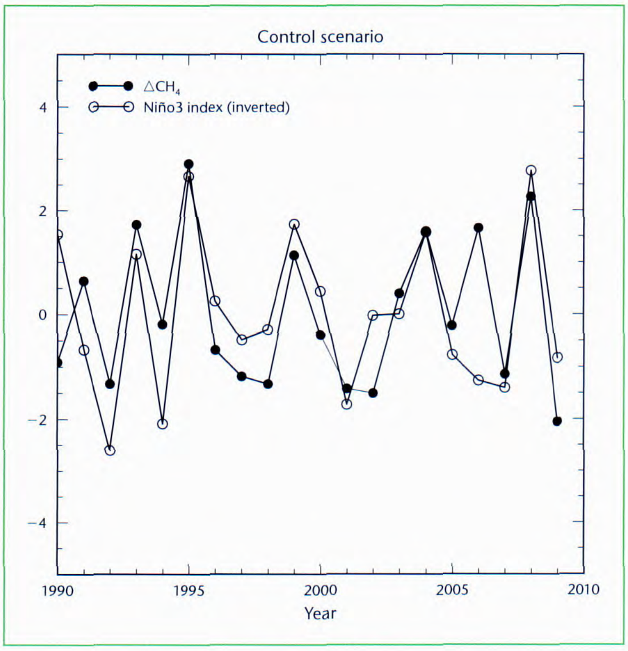

Figure 57. Interannual variability in the growth rate of atmospheric CH_4 as modelled using STOCHEM coupled to HadCM3. The inverted Niño3 index is also plotted to demonstrate the extent to which the El Niño Southern Oscillation drives this variability.

Effects of soot aerosol

The radiative effects of aerosol particles are one of the key uncertainties in projections of 21st century climate change. Sulphate aerosols from anthropogenic activities are believed to have offset greenhouse warming since pre-industrial times, by reflecting solar radiation (the 'direct effect') and providing additional cloud condensation nuclei ('indirect effects'). However, other aerosol species can have a warming rather than a cooling effect. Black carbon or 'soot' aerosol absorbs solar radiation and thereby tends to heat the atmospheric column. Experiments to investigate the climate response to fossil fuel soot aerosol have been carried out using the atmospheric model HadAM4 coupled to a simple mixed-layer ocean model. Figure 58 shows the simulated surface temperature change in one experiment. Soot exerts a positive radiative forcing so the global mean effect is a warming, but note that there are areas of cooling, especially in the southern hemisphere where

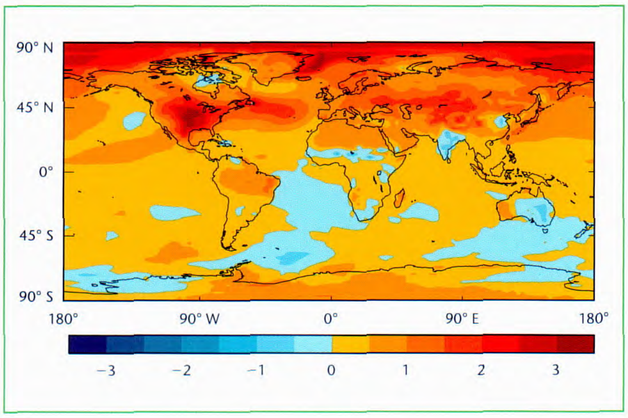

Figure 58. Modelled annual mean surface temperature change (°C) due to four times the fossil fuel soot aerosol emissions for 1985.

emissions are relatively low. In this model, the climate sensitivity to soot forcing appears to be significantly lower than for greenhouse gas forcing — a result that may have implications for policies on emissions.

Stratosphere–troposphere exchange

Previous work at the Met Office has suggested that the flux of air through the troposphere will increase in a warmer climate. STOCHEM was used within the climate model HadAM4, to investigate the influence of climate change on the stratosphere–troposphere exchange of ozone. The stratospheric ozone concentrations were held constant for this experiment to isolate the changes due solely to transport. The study found an increase between the 1990s and 2090s of over 30% in the net downward flux of ozone across the 200 hPa surface. The effect of this flux can be seen in Fig. 59, which shows the fractional change in ozone using a 2090s climate compared to a 1990s climate (emissions were fixed at 1990s levels). Although the ozone generally decreases (due to a warmer, wetter climate in the future), there are significant increases in ozone in the upper troposphere that will have implications for the radiative forcing from tropospheric ozone. This study also demonstrates the important influence that stratospheric processes can have on tropospheric chemistry.

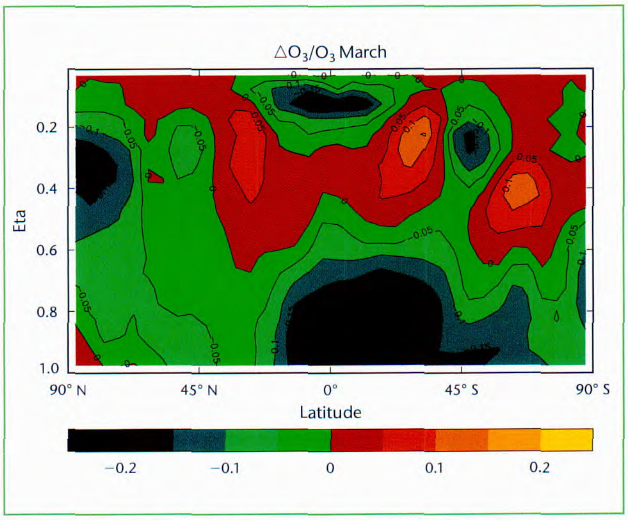

Figure 59. Fractional change in ozone mixing ratio between 2090s and 1990s.

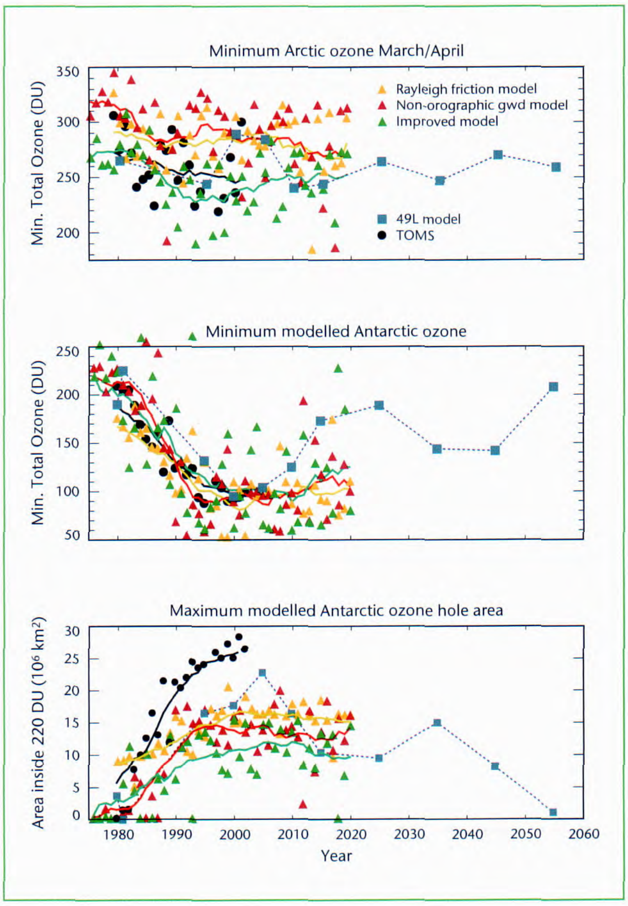

Figure 60. Total ozone amounts in the model experiments averaged over the latitude range 65° N-65° S, compared with observations from the Total Ozone Mapping Spectrometer.

Stratospheric processes research

A policy of continual model development has been pursued with the aim of obtaining improved simulations of the chemistry and dynamics of the stratosphere with which to investigate the impact of the stratosphere on the troposphere. The UM was previously established at the National Institute of Water and Atmospheric Research (NIWA, New Zealand) and this Met Office collaboration was developed further by setting up the coupled chemistry code at NIWA. The model has been improved further in collaboration with NIWA by incorporating a simple tropospheric chemistry scheme and improving the tracer transport. A simulation with the new chemistry-climate model has now been completed for the period 1975–2020, showing improved overall characteristics compared with the previous model. In particular, the overall bias in column average ozone is considerably reduced because of improved nitrogen oxide simulations. Figure 60 shows the results of column ozone averaged over the latitude range 65° N–65° S obtained for the different versions of the model, in comparison with observations. In each of the model results, the annual variation is given by the broken lines, while the solid lines indicate the smoothed values.The improved model (green line), including improved nitrogen oxides and a simple tropospheric chemistry scheme, has ozone values in much better agreement with the observations (blue line).

The results of the improved model are being analysed to try to determine the impact of climate change on ozone and the impact of ozone change on tropospheric quantities such as tropopause height, cloud amount, precipitation rates and large-scale atmospheric structure.

Operational ocean modelling

Forecasting Ocean Assimilation Model

Each day we run a global version of our Forecasting Ocean Assimilation Model (FOAM) with 1° resolution, and a nested regional Atlantic and Arctic Ocean FOAM at 1/3°, to provide forecasts of ocean temperature, salinity, currents and sea ice. A 1/9° (~11 km) North Atlantic FOAM is being run as a contribution to the Global Ocean Data Assimilation Experiment (GODAE). 1/3° and 1/9° FOAM configurations are also run operationally for the Indian Ocean and Arabian Sea. Yet higher-resolution FOAM models have been set up during the year in support of naval exercises, e.g. for the Tyrrhenian Sea (Fig. 61).

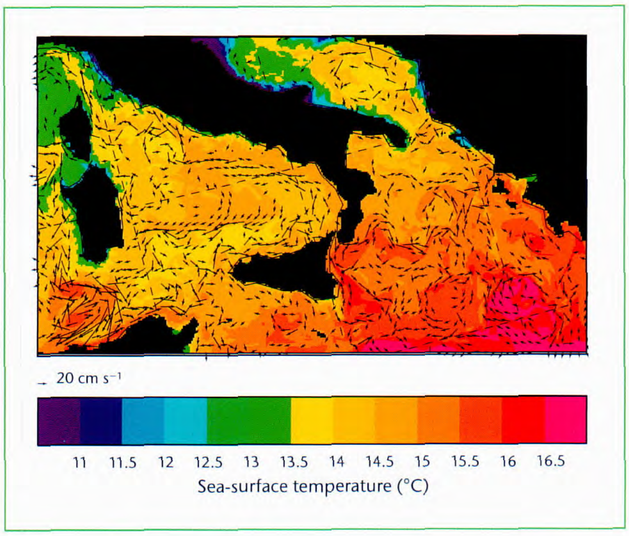

Figure 61. Example showing the sea-surface temperature and currents predicted with the 1/27° resolution Tyrrhenian Sea FOAM.

New methods for assimilation of in-situ and satellite altimeter data into the model have been implemented. These enable observations to make their full impact on the day they are received. They also use spatially varying statistics of the model's error at both atmospheric 'synoptic' scales and oceanographic 'mesoscales' (Fig. 62).

The Atlantic Margin shelf-seas model

During 2002, the operational ocean model for the north-west European shelf was upgraded. The new Atlantic Margin model covers a larger region that includes the full shelf break (Fig. 63). It uses the latest formulation of the Proudman Oceanographic Laboratory Coastal Ocean Modelling System (POLCOMS), with a hybrid vertical co-ordinate to improve representation of near-surface temperature in deeper waters. At the deep ocean boundaries, the Atlantic

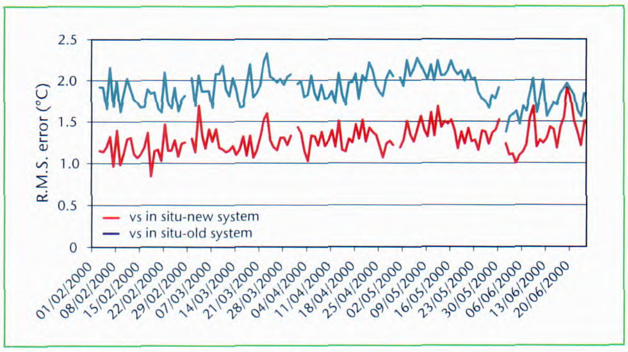

Figure 62. Time-series of root mean-square errors for model forecasts of surface temperature in the north-west Atlantic for the new and old methods for assimilating in-situ observations.

Margin model is nested into 1/3° Atlantic/Arctic FOAM for temperature and salinity conditions and barotropic currents. The Atlantic Margin model, in turn, provides boundary forcing for nested higher-resolution models of coastal waters, such as the Irish Sea model (Fig. 64).

Wave modelling

As part of the European Commission project MAXWAVE, we are developing a greater understanding of the likelihood of occurrence of extreme waves. Techniques are being developed to examine the 'peakedness' of modelled and observed wave energy

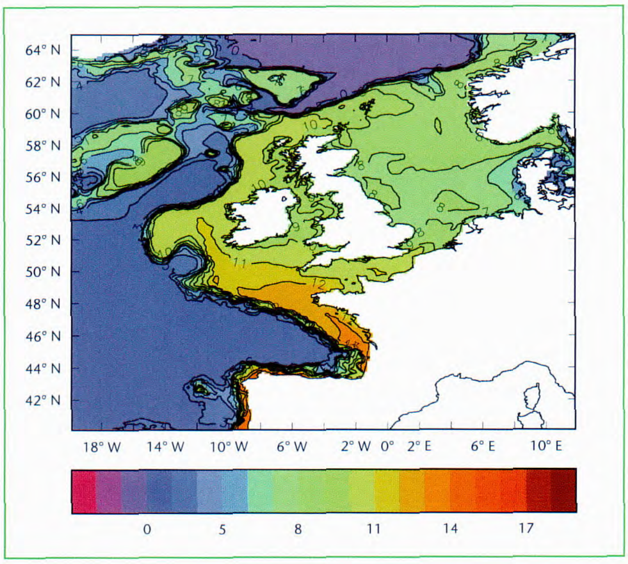

Figure 63. The Atlantic Margin model domain, showing predicted bed temperature (° C) for 17 March 2001.

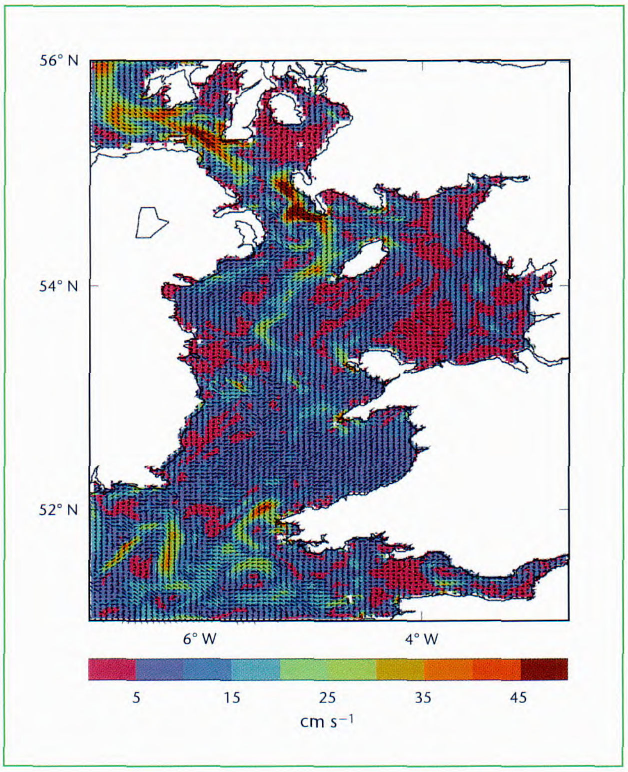

Figure 64. Instantaneous surface currents in the nested Irish Sea model.

spectra around the time and location of extreme wave events and it has been found that the peakedness can be much higher than previously thought. The wave model is being modified to provide estimates of the peakedness of the wave energy spectrum, to assist in predicting the likelihood of occurrence of an extreme wave.

During 2002, a collaboration with HR Wallingford was established to allow us to run the HR Floodworks system. This has extended our capability for wave prediction from offshore to near-shore. The system has been run in support of various commercial customers and the Royal Navy.

Seasonal climate modelling and prediction

Seasonal forecasts with an atmospheric model

A seasonal prediction system is run to generate experimental seasonal predictions for all areas of the globe. The atmospheric model is a version of the HadAM3 climate prediction model, integrated forward from current conditions out to six months. The expected SST evolution is based on persistence of observed SST anomalies. From May 2002, forecast maps have been freely available on our public web site (www.metoffice.com/research/seasonal/).

In 2002, warm SST anomalies in the tropical east Pacific became established in March and increased in magnitude over the following months to signal the onset of El Niño conditions. The seasonal precipitation forecast for September to November (Fig. 65 (a)), confirmed the likelihood of drier than usual conditions

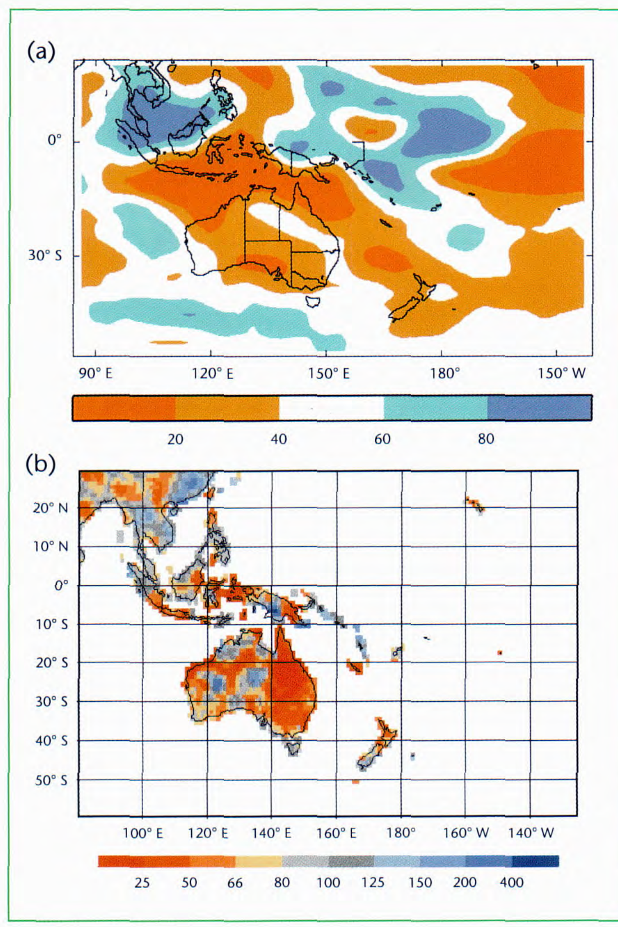

Figure 65. (a) Forecast probability of a positive anomaly in September-October-November 2002 precipitation totals, issued on 9 September 2002. (b) Observed precipitation anomalies as a percentage of the 1961–1990 average (from the Global Precipitation Climatology Centre).

over much of Australia and southern Indonesia, but suggested an atypical 'wetter' than normal response was more likely over northern Indonesia and Indochina. The forecast provided good guidance for both regions: dry conditions being observed over much of Australia and southern Indonesia, while over Indochina precipitation was generally average to above average (Fig. 65 (b)).

Ocean–atmosphere forecasts

We run a coupled ocean–atmosphere model to include the effects of air–sea interactions and feedbacks in seasonal forecasts. The Global Seasonal (GloSea) prediction system is based on the Hadley Centre HadCM3 ocean–atmosphere climate model with several added features, such as enhanced ocean resolution.

Since January 2002, trial forecasts have been produced using GloSea. Figure 66 shows a recent forecast for sea-surface temperature in the tropical Pacific, predicting a decline of the El Niño event.

Ocean modelling for climate

The ocean and sea-ice components of the HadGEM1 model (known as HadGOM1) will include a number of recent developments to both the ocean and sea-ice models. HadGOM1 will have a horizontal resolution of 1° (increasing in the tropics to 1/3° meridionally) and 40 vertical levels. Development work has focused on the introduction of a bottom boundary layer scheme into the model; this improves the representation of Arctic origin water flowing over the Denmark Strait into the subpolar North Atlantic and leads to a more realistic representation of the large-scale circulation in the North Atlantic basin.

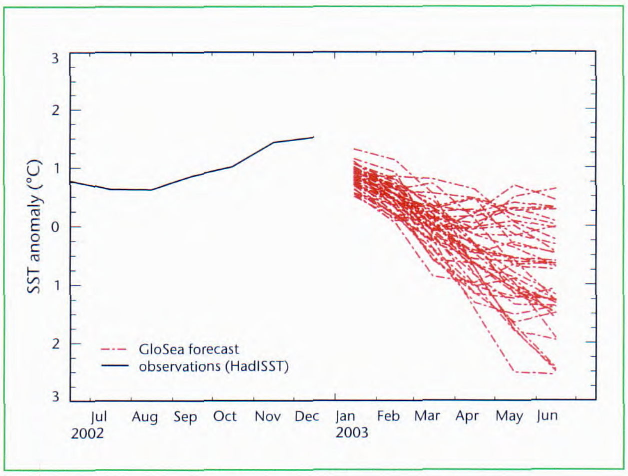

Figure 66. Ensemble forecast of SST anomalies in the central-east tropical Pacific Niño3 region, from 1 January 2003, predicting the decline in 2003 of the El Niño event that occurred in 2002. The dashed lines indicate monthly-mean forecast values for the separate ensemble members.

The model HadCEM (Coupled Eddy-permitting Model), developed over the past two years, has been run under an idealised scenario of increasing greenhouse gas concentrations. This is the first transient climate change experiment to be run using an ocean model with sufficient resolution to allow mesoscale eddies. Initial results suggest that the global mean temperature response is somewhat stronger than in the standard HadCM3 model (which has an identical atmospheric component). This is due in part to a smaller weakening of the North Atlantic thermohaline circulation (THC) in HadCEM than in HadCM3.

The role of the ocean in climate

Previous work identifying the processes responsible for the relative stability of the THC in the HadCM3 model has been extended to show that these processes are robust across a number of model runs. The analysis highlights the fundamental role played by fresh water transport in the North Atlantic Ocean on the salinity of the subpolar North Atlantic. Recent observations have identified decadal changes in North Atlantic salinity, and a current focus is on using models to understand the causes of these changes. To complement the analysis of coupled model runs using anthropogenic and natural climate forcings, an ocean-only model has been run using historical ('re-analysed') atmospheric forcing. This will allow assessment of how much of the observed variability may be due to internal ocean processes and how much is forced by the atmosphere.

Ocean carbon cycle

Ongoing collaboration with scientists at Southampton Oceanography Centre has yielded major advancements in the ocean carbon cycle model HadOCC, integrating into the model more realistic controls on ocean plankton growth and hence giving improved simulations of ocean carbon cycling. Work has begun on performing simulations of the variability of the ocean carbon cycle for the last 50 years.

Ocean observations (Argo)

Argo will be an international array of 3,000 free-drifting profiling floats to measure the temperature and salinity of the upper 2,000 m of the ocean, with expectations for the global 3,000-float array being in place by 2006. Since 2001, over 70 UK floats have been deployed in support of Argo (Fig. 67), with another 60 or so floats planned for deployment in 2003.

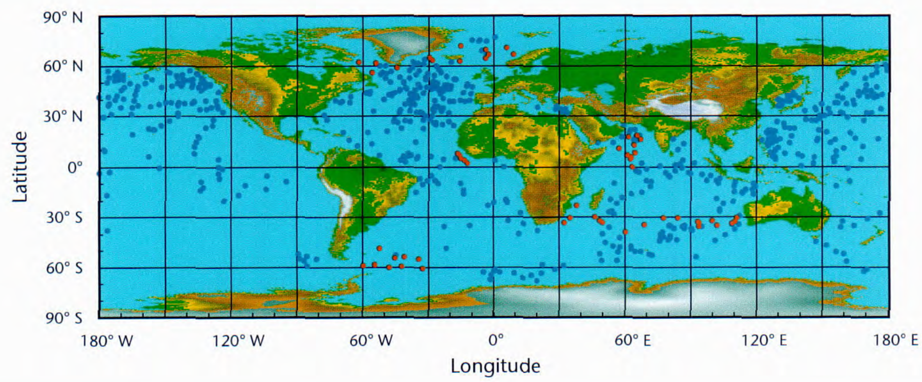

Figure 67. Coverage of Argo floats in mid February 2003. The red positions show the locations of active UK floats.

Bibliography

ALLAN, R., 2003: El Niño — a world perspective and what it means in Australia. Ecology: An Australian perspective. P. Attiwell and B. Wilson (Eds). Oxford University Press.

ALLAN, R.J., Reason, C.J.C., Carroll, P. and Jones, P.D., 2002: A reconstruction of Madras (Chennai) mean sea-level pressure using instrumental records from the late 18th and early 19th centuries. *Int J Climatol*, **22**, 1,119–1,142.

ALLAN, R.P. and SLINGO, A., 2002: Can current climate forcings explain the spatial and temporal signatures of decadal OLR variations? *Geophys Res Lett*, **29**, 45-1 to 45-4.

ALLAN, R.P., Ramaswamy, V. and SLINGO, A., 2002: Diagnostic analysis of atmospheric moisture and clear-sky radiative feedback in the Hadley Centre and Geophysical Fluid Dynamics Laboratory climate models. *J Geophys Res*, **107 (D17)**, ACL 4-1 to ACL 4-7.

ALLAN, R.P., SLINGO, A. and Ramaswamy, V., 2002: Analysis of moisture variability in the European Centre for Medium-Range Weather Forecasts 15-year reanalysis over the tropical oceans. *J Geophys Res*, **107 (D15)**, ACL 1-1 to ACL 1-5.

ALLAN, R.P., SLINGO, A. and RINGER, M.A., 2002: Influence of dynamics on the changes in tropical cloud radiative forcing during the 1998 El Niño. *J Clim*, **15**, 1,979–1,986.

Allen, M.R. and INGRAM, W.J., 2002: Constraints on future changes in climate and the hydrological cycle. *Nature*, **419**, 224–232.

ATHANASSIADOU, M., 2003: Wave and form drag: their relation in the linear gravity wave regime. *Tellus*, **55A**, 173–180.

AUSTIN, J. and KNIGHT, J.R., 2002: The Unified Model with Eulerian transport and chemistry: code description and testing procedure. Met Office internal document.

AUSTIN, J., et al., 2003: Uncertainties and assessments of chemistry-climate models of the stratosphere. *Atmos Chem Phys*, **3**, 1–27.

BANKS, H. and WOOD, R., 2002: Where to look for anthropogenic climate change in the ocean. *J Clim*, **15**, 879–891.

BANKS, H., WOOD, R. and GREGORY, J., 2002: Changes to Indian Ocean subantarctic mode water in a coupled climate model as CO_2 forcing increases. *J Phys Oceanogr*, **32**, 2,816–2,827.

BANKS, H.T. and Bindoff, N.L., 2003: Comparison of observed temperature and salinity changes in the Indo-Pacific with results from the coupled climate model HadCM3: processes and mechanisms. *J Clim*, **16**, 156–166.

BARAN, A.J., FRANCIS, P.N. and Yang, P., 2003: A process study of the dependence of ice crystal absorption on particle geometry: application to aircraft radiometric measurements of cirrus cloud in the terrestrial window region. *J Atmos Sci*, **60**, 417–427.

BEARE, R.J., Thorpe, A.J. and WHITE, A.A., 2003: The predictability of extratropical cyclones: nonlinear sensitivity to localized potential-vorticity perturbations. *QJR Meteorol Soc*, **129**, 219–237.

Bouwman, A.F., van Vuuren, D.P., DERWENT, R.G. and Posch, M., 2002: A global analysis of acidification and eutrophication of terrestrial ecosystems. *Water, Air & Soil Pollut*, **141**, 349–382.

Braganza, K. et al. (including STOTT, P.), 2003: Simple indices of global climate variability and change: Part I — variability and correlation structure. *Clim Dyn*, **20**, 491–502.

BROWN, A.R., LOCK, A.P., MACVEAN, M.K., et al., 2002: Large-eddy simulation of the diurnal cycle of shallow cumulus convection over land. *QJR Meteorol Soc*, **128**, 1,075–1,093.

Cardwell, J.R., Choularton, T.W., WILSON, D. and KERSHAW, R., 2002: Use of an explicit model of the microphysics of precipitating stratiform cloud to test a bulk microphysics scheme. *QJR Meteorol Soc*, **128**, 573–592.

Cavalcanti, I.F.A., FOLLAND, C.K., and COLMAN, A.W., 2002: Note on "Predictability of Northeast Brazil rainfall and real-time forecast skill, 1987–98". *J Clim*, **15**, 1,993–1,996.

Champion, H.J. et al. (including GLOSTER, J. and RYALL, D.B.), 2002: Investigation of the possible spread of foot-and-mouth disease virus by the burning of animal carcases on open pyres. *Vet Rec*, **151**, 593–600.

Chédin, A. et al. (including SAUNDERS, R.), 2003: The feasibility of monitoring CO_2 from high resolution infrared sounders. *J Geophys Res*, **108 (D2)**, ACH 6-1 to ACH 6-19.

Collier, C.G., Illingworth, A.J. and GOLDING, B.W., 2002: UWERN Report No. 5: Quantitative precipitation forecasts. *Weather*, **57**, 59–68.

Collins, M., Osborn, T.J., TETT, S.F.B., Briffa, K.R. and Schweingruber, F.H., 2002: A comparison of the variability of a climate model with paleotemperature estimates from a neural network of tree-ring densities. *J Clim*, **15**, 1,497–1,515.

COLLINS, W.J., DERWENT, R.G., JOHNSON, C.E. and STEVENSON, D.S., 2002: A comparison of two schemes for the convective transport of chemical species in a Lagrangian global chemical model. *QJR Meteorol Soc*, **128**, 991–1,009.

COLMAN, A., 2002: Experimental forecast of east African rainfall for October–December 2002. COLA. *Exp Long-Lead Forecast Bull*, **11**, Nos 3-4, 53–57 (available online at http://grads.iges.org/ellfb/Sep02/Colman/colman.htm).

COLMAN, A. and DAVEY, M., 2002: Experimental forecast of 2002 seasonal rainfall in the Sahel and other regions of tropical north Africa. *Exp Long-Lead Forecast Bull*, **11**, No. 2, 51–55 (available online at http://grads.iges.org/ellfb/Jun02/colman/colman.htm).

COTTON, R.J. and FIELD, P.R., 2002: Ice nucleation characteristics of an isolated wave cloud. *QJR Meteorol Soc*, **128**, 2,417–2,437.

DERWENT, R.G., COLLINS, W.J., JOHNSON, C.E. and STEVENSON, D.S., 2002: Global ozone concentrations and regional air quality. *Environ Sci & Technol*, **36**, 379A–382A.

DERWENT, R.G., COLLINS, W.J., Jenkin, M.E., JOHNSON, C.E. and STEVENSON, D.S., 2003: The global distribution of secondary particulate matter in a 3-D Lagrangian chemistry transport model. *J Atmos Chem*, **44**, 57–95.

DERWENT, R.G., RYALL, D.B., MANNING, A.J., et al., 2002: Continuous observations of carbon dioxide at Mace Head, Ireland from 1995 to 1999 and its net European ecosystem exchange. *Atmos Environ*, **36**, 2,799–2,807.

Diaz, H.F. et al. (including FOLLAND, C.K. and PARKER, D.E.), 2002: Workshop on advances in the use of historical marine climate data (Boulder, Co., USA, 29 January – 1 February 2002). *WMO Bull*, **51**, 377–380.

Dixon, R.S., Browning, K.A. and SHUTTS, G.J., 2002: The relation of moist symmetric instability and upper-level potential-vorticity anomalies to the observed evolution of cloud heads. *QJR Meteorol Soc*, **128**, 839–859.

FIELD, P.R. and Heymsfield, A.J., 2003: Aggregation and scaling of ice crystal size distributions. *J Atmos Sci*, **60**, 544–560.

FIELD, P.R., BROWN, P.R.A., SMITH, J.A., et al., 2003: Ice particle interarrival times measured with a fast FSSP. *J Atmos and Oceanic Technol*, **20**, 249–261.

FOLLAND, C. and COLMAN, A., 2002: Empirical prediction of the global temperature anomaly for 2003. *Exp Long-Lead Forecast Bull*, **11**, Nos 3-4, 115–119 (available online at http://grads.iges.org/ellfb/Dec02/Colman/colman.htm).

FOLLAND, C.K. and Anderson, C., 2002: Estimating changing extremes using empirical ranking methods. *J Clim*, **15**, 2,954–2,960.

FOLLAND, C.K., Karl, T.R. and Salinger, M.J., 2002: Observed climate variability and change. *Weather*, **57**, 269–278.

FOLLAND, C.K., Renwick, J.A., Salinger, M.J. and Mullan, A.B., 2002: Relative influences of the Interdecadal Pacific Oscillation and ENSO on the South Pacific Convergence Zone. *Geophys Res Lett*, **29**, 21-1 to 21-4.

FORBES, R.M. and CLARK, P.A., 2003: Sensitivity of extratropical cyclone mesoscale structure to the parametrization of ice microphysical processes. *QJR Meteorol Soc*, **129**, 1,123–1,148.

Free, M. et al. (including PARKER, D. and GORDON, M.), 2002: Creating climate reference datasets: CARDS Workshop on adjusting radiosonde temperature data for climate monitoring: Meeting Summary. *Bull Am Meteorol Soc*, **83**, 891–899.

Frei, C. et al. (including JONES, R.G.), 2003: Daily precipitation statistics in regional climate models: Evaluation and intercomparison for the European Alps. *J Geophys Res*, **108 (D3)**, ACL 9-1 to ACL 9-19.

Gillett, N.P. et al. (including MCDONALD, R.E.), 2002: How linear is the Arctic oscillation response to greenhouse gases? *J Geophys Res*, **107 (D3)**, ACL 1-1 to ACL 1-7.

Gillett, N.P., Allen, M.R. and WILLIAMS, K.D., 2002: The role of stratospheric resolution in simulating the Arctic oscillation response to greenhouse gases. *Geophys Res Lett*, **29**, 138-1 to 138-4.

Gillett, N.P., Allen, M.R. and WILLIAMS, K.D., 2003: Modelling the atmospheric response to doubled CO_2 and depleted stratospheric ozone using a stratospheric-resolving coupled GCM. *QJR Meteorol Soc*, **129**, 947–966.

Gillett, N.P. et al. (including STOTT, P.A.), 2002: Detecting anthropogenic influence with a multi-model ensemble. *Geophys Res Lett*, **29**, 31-1 to 31-4.

Gillett, N.P., Zwiers, F.W., Weaver, A.J. and STOTT, P.A., 2003: Detection of human influence on sea-level pressure. *Nature*, **421**, 292–294.

Glantz, P., Noone, K.J. and OSBORNE, S.R., 2003: Comparisons of airborne CVI and FSSP measurements of cloud droplet number concentrations in marine stratocumulus clouds. *J Atmos and Oceanic Technol*, **20**, 133–142.

GOEBER, M. and MILTON, S.F., 2002: On the use of radar data to verify mesoscale model precipitation forecasts. *In* Workshop report of the first SRNWP mesoscale verification workshop, 23–24 April 2001. De Bilt, KNMI.

GOEBER, M., MILTON, S.F. and WILSON, C.A., 2002: WGNE assessment of quantitative precipitation forecasts from operational numerical weather prediction models over the U.K. 2002 WGNE Blue Book, WMO/ICSU/IOC Joint Scientific Committee For the World Climate Research Programme, WMO Commission for atmospheric sciences, CAS/JSC Working Group on numerical experimentation.

GOLDING, B.W., 2002: Numerical weather prediction: regional prediction models. *In* Encyclopedia of atmospheric sciences. J.R. Holton, J.A. Curry and J.A. Pyle (Eds). Academic Press.

GREGORY, D., WILSON, D. and BUSHELL, A., 2002: Insights into cloud parameterization provided by a prognostic approach. *QJR Meteorol Soc*, **128**, 1,485–1,504.

GREGORY, J.M. and Church, J.A., 2002: Changes in sea-level. *Weather*, **57**, 287–295.

GREGORY, J.M., STOTT, P.A., CRESSWELL, D.J., RAYNER, N.A., GORDON, C. and SEXTON, D.M.H., 2002: Recent and future changes in Arctic sea ice simulated by the HadCM3 AOGCM. *Geophys Res Lett*, **29**, 28-1 to 28-4.

GREGORY, J.M., Stouffer, R.J., Raper, S.C.B., STOTT, P.A. and RAYNER, N.A., 2002: An observationally based estimate of the climate sensitivity. *J Clim*, **15**, 3,117–3,121.

Hansen, J. et al. (incuding LEAN, J., RAYNER, N. and PARKER, D.), 2002: Climate forcings in Goddard Institute for Space Studies SI2000 simulations. *J Geophys Res*, **107 (D18)**, ACL 2-1 to ACL 2-37.

HAYWOOD, J.M., OSBORNE, S.R., FRANCIS, P.N., KEIL, A., et al., 2003: The mean physical and optical properties of regional haze dominated by biomass burning aerosol measured from the C-130 aircraft during SAFARI 2000. *J Geophys Res*, **108 (D13)**, SAF 9-1 to SAF 9-14.

HAYWOOD, J.M., FRANCIS, P.N., Dubovik, O., GLEW, M.D. and Holben, B.N., 2003: Comparison of aerosol size distributions, radiative properties, and optical depths determined by aircraft observations and Sun photometers during SAFARI 2000. *J Geophys Res*, **108 (D13)**, SAF 7-1 to SAF 7-12.

Hewitt, C.D., Stouffer, R.J., Broccoli, A.J. and MITCHELL, J.F.B., 2003: The effect of ocean dynamics in a coupled GCM simulation of the last glacial maximum. *Clim Dyn*, **20**, 203–218.

Heymsfield, A.J. et al. (including FIELD, P.R.), 2002: Observations and parameterizations of particle size distributions in deep tropical cirrus and stratiform precipitating clouds: Results from in situ observations in TRMM field campaigns. *J Atmos Sci*, **59**, 3,457–3,491.

HORROCKS, L.A., CANDY, B., SAUNDERS, R.W., O'CARROLL, A., et al., 2003: Parameterizations of the skin effect and implications for satellite-based measurement of sea-surface temperature. *J Geophys Res*, **108 (C3)**, 41-1 to 41-11.

HORT, M.C. and Robins, A.G., 2002: The dispersion of fugitive emissions from storage tanks. *J Wind Eng and Ind Aerodyn*, **90**, 1,321–1,348.

HORT, M.C., DEVENISH, B.J. and THOMSON, D.J., 2002: Building affected dispersion: development and initial performance of a new Lagrangian particle model. *In* 15th Conference on boundary layers and turbulence. American Meteorological Society.

Hulme, M. et al. (including JENKINS, G., JONES, R., MURPHY, J., HASSELL, D., BOORMAN, P., MACDONALD, R. and HILL, S.), 2002: Climate-change scenarios for the United Kingdom: The UKCIP02 Scientific Report. Tyndall Centre for Climate Change Research, School of Environmental Sciences, University of East Anglia, Norwich, UK.

INGRAM, W.J., 2002: On the robustness of the water vapor feedback: GCM vertical resolution and formulation. *J Clim*, **15**, 917–921.

INVERARITY, G.W., 2002: Fast computation of multi-dimensional Fourier integrals. *SIAM J Sci Comput*, **24**, 645–651.

JOHNS, T.C., GREGORY, J.M., INGRAM, W.J., JOHNSON, C.E., JONES, A., LOWE, J.A., MITCHELL, J.F.B., ROBERTS, D.L., SEXTON, D.M.H., Stevenson, D.S., TETT, S.F.B. and WOODAGE, M.J., 2003: Anthropogenic climate change for 1860 to 2100 simulated with the HadCM3 model under updated emissions scenarios. *Clim Dyn*, **20**, 583–612.

JOHNSON, C.E., STEVENSON, D.S., COLLINS, W.J. and DERWENT, R.G., 2003: Interannual variability in methane growth rate simulated with a coupled ocean-atmosphere-chemistry model. *Geophys Res Lett*, **29**, 9-1 to 9-4.

JONES, G.S., TETT, S.F.B. and STOTT, P.A., 2003: Causes of atmospheric temperature change 1960–2000: A combined attribution analysis. *Geophys Res Lett*, **30**, 32-1 to 32-4.

KEIL, A. and HAYWOOD, J.M., 2003: Solar radiative forcing by biomass aerosol particles over marine clouds during SAFARI-2000. A case study based on measured aerosol and cloud properties. *J Geophys Res*, **108 (D13)**, SAF 3-1 to SAF 3-10.

Kiktev, D., SEXTON, D., ALEXANDER, L. and FOLLAND, C., 2002: Trends in fields of precipitation and surface temperature annual extremes during the second half of the 20th century. *Meteorol and Hydrol*, **N11**, 5–15.

Klein Tank, A.M.G. et al. (including ALEXANDER, L.V.), 2002: Daily dataset of 20th-century surface air temperature and precipitation series for the European Climate Assessment. *Int J Climatol*, **22**, 1,441–1,453.

Labitzke, K. et al. (including AUSTIN, J., BUTCHART, N. and KNIGHT, J.), 2002: The global signal of the 11-year solar cycle in the stratosphere: observations and models. *J Atmos & Sol-Terr Phys*, **64**, 203–210.

Leach, H., Bowerman, S.J. and McCULLOCH, M.E., 2002: Upper ocean eddy transports of heat, potential vorticity and volume in the northeastern North Atlantic — "Vivaldi 1991". *J Phys Oceanogr*, **32**, 2,926–2,937.

LEGG, T.P., MYLNE, K.R. and WOOLCOCK, C., 2002: Use of medium-range ensembles at the Met Office. 1: PREVIN — a system for the production of probabilistic forecast information from the ECMWF EPS. *Meteorol Appl*, **9**, 255–271.

LORENC, A., 2002: Weather prediction: data assimilation. *In* Encyclopedia of atmospheric sciences. J.R. Holton, J.A. Curry and J.A. Pyle (Eds). Academic Press.

McFarquhar, G.M., Yang, P., Macke, A. and BARAN, A.J., 2002: A new parameterization of single-scattering solar radiative properties for tropical anvils using observed ice crystal size and shape distributions. *J Atmos Sci*, **59**, 2,458–2,478.

McIntyre, M.E. and ROULSTONE, I. 2002: Are there higher-accuracy analogues of semi-geostrophic theory? *In* Large-scale atmosphere–ocean dynamics. Vol. 2, Geometric methods and models. J. Norbury and I. ROULSTONE (Eds.). Cambridge University Press.

Manney, G.L. et al. (including SWINBANK, R.), 2003: Lower stratospheric temperature differences between meteorological analyses in two cold Arctic winters and their impact on polar processing studies. *J Geophys Res*, **108 (D5)**, SOL 71-1 to SOL 71-18.

MANSFIELD, D., 2002: Synoptic meteorology: forecasting. *In* Encyclopedia of atmospheric sciences. J.R. Holton, J.A. Curry and J.A. Pyle (Eds). Academic Press.

MARTIN, M.J., BELL, M.J. and Nichols, N.K., 2002: Estimation of systematic error in an equatorial ocean model using data assimilation. *Int J Num Meth Fluids*, **40**, 435–444.

MASON, P.J. and THOMSON, D.J., 2002: Boundary layers: overview. *In* Encyclopedia of atmospheric sciences. J.R. Holton, J.A. Curry and J.A. Pyle (Eds). Academic Press.

Metcalfe, S.E., Whyatt, J.D., DERWENT, R.G. and O'Donoghue, M., 2002: The regional distribution of ozone across the British Isles and its response to control strategies. *Atmos Environ*, **36**, 4,045–4,055.

MYLNE, K.R., 2002: Decision-making from probability forecasts based on forecast value. *Meteorol Appl*, **9**, 307–315.

NEWMAN, S.M. and TAYLOR, J.P., 2002: Impact of updates to the HITRAN spectroscopic database on the modeling of clear-sky infrared radiances. *Geophys Res Lett*, **29**, 18-1 to 18-4.

Norbury, J. and ROULSTONE, I. (Eds), 2002: Large-scale atmosphere-ocean dynamics. Vol. I Analytical methods and numerical models: Vol. 2 Geometric methods and models. Cambridge University Press.

PARKER, D.E., 2002: Reply to correspondent on calculation of global warming. *Weather*, **57**, 147–148.

PARKER, D.E. and ALEXANDER, L.V., 2002: Global and regional climate in 2001. *Weather*, **57**, 328–340.

PETCH, J.C., BROWN, A.R. and GRAY, M.E.B., 2002: The impact of horizontal resolution on the simulations of convective development over land. *QJR Meteorol Soc*, **128**, 2,031–2,044.

Peterson, T.C. et al. (including ALEXANDER, L.), 2002: Recent changes in climate extremes in the Caribbean region. *J Geophys Res*, **107 (D21)**, ACL 16-1 to ACL 16-9.

Pielke, R.A. et al. (including BETTS, R.A.), 2002: The influence of land-use change and landscape dynamics on the climate system: relevance to climate change policy beyond the radiative effect of greenhouse gases. *Philos Trans R Soc London*, **A360**, 1,705–1,719.

Pielke, R.A. et al. (including BETTS, R.A.), 2003: The influence of land-use change and landscape dynamics on the climate system: relevance to climate change-policy beyond the radiative effect of greenhouse gases. *In* Capturing carbon and conserving biodiversity, Part 2: Environmental services. I.R. Swingland (Ed.). London, Earthscan Publications Ltd.

Ponte, R.M., Rajamony, J. and GREGORY, J.M., 2002: Ocean angular momentum signals in a climate model and implications for Earth rotation. *Clim Dyn*, **19**, 181–190.

POPE, V. and Davies, T., 2002: Testing and evaluating atmospheric climate models. *Comput in Sci and Eng*, **4**, 64–69.

POPE, V.D. and STRATTON, R.A., 2002: The processes governing horizontal resolution sensitivity in a climate model. *Clim Dyn*, **19**, 211–236.

PRICE, J.D. and WOOD, R., 2002: Comparison of probability density functions for total specific humidity and saturation deficit humidity, and consequences for cloud parametrization. *QJR Meteorol Soc*, **128**, 2,059–2,072.

Pyle, J.A. et al. (including AUSTIN, J.), 2003: Polar stratospheric ozone. *In* Stratospheric processes: observations and interpretation. WMO Global Ozone Research and Monitoring Project Report. Geneva, WMO.

Randel, W. et al. (including SWINBANK, R.), 2002: SPARC intercomparison of middle atmosphere climatologies. WCRP-116, WMO/TD No. 1142, SPARC Report No. 3. Geneva, World Meteorological Organization.

Raper, S.C.B., GREGORY, J.M. and Stouffer, R.J., 2002: The role of climate sensitivity and ocean heat uptake on AOGCM transient temperature response. *J Clim*, **15**, 124–130.

REDINGTON, A.L. and DERWENT, R.G., 2002: Calculation of sulphate and nitrate aerosol concentrations over Europe using a Lagrangian dispersion model. *Atmos Environ*, **36**, 4,425–4,439.

Reynolds, R.W. et al. (including RAYNER, N.A.), 2002: An improved in situ and satellite SST analysis for climate. *J Clim*, **15**, 1,609–1,625.

Richards, K.J. and BANKS, H.T., 2002: Characteristics of interleaving in the western equatorial Pacific. *J Geophys Res*, **107 (C12)**, 24-1 to 24-12.

RINGER, M.A., EDWARDS, J.M. and SLINGO, A., 2003: Simulation of satellite channel radiances in the Met Office Unified Model. *QJR Meteorol Soc*, **129**, 1,169–1,190.

ROBERTS, N.M. and FORBES, R.M., 2002: An observational study of multiple cloud head structure in the FASTEX IOP 16 cyclone. *Atmos Sci Lett*, **3**, 59–70.

RODWELL, M.J., 2003: On the predictability of North Atlantic climate. The North Atlantic Oscillation. J.W. Hurrell, Y. Kushnir, G. Ottersen and M. Visbeck (Eds). *Geophys Monogr*, **134**, 173–192.

RODWELL, M.J. and FOLLAND, C.K., 2002: Atlantic air–sea interaction and seasonal predictability. *QJR Meteorol Soc*, **128**, 1,413–1,443.

RODWELL, M.J. and FOLLAND, C.K., 2003: Atlantic air–sea interaction and model validation. *Ann of Geophys*, **46**, 47–56.

Rohn, M., Kelly, G. and SAUNDERS, R.W., 2001: Impact of new cloud motion wind product from Meteosat on NWP analyses and forecasts. *Mon Weather Rev*, **129**, 2,392–2,403.

Ross, A.N. and VOSPER, S.B., 2003: Numerical simulations of stably stratified flow through a mountain pass. *QJR Meteorol Soc*, **129**, 97–115.

ROULSTONE, I., 2002: Lagrangian dynamics. *In* Encyclopedia of atmospheric sciences. J.R. Holton, J.A. Curry and J.A. Pyle (Eds). Academic Press.

ROWELL, D.P., 2003: The impact of Mediterranean SSTs on the Sahelian rainfall season. *J Clim*, **16**, 849–862.

Saenko, O.A., GREGORY, J.M., Weaver, A.J. and Eby, M., 2002: Distinguishing the influences of heat, freshwater, and momentum fluxes on ocean circulation and climate. *J Clim*, **15**, 3,686–3,697.

Saunders, S.M. et al. (including DERWENT, R.G.), 2003: Protocol for the development of the Master Chemical Mechanism, MCM v3 (Part A): Tropospheric degradation of non-aromatic volatile organic compounds. *Atmos Chem Phys*, **3**, 161–180.

SCAIFE, A.A., BUTCHART, N., Warner, C.D. and SWINBANK, R., 2002: Impact of a spectral gravity wave parameterization on the stratosphere in the Met Office Unified Model. *J Atmos Sci*, **59**, 1,473–1,489.

SENIOR, C.A., JONES, R.G., LOWE, J.A., DURMAN, C.F. and Hudson, D., 2002: Predictions of extreme precipitation and sea-level rise under climate change. *Philos Trans R Soc London*, **A360**, 1,301–1,311.

Sheppard, C.R.C. and RAYNER, N., 2002: Utility of the Hadley Centre sea-ice and sea surface temperature data set (HadISST1) in two widely contrasting coral reef areas. *Mar Pollut Bull*, **44**, 303–308.

SHUTTS, G., 2003: Inertia-gravity wave and neutral Eady wave trains forced by directionally sheared flow over isolated hills. *J Atmos Sci*, **60**, 593–606.

SHUTTS, G.J., 2003: Some interpretations of stochastic physical parametrizations. ECMWF Seminar Proceedings, 3–7 Sept. 2001. Reading, ECMWF.

STANIFORTH, A., WOOD, N. and Côté, J., 2002: A simple comparison of four physics–dynamics coupling schemes. *Mon Weather Rev*, **130**, 3,129–3,135.

STANIFORTH, A., WOOD, N. and Côté, J., 2002: Analysis of physics–dynamics coupling. *QJR Meteorol Soc*, **128**, 2,779–2,800.

STOTT, P.A. and Kettleborough, J.A., 2002: Origins and estimates of uncertainty in predictions of twenty-first century temperature rise. *Nature*, **416**, 723–726.

Struthers, H. et al. (including SWINBANK, R.), 2002: Assimilation of ozone profiles and total column measurements into a global general circulation model. *J Geophys Res*, **107 (D20)**, ACH 10-1 to ACH 10-14.

Swap, R.J. et al. (including HAYWOOD, J.M.), 2002: The Southern African Regional Science Initiative (SAFARI 2000): overview of the dry season field campaign. *S African J of Sci*, **98**, 125–130.

TETT, S.F.B., JONES, G.S., STOTT, P.A., Hill, D.C., MITCHELL, J.F.B., Allen, M.R., INGRAM, W.J., JOHNS, T.C., JOHNSON, C.E., JONES, A., ROBERTS, D.L., SEXTON, D.M.H. and WOODAGE, M.J., 2002: Estimation of natural and anthropogenic contributions to twentieth century temperature change. *J Geophys Res*, **107 (D16)**, ACL 10-1 to ACL 10-24.

THOMSON, D.J., 2002: Meteorology. *In* Encyclopedia of environmetrics. A.H. El-Shaarawi and W.W. Piegorsch (Eds). Wiley.

THOMSON, D.J., 2003: Dispersion of particle pairs and the decay of scalar fields in isotropic turbulence. *Phys Fluids*, **15**, 801–813.

Thorncroft, C.D. et al. (including DEVEREAU, S., DUMELOW, R., KINDRED, D.R. and PRICE, N.M.), 2003: The JET2000 project: Aircraft observations of the African easterly jet and African easterly waves. *Bull Am Meteorol Soc*, **84**, 337–351.

THORNE, P.W., TETT, S.F.B., PARKER, D.E., STOTT, P.A., JONES, G.S., et al., 2002: Assessing the robustness of zonal mean climate change detection. *Geophys Res Lett*, **29**, 26-1 to 25-4.

Thuburn, J., WOOD, N. and STANIFORTH, A., 2002: Normal modes of deep atmospheres. I: Spherical geometry. *QJR Meteorol Soc*, **128**, 1,771–1,792.

Thuburn, J., WOOD, N. and STANIFORTH, A., 2002: Normal modes of deep atmospheres. II: *f-F*-plane geometry. *QJR Meteorol Soc*, **128**, 1,793–1,806.

Tjemkes, S.A. et al. (including CLOUGH, S.A., RAYER, P. and TAYLOR, J.P.), 2003: The ISSWG line-by-line inter-comparison experiment. *J Quant Spectrosc and Radiat Transfer*, **77**, 433–453.

Trenberth, K.E. et al. (including ALLAN, R.P. and SLINGO, A., 2002: Changes in tropical cloud and radiation. *Science*, **296**, 2095a.

Vaughan, J.M., MARYON, R.H. and Geddes, N.J., 2002: Comparison of atmospheric aerosol backscattering and air mass back trajectories. *Meteorol Atmos Phys*, **79**, 33–46.

VELLINGA, M. and WOOD, R.A., 2002: Global climatic impacts of a collapse of the Atlantic thermohaline circulation. *Clim Change*, **54**, 251–267.

VOSPER, S.B., Mobbs, S.D. and Gardiner, B.A., 2002: Measurements of the near-surface flow over a hill. *QJR Meteorol Soc*, **128**, 2,257–2,280.

VOSPER, S.B. 2003: Development and testing of a high resolution mountain-wave forecasting system. *Meteorol Appl*, **10**, 75–86.

Waple, A.M. et al. (including ALEXANDER, L.), 2002: Climate assessment for 2001. *Bull Am Meteorol Soc*, **83**, 938.

WEBSTER, H., THOMSON, D., REDINGTON, A. and RYALL, D., 2002: Validation of a Lagrangian model plume rise scheme against the Kincaid data set. *In* Eighth international conference on harmonisation within atmospheric dispersion modelling for regulatory purposes. E. Batchvarova and D. Syrakov (Eds). Sofia, Demetra Ltd.

WEBSTER, H.N. and THOMSON, D.J., 2002: Validation of a Lagrangian model plume rise scheme using the Kincaid data set. *Atmos Environ*, **36**, 5,031–5,042.

WHITE, A.A., 2002: Dynamic meteorology — primitive equations. *In* Encyclopedia of atmospheric sciences. J.R. Holton, J.A. Curry and J.A. Pyle (Eds). Academic Press.

WHITE, A.A., 2002: A view of the equations of meteorological dynamics and various approximations. *In* Large-scale atmosphere–ocean dynamics, Vol. I, Analytical methods and numerical models. J. Norbury and I. ROULSTONE (Eds). Cambridge University Press.

WHITE, A.A., 2003: Dynamical equivalence and the departure-point equation in semi-Lagrangian numerical models. *QJR Meteorol Soc*, **129**, 1,317–1,324.

White, W.B., Chen, S.-C., ALLAN, R.J. and Stone, R.C., 2002: Positive feedbacks between the Antarctic circumpolar wave and the global el Niño-Southern Oscillation wave. *J Geophys Res*, **107 (C10)**, 29-1 to 29-17.

Williams, R.G., Day, K., Roussenov, V. and WOOD, R.A., 2002: The role of overturning circulation in determining the potential vorticity over the abyssal ocean. *J Geophys Res*, **107 (C10)**, 34-1 to 34-12.

WOOD, N. and STANIFORTH, A., 2003: The deep-atmosphere Euler equations with a mass-based vertical coordinate. *QJR Meteorol Soc*, **129**, 1,289–1,300.

WOOD, R., FIELD, P.R. and Cotton, W.R., 2002: Autoconversion rate bias in stratiform boundary layer cloud parameterizations. *Atmos Res*, **65**, 109–128.

WOOD, R.A. and Killworth, P.D., 2002: Has WOCE helped deliver ocean models suitable for predicting climate change? *Int WOCE Newsl*, **43**, 10–14.

WU, P. and GORDON, C., 2002: Oceanic influence on North Atlantic climate variability. *J Clim*, **15**, 1,911–1,925.

Xie, S. et al. (including PETCH, J.C.), 2002: Intercomparison and evaluation of GCM cumulus parametrizations under summertime midlatitude continental conditions. *QJR Meteorol Soc*, **128**, 1,095–1,136.

Xu, K.-M. et al. (including PETCH, J.C.), 2002: An intercomparison of cloud-resolving models with the atmospheric radiation measurement summer 1997 intensive observation period data. *QJR Meteorol Soc*, **128**, 593–624.

YOUNG, M.V. and CARROLL, E.B., 2002: The use of medium-range ensembles at the Met Office. 2: Applications for medium-range forecasting. *Meteorol Appl*, **9**, 273–288.

ZERROUKAT, M., WOOD, N. and STANIFORTH, A., 2002: SLICE: A Semi-Lagrangian Inherently Conserving and Efficient scheme for transport problems. *QJR Meteorol Soc*, **128**, 2,801–2,820.

Zhu, Y. et al. (including MYLNE, K.), 2002: The economic value of ensemble-based forecasts. *Bull Am Meteorol Soc*, **83**, 73–83.

Acronyms

AATSR	Advanced Along-track Scanning Radiometer
AIRS	Advanced Infrared Sounder
AMSU	Advanced Microwave Sounding Unit
ATOVS	Advanced TIROS Operational Vertical Sounder
AVHRR	Advanced Very High Resolution Radiometer
CET	Central England Temperature
ECMWF	European Centre for Medium-range Weather Forecasts
ENSO	El Niño Southern Oscillation
EPS	Ensemble Prediction System
ESA	European Space Agency
FAAM	Facility for Airborne Atmospheric Measurements
FM	Fields Modification
FOAM	Forecasting Ocean Assimilation Model
GANDOLF	Generating Advanced Nowcasts for Deployment in Operational Land-based flood Forecasts
GCM	General circulaton model
GODAE	Global Ocean Data Assimilation Experiment
GPS	Global Positioning System
GloSea	Global Seasonal
IASI	Infrared Atmospheric Sounding Interferometer
IPCC	Intergovernmental Panel on Climate Change
LES	Large Eddy Simulation
LCBR	Laser cloud-base recorder
MORSN	Met Office Remote Sites Network
MOSES	Met Office Surface Exchange Scheme
MSLP	Mean sea-level pressure
NASA	National Aeronautics and Space Administration (USA)
NCEP	National Centers for Environmental Prediction (part of NOAA)
NERC	Natural Environment Research Council
NESDIS	National Environmental Satellite, Data, and Information Service (part of NOAA)
NOAA	National Oceanic and Atmospheric Administration (USA)
NWP	Numerical weather prediction
NMAT	Night-time marine air temperatures
OFC	Optical Flow Constraint
POLCOMS	Proudman Oceanographic Laboratory Coastal Ocean Modelling System
RMSE	Root-mean-square error
SAMOS	Semi-automatic Meteorological Observing System
SEVIRI	Spinning Enhanced Visible and Infrared Imager
SID	Small Ice Detector
SOAP	Simulations, Observations and Palaeoclimate data
SMOK	Hydrological and Meteorological Monitoring and Forecasting System
SST	Sea-surface temperature
THC	Thermohaline circulation
TOMS	Total Ozone Mapping Spectrometer
UM	Unified Model
VOC	Volatile organic compounds

Notes

Copies of the *Scientific and Technical Review 2002/3* can be obtained from the Met Office on 01344 854623.

The *Scientific and Technical Review 2002/3* and the *Annual Report and Accounts 2002/3* can also be accessed from our web site at

www.metoffice.com

All other enquiries, including those relating to products and services, should be directed to our Customer Centre on 0845 300 0300.

Designed and produced by the Met Office.

02/0753

Printed on totally chlorine-free paper.

ISBN 0 86180 369 8

Met Office London Road Bracknell Berkshire RG12 2SZ United Kingdom
Tel: +44 (0)1344 855680 Fax: +44 (0)1344 855681
E-mail: enquiries@metoffice.com www.metoffice.com

From 1 September 2003 the new address will be
Met Office FitzRoy Road Exeter EX1 3PB United Kingdom